

MODELING AND OPTIMIZATION OF DEMAND-SIDE AND SUPPLY-SIDE
ENERGY MANAGEMENT IN ELECTRICITY MARKETS

by

Behdad Vatani

A dissertation submitted to the faculty of
The University of North Carolina at Charlotte
in partial fulfillment of the requirements
for the degree of Doctor of Philosophy in
Electrical Engineering

Charlotte

2018

Approved by:

Dr. Badrul Chowdhury

Dr. Valentina Cecchi

Dr. Churlzu Lim

Dr. Robert Cox

ABSTRACT

BEHDAD VATANI. Modeling and Optimization of Demand-Side and Supply-Side Energy Management in Electricity Markets. (Under the direction of DR. BADRUL CHOWDHURY)

An energy management system (EMS) is a system designed for owners of generation companies (GenCos), operators of electricity markets and electric utility grids, as well as consumers and aggregators to monitor, control, and optimize the performance of the generation, transmission, and demand systems.

This Ph.D. dissertation is devoted to studying the modeling and optimization of energy management problems associated with demand-side and supply-side of the electricity market comprising of a comprehensive comparison amongst several robust self-scheduling models of GenCos using real-world electricity market prices in which different self-scheduling strategies are proposed based on the price data and the generation company's desired robustness level. Moreover, to practically evaluate the performance of various methodologies, a post-optimization procedure has been proposed to determine the actual profit of each method in different real-market-environment cases. The conclusions drawn from the evaluations can help GenCos select and model the most appropriate non-deterministic self-scheduling approach based on the price information and price forecast method that they have adopted, as well as the robustness level that they desire in their solution.

In addition, a novel integrated capacity market and demand response model is introduced as an alternative solution to the transmission expansion planning problem. This strategy includes the use of the demand response resources (DRRs) as power supply resources to participate in the capacity market. The proposed model is implemented on the Base Residual Auction (BRA) of 2020/2021 PJM capacity market real data, and the influence of several important parameters are investigated in detail.

As a final step, a comprehensive transactive energy system framework is proposed

for the integration of the aggregated load reduction demand response (DR) such as load curtailment and load shifting, and plug-in electric vehicle (PEV). It is observed that utilizing other distributed energy resources (DERs) including on-site renewable energy (RE) resources and behind-the-meter energy storage (ES) systems can increase the obtained profits from day-ahead electricity markets, and improve interactions of aggregators with retail customers.

DEDICATION

This thesis work is dedicated to love of my life, my wife Mandana who has been a constant source of love, support and encouragement during the challenges of graduate school and life. Also, I dedicate this work to my parents, Sharareh and Behrooz who always offered love and support although I was too many miles away from them. I am very thankful for having them in my life.

ACKNOWLEDGEMENTS

Special thanks must go to my advisor, Dr. Badrul Chowdhury for his support and guidance. He always, dedicated generously his time and vast knowledge whenever I needed him. It was absolutely great opportunity to work under his supervision.

I would also like to thank Dr. Shahab Dehghan for dedicating his time and providing constructive comments.

In addition, a thank you to my committee members: Dr. Valentina Cecchi, Dr. Churlzu Lim, Dr. Robert Cox, and Dr. Babak Parkhideh for their time and valuable comments.

I was supported by the Graduate Assistant Support Plan tuition award from the University of North Carolina at Charlotte Graduate School throughout my graduate studies. I am thankful for the research assistantship provided in Dr. Badrul Chowdhury research group and teaching assistantship provided by the Department of Electrical and Computer Engineering.

TABLE OF CONTENTS

LIST OF FIGURES	x
LIST OF TABLES	xii
CHAPTER 1: INTRODUCTION	1
1.1. Supply-Side Energy Management	1
1.2. Demand-Side Energy Management	4
1.3. Outline and Overview of the Dissertation	7
CHAPTER 2: A CRITICAL REVIEW OF ROBUST SELF-SCHEDULING FOR GENERATION COMPANIES UNDER ELECTRICITY PRICE UNCERTAINTY	10
2.1. Introduction	13
2.1.1. Background and Motivation	13
2.1.2. Contributions	15
2.1.3. Assumptions	16
2.2. Deterministic and Non-Deterministic Self-Scheduling Models	16
2.2.1. Deterministic Self-Scheduling Model	16
2.2.2. Non-deterministic Self-Scheduling Models	18
2.2.3. Construction of Hourly Offer Curve	26
2.2.4. Post-Optimization Procedure	27
2.3. Case Studies	29
2.4. Conclusion	40

CHAPTER 3: The ROLE OF DEMAND RESPONSE AS AN ALTERNATIVE TRANSMISSION EXPANSION SOLUTION IN A CAPACITY MARKET	42
3.1. Introduction	44
3.1.1. Background and Motivation	44
3.1.2. Contributions	45
3.2. PJM Capacity Market	46
3.3. Proposed Integrated Capacity Market and Demand Response Model	48
3.3.1. Capacity Market Model Considering Transmission Upgrade	49
3.3.2. Integrated Capacity Market and Demand Response Model	53
3.4. Case Studies	56
3.4.1. Impact of DR on the Proposed Model	57
3.4.2. Impact of Generation Capacities on the Proposed Model	59
3.4.3. Impact of <i>CETO</i> on the Proposed Model	61
3.5. Conclusion	62
CHAPTER 4: ROBUST TRANSACTIVE ENERGY SYSTEM FRAMEWORK WITH INTEGRATED DEMAND RESPONSE AND DER USING EXTENDED LINEAR DECISION RULES	63
4.1. Introduction	66
4.1.1. Background and Motivation	66
4.1.2. Contributions	68
4.2. Problem Description	69
4.2.1. Deterministic TES Model	69

	ix
4.2.2. ELDR-based Robust TES Framework	73
4.2.3. Mathematical Formulation	75
4.3. Numerical Results	76
4.3.1. Data	76
4.3.2. Evaluation of the Proposed Deterministic TES	77
4.3.3. Evaluation of the Proposed ELDR-based Robust TES	80
4.4. Conclusion	82
CHAPTER 5: CONCLUSIONS	84
5.1. Contributions	85
5.2. Future Work	87
REFERENCES	88
APPENDIX A: The LINEARIZATION OF THE GENERATION COST FUNCTIONS	96
APPENDIX B: THE GENERATOR DATA OF IEEE 30 AND 118-BUS TEST SYSTEMS	97
APPENDIX C:	100
APPENDIX D:	103
APPENDIX E:	104

LIST OF FIGURES

FIGURE 1.1: The three-stage parametric probabilistic forecasting algorithm [6].	2
FIGURE 1.2: Structure of the proposed hybrid decomposition strategy [9].	3
FIGURE 1.3: Demand-side management categories [11].	5
FIGURE 1.4: Overview of the proposed methodology [14].	6
FIGURE 1.5: a) Equivalent circuit of power system with the decentralized active demand response, b) block diagram of frequency system [15].	7
FIGURE 2.1: Schematic of the proposed self-scheduling framework.	28
FIGURE 2.2: Offer curves of unit 39 in hour 10 on January 18 th , April 14 th , and July 7 th .	39
FIGURE 3.1: PJM capacity market (i.e. RPM) structure.	47
FIGURE 3.2: Zonal LDAs.	49
FIGURE 3.3: Global LDAs.	49
FIGURE 3.4: Generation offering and VRR bidding curves.	51
FIGURE 3.5: Total profit of consumers vs. different maximum capacity of DR (P is $P_{c,b}^{DR,max}$).	58
FIGURE 3.6: Total capacity of generation, VRR, upgrade, and DR vs. different maximum capacity of DR.	59
FIGURE 3.7: Total capacity of generation, VRR, and DR vs. different maximum capacity of generation resource.	60
FIGURE 3.8: Capacity market locational marginal price vs. different maximum capacity of generation resource.	60
FIGURE 3.9: Capacity market locational marginal price vs. different $CETO$ values.	62
FIGURE 4.1: TES conceptual diagram.	71

FIGURE 4.2: Total power of load reduction, grid, home, and battery storage. 78

FIGURE 4.3: Total power of load reduction, grid, home, and battery storage. 79

FIGURE C.1: BRO (a.), BERO (b.), and BPRO (c.) uncertainty set for $DR = DR^{\max}$. 102

LIST OF TABLES

TABLE 2.1: Actual profit of deterministic and robust approaches for four months using the IEEE 30-bus test system (\$)	30
TABLE 2.2: Actual profit of deterministic and robust approaches for four months using the IEEE 118-bus test system (\$)	31
TABLE 2.3: Actual profit of RO approaches vs. DR for the IEEE 30-bus test system (\$)	33
TABLE 2.4: Actual profit of RO approaches vs. DR for the IEEE 118-bus test system (\$)	34
TABLE 2.5: Actual profit of robust approaches vs. forecast error for the IEEE 30-bus test system (\$)	35
TABLE 2.6: Actual profit of robust approaches vs. forecast error for the IEEE 118-bus test system (\$)	36
TABLE 2.7: Computation time (s) of the robust approaches on the test case	39
TABLE 2.8: Summary of the self-scheduling strategies for difference real-market-environment cases	40
TABLE 3.1: The capacity market cost, revenue, and costs vs. different maximum capacity of DR (\$/Day)	57
TABLE 4.1: The TES profit vs. different scenarios (\$)	78
TABLE 4.2: The total profit (\$) and computation time (s) of the proposed robust TES model vs. budget of uncertainty	81
TABLE 4.3: The total profit and out-of-sample results	82
TABLE B.1: IEEE 30-bus Generator Data	97
TABLE B.2: IEEE 118-bus Generator Data	97

CHAPTER 1: INTRODUCTION

An energy management system (EMS) is a system designed for owners of generation companies (GenCos), operators of electricity markets and electric utility grids, as well as consumers and aggregators to monitor, control, and optimize the performance of the generation, transmission, and demand systems [1]. The EMS includes supply-side energy management (SSEM) and demand-side energy management (DSEM) systems. GenCo owners and/or grid operators can use SSEM to increase profit, improve system operation, enhance grid reliability, increase grid capacity, and optimize energy usage to reduce cost [2, 3]. The benefits from DSEM are potentially two-fold; first, consumers can reduce their electricity bills by adjusting the timing and amount of electricity use, while providing electric utilities a means to improve customer service. Second, DSEM can provide cost-effective energy and capacity resources to help defer the need for new sources of power, including generating facilities, power purchases, and transmission and distribution capacity additions [4, 5].

In the following sections, supply-side energy management systems including generation and transmission systems are reviewed. Also, demand-side energy management systems and methodologies are reviewed. Finally, the outline and overview of the dissertation will be discussed.

1.1 Supply-Side Energy Management

Owners of generation companies, regardless of whether they are traditional regulated entity, a renewable energy provider, or an independent power producer, can face several challenges, as well as uncertainty in their forecasts (such as price, forced outages, wind energy availability, and so on). Hence, integration and coordination of a more

diverse mix of generations are needed to manage such a complex system with so many constraints.

An offer curve construction process for wind power producers in the day-ahead electricity market is presented in [6]. The algorithm is based on the multivariate distribution of the real-time price and wind power forecasting errors, since the bivariate distribution results in more profitable offers based on the conditional probability of wind power forecasting errors with regard to the RT price forecasting errors. Figure 1.1 illustrates a three-stage parametric probabilistic wind power forecasting algorithm proposed to decrease the standard deviation of the bivariate distribution, and further increase the profitability from the offer curve.

The self-scheduling models for GenCos are presented in [7, 8] in which uncertainties of generating units' forced outage and market price are modeled via stochastic optimization approach. This framework allows the producer to maximize its profit while controlling the risk of profit variability through well-known conditional value-at-risk index.

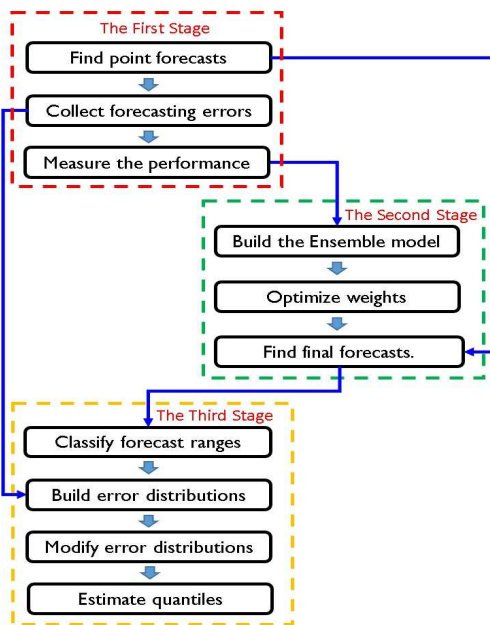


Figure 1.1: The three-stage parametric probabilistic forecasting algorithm [6].

A new stochastic security-constrained hydrothermal unit commitment model for an electricity market operator is proposed in [9], in which the uncertainty of load forecast prediction of inflows to hydro reservoirs and unavailability of units is considered. Also, to obtain more realistic results, an AC network modeling is included in the model. To solve the large-scale and mixed-integer non-linear nature of the model, a new hybrid decomposition strategy composed of generalized Benders decomposition and outer approximation/ equality relaxation (OA/ER) as shown in Figure 1.2 is introduced.

Current models of capacity market designs in the U.S. and elsewhere ignore the important issue of carbon emission produced by electric power plants. While the current designs may produce optimal and efficient capacity market prices, these designs contribute little or nothing to reduce such emissions. In [10], a novel alternative to the current capacity market design which can realistically achieve the noble goal of power system decarbonization is presented. While there are a number of possible design choices, the new design developed in the work explicitly models carbon pricing in the market clearing problem. Using PJM capacity market as a base model, it is shown

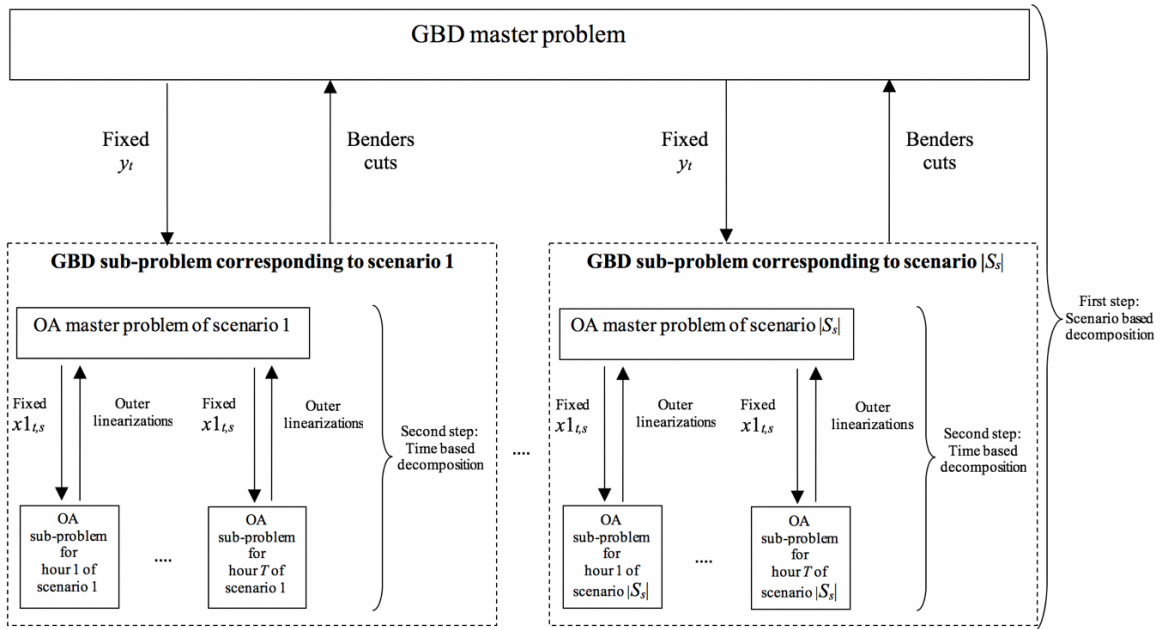


Figure 1.2: Structure of the proposed hybrid decomposition strategy [9].

that the new capacity market design can achieve the decarbonization goal with some reasonable increase of capacity market prices.

1.2 Demand-Side Energy Management

According to Figure 1.3 of North American Electric Reliability Corporation (NERC), DSEM includes two main categories: demand response (DR), and energy efficiency [11]. Based on the U.S. Energy Information Administration (EIA), DSEM does not refer to energy and load-shape changes arising from the normal operation of the marketplace or from government-mandated energy-efficiency standards [4]. The main DSEM category is DR which based on Federal Energy Regulator Commission (FERC), is a reduction in the consumption of electric energy by customers from their expected consumption in response to an increase in the price of electric energy or to incentive payments designed to induce lower consumption of electric energy [12]. DR offers a variety of financial and operational benefits for electricity customers, load-serving entities and grid operators. Power systems have three important characteristics:

1. Due to the fact that electricity cannot be stored economically, electricity supply of and demand must be maintained in balance in real-time.
2. Grid conditions can change significantly from day-to-day, hour-to-hour, and even within moments. Demand levels also can change quite rapidly and unexpectedly, and resulting mismatches in supply and demand can threaten the integrity of the grid over very large areas within seconds.
3. The power system is highly capital-intensive, and generation and transmission system investments have long lead times and multi-decade economic lifetimes.

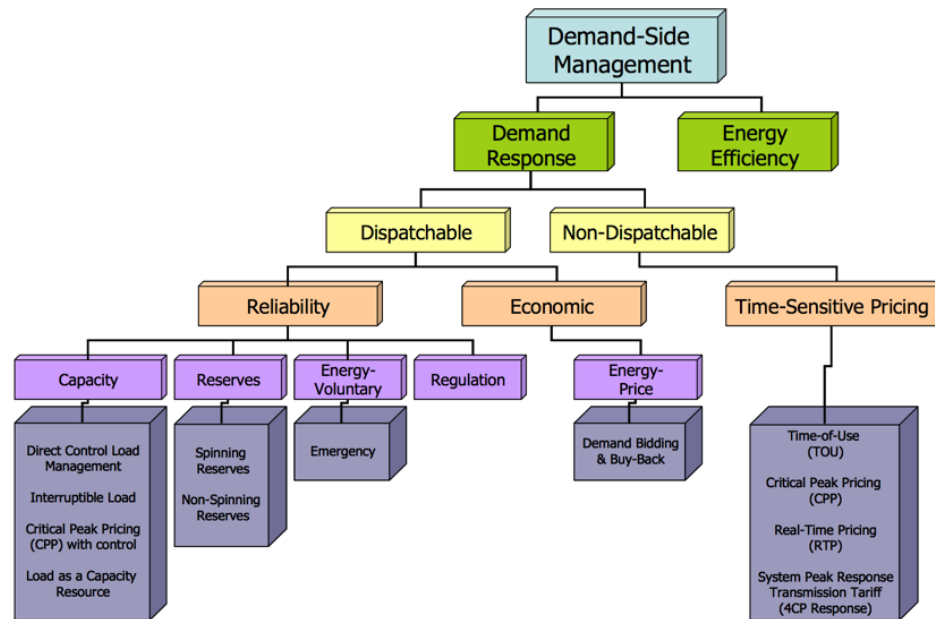


Figure 1.3: Demand-side management categories [11].

These challenges and uncertainties are what make DR so valuable [13].

A two-stage stochastic joint energy and reserve day-ahead market structure incorporating the participation of demand side resources in the provision of load following reserves is presented in [14]. Since a load that incurs a demand reduction may need to recover this energy in other periods, different types of load recovery requirements are modeled. Furthermore, in order to evaluate the risk associated with the decisions of the system operator and to assess the effect of procuring and compensating load reductions, the Conditional Value-at-Risk metric is employed. In order to solve the resulting multi-objective optimization problem, a new approach based on an improved variant of the epsilon-constraint method is adopted. The overview of the proposed methodology is shown in Figure 1.4.

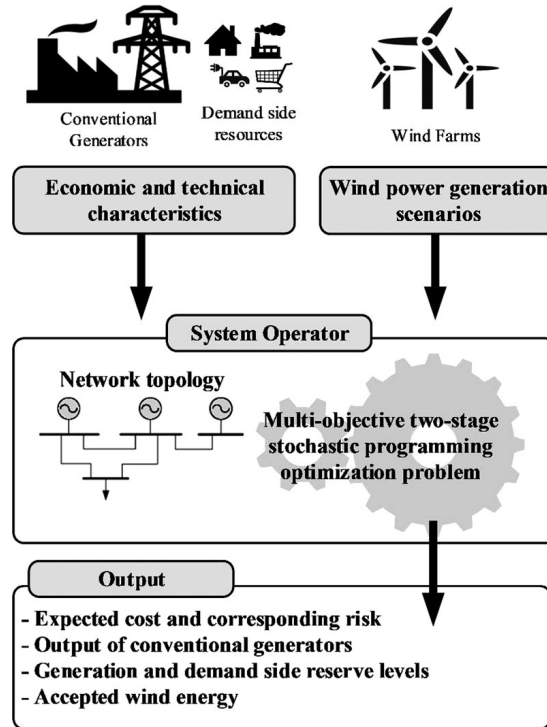


Figure 1.4: Overview of the proposed methodology [14].

A stochastic decentralized active demand response system including a mathematical model of the decentralized active demand response system comprising of functional and technical requirements as well as general principles of decentralized active demand response operation and control algorithm is presented in [15]. Due to the high dynamic response of the system in dealing with disturbance phenomena, the strategy may be used as part of both the primary and the secondary load frequency control in electrical power systems. Fulfillment of all assumed decentralized active demand response system requirements concerning high dynamic, fair share in service as well as minimization of degradation in comfort of use of decentralized active demand response controlled devices were evaluated. Figure 1.5 illustrates the equivalent circuit of the power system with the decentralized active demand response, as well as a block diagram of frequency system.

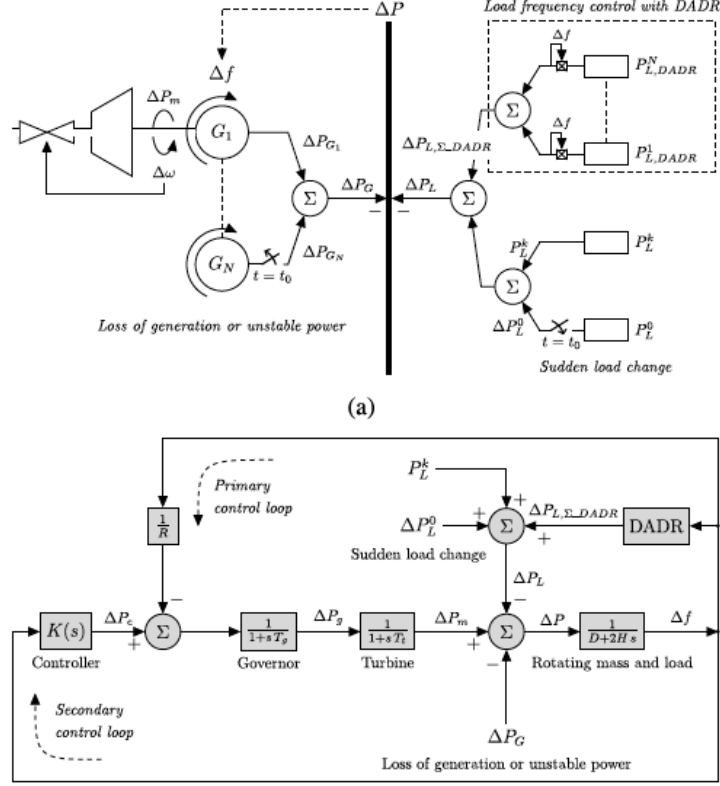


Figure 1.5: a) Equivalent circuit of power system with the decentralized active demand response, b) block diagram of frequency system [15].

1.3 Outline and Overview of the Dissertation

This Ph.D. dissertation is devoted to studying the modeling and optimization of problems associated with generation, transmission, and demand sides of the different electricity markets. It comprise of a comprehensive comparison amongst several robust self-scheduling models of GenCos using real-world electricity market prices, a novel integrated capacity market and demand response model as an alternative solution to the transmission expansion planning problem, and a comprehensive transactive energy system framework for the integration of the aggregated load reduction DR and plug-in electric vehicle (PEV).

For a generation company trading in an electricity market, efficient control of the financial risks and robustness is as vital as maximizing profit. A robust approach is preferred since the generation company can obtain an optimal self-schedule considering

price volatility as a source of uncertainty. In Chapter 2, different robust approaches such as robust optimization methods with different uncertainty sets, conditional value-at-risk based stochastic programming, and information gap decision theory for self-scheduling of generation companies are implemented and compared. Moreover, all robust frameworks are utilized to test systems with different price behaviors in the long-run to illustrate the performance and features of each method. Finally, the different self-scheduling strategies based on the price data and the generation company's desired robustness level are proposed.

DR cannot only be used as an electric power supply resource to produce a megawatt in high power prices or when the reliability of the grid is threatened, but also can be utilized to resolve a transmission expansion planning problem instead of implementing a costly and complex transmission upgrade solution. Essentially, the demand response resources (DRRs) can relieve the capacity requirement for a load area, and thereby relieve the import transmission requirement. In Chapter 3, the role of DRRs as an alternative solution to the required transmission upgrades in the context of a proposed capacity market modeled based on PJM's capacity market model is explored. Results show that the DRRs can indeed replace the needed transmission upgrades.

Increasing the penetration of DR, ES, and PEVs exploits the integration of RE resources and electricity demand, which can lead to addressing resource adequacy, enhancing wholesale electricity market reliability and flexibility, and facilitating customer behavior changes. In Chapter 4, a design of a novel day-ahead transactive energy system (TES) framework is proposed for the integration of the aggregated DR and PEV as well as other DERs including on-site RE resources and behind-the-meter ES systems to enhance demand-side energy management. My methodology not only provides the amount of offered DR, but also determines optimal PEV schedules to increase the profit while considering customers' willingness. DR providers and aggregators can take into account the influence of the customers' willingness on their offers by utilizing

the proposed comfort index. Finally, to derive a tractable optimization problem, while handling the uncertainty of electricity market clearing prices and renewable power generations, the TES framework is reformulated as an affinely adjustable robust model using extended linear decision rules (ELDR). Simulation results on a large-scale case study demonstrate the applicability and effectiveness of the proposed model.

CHAPTER 2: A CRITICAL REVIEW OF ROBUST SELF-SCHEDULING FOR GENERATION COMPANIES UNDER ELECTRICITY PRICE UNCERTAINTY

For a generation company trading in an electricity market, efficient control of the financial risks and robustness is as vital as maximizing profit. A robust approach is preferred since the generation company can obtain an optimal self-schedule considering price volatility as a source of uncertainty. The goal of this chapter of the dissertation is to implement and compare different robust approaches such as robust optimization methods with different uncertainty sets, conditional value-at-risk based stochastic programming, and information gap decision theory for self-scheduling of generation companies. Moreover, all robust methods are applied to test cases with different price behaviors in the long-run to demonstrate the performance and features of each method. Finally, the different self-scheduling strategies based on the price data and the generation company's desired robustness level are proposed.

Nomenclature

A. Functions

$f_u(\cdot)$ Generation cost function of unit u .

B. Parameters

A_u Coefficient of the piecewise linear generation cost function of unit u .

a_u, b_u, c_u Coefficients of the quadratic generation cost function of unit u .

$B_{ut}^{ss'}$ Binary parameter for unit u in hour t , which is zero if $e_{ts} = e_{ts'}$ and one otherwise.

CSC_u Cold startup cost of unit u (\$).

$Diff_t$ Difference between maximum and minimum prices of each price interval

in hour t (\$/MWh).

$Diff_{DP}$	Difference between maximum and minimum deterministic profits of each profit interval (\$).
E_t	Predicted electricity price for hour t (\$/MWh).
E_{ts}	Electricity price of hour t in scenario s (\$/MWh).
\hat{E}_t	Respective range of \tilde{E}_t (\$/MWh).
E_t^{\max}, E_t^{\min}	Upper and lower limit E_t (\$/MWh).
HSC_u	Hot startup cost of unit u (\$).
i, j	Loop counters.
J	Set of uncertain electricity market prices.
$ J $	Number of elements for the uncertainty set J .
MD_u, MU_u	Minimum down and up time of unit u , respectively (h).
N_i	Number of electricity price intervals.
N_j	Number of profit intervals.
N_u^l	Number of blocks of the piecewise linear generation cost function of unit u .
N_s	Number of scenarios.
P_u^l	Upper limit of block l of the piecewise linear generation cost function of unit u (MW).
P_u^{\max}, P_u^{\min}	Upper and lower limit for unit u , respectively (MW).
RD_u, RU_u	Ramp down and ramp up limit of unit u , respectively (MW/h).
S_{lu}	Slope of block l of the piecewise linear generation cost function of unit u .
SDR_u, SUR_u	Shutdown and startup ramp limit of unit u , respectively (MW/h).
$SU_{u\tau}$	Startup cost of unit u after τ hours down time (\$).
T_u^{cold}	Required time to cool down unit u (h).
T	Total hours of the scheduling period.

U	Total number of units.
Ψ_B	Degree of robustness for the box uncertainty set.
Ψ_E	Degree of robustness for the ellipsoidal uncertainty set.
Ψ_P	Degree of robustness for the polyhedral uncertainty set.
λ	A non-negative weight factor that weighs conditional robust profit against expected profit.
Π_s	Probability of scenario s .
α	Per unit confidence level.
σ	Profit deviation factor.

C. Variables

h_t, q_t, v	Continuous auxiliary robust modeling variables.
$m_{ut}^{ss'}$	Non-negative auxiliary variable used for modeling non-decreasing constraints.
p_{ut}	Power offered by unit u in hour t for energy auction; p_{uts} is p_{ut} value in scenario s (MW).
pb_{lut}	Power in block l of the piecewise linear generation cost function of unit u in hour t (MW).
$r_{ut}^{ss'}$	Free auxiliary variable used for modeling non-anticipativity constraints.
u_{ut}^{su}	Startup cost of unit u in hour t (\$).
x_{ut}, y_{ut}	Binary variables indicating startup and shutdown status of unit u in hour t , respectively.
z_{ut}	Binary variable indicating status of unit u in energy auction in hour t (1/0 for accepted/not-accepted).
\tilde{e}_t	Uncertain electricity price in hour t (\$/MWh).
β_s	Continuous auxiliary stochastic modeling variable.
μ	Value-at-risk (VaR).
θ	Uncertainty parameter for information gap decision theory.

2.1 Introduction

2.1.1 Background and Motivation

In a competitive market environment, a generation company (GenCo), as a decision-maker, not only tries to attain a profitable bidding strategy, but also strives to achieve a robust position (i.e. a strategy hedged against any realization of the uncertainty as the difference between the forecasted and actual values). The self-scheduling of a GenCo is a complex and difficult optimization problem, not only due to the need for meeting all equality and inequality constraints of the generating units during the entire scheduling period, such as minimum on/off duration, generation capacity limits, ramping up/down limits of generating units, but also due to all issues affecting electricity market prices and increasing their volatility, such as system load forecasting, predicting rival GenCos' bidding strategies, and transmission congestion. In other words, electricity market prices and their volatility are the key factors complicating the self-scheduling problem of a GenCo. The price signal forces the on/off status of a generation unit and its volatility significantly affects the self-scheduling problem of a GenCo. Since the forecasted electricity market prices are subject to uncertainty due to their high volatility [16], it is necessary to characterize the uncertainty of the forecasted electricity market prices aiming at hedging the self-schedules of GenCos against different realizations of uncertain electricity market prices. In other words, a GenCo should adopt optimization methods considering uncertainty for its self-scheduling approach. This has led to a growth in non-deterministic self-scheduling methods. These methods include robust optimization (RO) with different uncertainty sets [17, 18, 19, 20], conditional value-at-risk based stochastic programming (CVaR-SP) [21, 22], and information gap decision theory (IGDT) [23, 24].

The RO methodology models uncertainty sets as bounded intervals, such as box, ellipsoidal, and polyhedral uncertainty sets [25]. The ellipsoidal uncertainty set has

been applied to the self-scheduling problem leading to a second-order cone model in [17]. An ellipsoidal RO method has also been used in [18] to determine the worst-case robust profit of the self-scheduling problem. Besides, there is some research work concentrated on the combination of the uncertainty sets with each other. The combination of the box and polyhedral uncertainty sets for RO as a linear optimization framework has been presented in [26]. Moreover, this combined uncertainty set has been used to construct the offer curve of a generation company in [19]. The RO approach presented in [26] has been implemented to construct the bidding strategy of a wind farm and energy storage devices in [20]. In addition, the combined box and ellipsoidal uncertainty set for RO has been introduced in [27]. In RO methods including various uncertainty sets, a decision-maker can change the robustness of the solution by changing a specific parameter named the degree of robustness (DR).

The stochastic programming (SP) approach uses scenarios to model uncertainty sources [28]. In this method, the scenarios are generated by using the probability distribution function (PDF) of uncertain variables. Also, to model the financial risk, conditional value-at-risk (CVaR) index has been used in the stochastic framework [29]. The CVaR-SP has been applied to the weekly self-scheduling and offering problem of a GenCo in [5]. In this model, a forward contract is considered as the first-stage of the CVaR-SP framework and pool market as the second-stage. The CVaR-SP method has also been used to model the day-ahead self-scheduling of a GenCo for multi-auction markets in [22]. The presented methodology simultaneously models two uncertainty sources of electricity market prices and unavailability of units. In both models, the producer, who is the decision-maker, can adjust the financial risk of the framework and switch from risk-averse to risk-seeker GenCo and vice versa, only by changing the weight factor of the CVaR index. In other words, CVaR-SP has the capability to control the robustness of the solution.

The information gap decision theory (IGDT) expounds that the decisions made

under severe uncertainty should not require more information than what is dependably provided by the decision-maker [30]. Moreover, the IGDT obtains optimal values of the uncertain variables with a guarantee that the objective function (OF) does not become worse than a definite threshold. In [23], the IGDT has been used to model non-deterministic self-scheduling problem considering electricity price uncertainty. The IGDT has been applied to the bidding strategy problem of a GenCo in which demand response is also modeled [24]. Note that the IGDT, like the RO approaches and CVaR-SP, can control the robustness of the problem by changing the horizon of uncertain variables.

2.1.2 Contributions

The main contributions of this chapter of the dissertation are:

1. The mathematical formulations of different robust approaches including Box RO (BRO), Ellipsoidal RO (ERO), Polyhedral RO (PRO), Box and Ellipsoidal RO (BERO), Box and Polyhedral RO (BPRO), CVaR-SP, and IGDT models are proposed. Also, the characteristics of the uncertainty sets corresponding to BRO, ERO, PRO, BERO, and BPRO are presented by means of relevant theorems and proofs. Previous research work in this area have either only used these approaches [17, 18, 19, 20, 21, 22, 23, 24] or compared these methods without any mathematical proof [31]. Accordingly, to the best of my knowledge, there is no existing research work that mathematically characterizes the robust approaches.
2. Various self-scheduling strategies based on the robust approaches are proposed for GenCos to participate in an electricity market considering the price data and desired robustness level.
3. To correctly analyze and compare the performance of these robust methodologies in the uncertain environment of self-scheduling, a post-optimization procedure

is proposed. This procedure evaluates the long-run performance of the robust methodologies encountering different realizations of uncertain electricity prices.

2.1.3 Assumptions

For simplicity and better illustration of the underlying ideas of the robust approaches in the self-scheduling models presented in this chapter of the dissertation, the following assumptions are made:

1. The GenCo is a price taker, in which the GenCo must accept prevailing prices (i.e. market clearing prices) in a market without the capability of changing it.
2. Only the uncertainty source of electricity price is considered. Based on [16], “in a power market, the price of electricity is the most important signal to all market participants.”
3. Only energy auction is taken into account.
4. Shutdown costs of units are neglected.

These assumptions are in line with many other self-scheduling research work such as [16, 17, 18, 19, 20, 21, 22, 32, 33].

2.2 Deterministic and Non-Deterministic Self-Scheduling Models

2.2.1 Deterministic Self-Scheduling Model

The deterministic self-scheduling model based on the mentioned assumptions can be formulated as a mixed-integer linear programming (MILP) problem given in (2.1)-(2.9) [34]:

$$\max_{\Omega} \left[\underbrace{\sum_{t=1}^T \sum_{u=1}^U (E_t \cdot p_{ut}) - \sum_{t=1}^T \sum_{u=1}^U u_{ut}^{su} - \sum_{t=1}^T \sum_{u=1}^U f_u(p_{ut})}_{DT} \right] \quad (2.1)$$

s.t.

$$u_{ut}^{su} \geq SU_{u\tau} \cdot (z_{ut} - \sum_{n=1}^{\tau} z_{u(t-n)}) \quad u_{ut}^{su} \geq 0 \quad \forall u, \forall t | \tau = 1, \dots, t \quad (2.2)$$

$$SU_{u\tau} = \begin{cases} CSC_u & \text{if } \tau > T_u^{cold} + MD_u \\ HSC_u & \text{if } \tau \leq T_u^{cold} + MD_u \end{cases} \quad \forall u \quad (2.3)$$

$$\sum_{n=t-MU_u+1}^t x_{un} \leq z_{ut} \quad \forall u, \forall t \quad (2.4)$$

$$z_{ut} + \sum_{n=t-MD_u+1}^t y_{un} \leq 1 \quad \forall u, \forall t \quad (2.5)$$

$$z_{u(t-1)} - z_{ut} + x_{ut} - y_{ut} = 0 \quad \forall u, \forall t \quad (2.6)$$

$$P_u^{\min} \cdot z_{ut} \leq p_{ut} \leq P_u^{\max} \cdot z_{ut} \quad \forall u, \forall t \quad (2.7)$$

$$p_{ut} \leq p_{u(t-1)} + RU_u \cdot z_{u(t-1)} + SUR_u \cdot x_{ut} \quad \forall u, \forall t \quad (2.8)$$

$$p_{u(t-1)} \leq p_{ut} + RD_u \cdot z_{ut} + SDR_u \cdot y_{u,t} \quad \forall u, \forall t \quad (2.9)$$

In (2.1), Ω includes the decision variables of the self-scheduling model: $\Omega = \{p_{ut}, z_{ut}, x_{ut}, y_{ut}\}$, $\forall u, \forall t$. The first, second and third terms of (2.1), denoted by DT , indicate revenue from selling energy, startup cost and operation cost of GenCo, respectively. The objective function of (2.1) represents profit of GenCo in the energy auction. The generation cost functions of $f_u(\cdot)$ are linearized by the piecewise linear approximation of [35], which is given in Appendix A. Constraints (2.2) and (2.3) model startup costs of units including the costs of hot and cold starts. Minimum up and down time limits of units are modeled in (2.4)-(2.6) based on three-binary variable formulation (including x_{ut} , y_{ut} , and z_{ut}), which is more effective than conventional one-binary variable formulation [32]. Unit generation limits are represented in (2.7). Ramp up and down rate limits of units considering startup and shutdown ramps are given in

(2.8)-(2.9).

2.2.2 Non-deterministic Self-Scheduling Models

To model electricity price uncertainty in the self-scheduling framework, various non-deterministic approaches comprising BRO, ERO, PRO, BERO, BPRO, CVaR-SP, and IGDT are proposed. These approaches provide robust solutions against the uncertainty source with the capability of modeling the solution robustness. Details of each non-deterministic self-scheduling model are presented in the following.

2.2.2.1 BRO-based Self-Scheduling Model

In this approach, the uncertainty source is modeled using infinite-norm as a box uncertainty set (BS):

$$BS = \left\{ \tilde{e}_j \in [E_j - \hat{E}_j, E_j + \hat{E}_j] \forall j \in J : \left\| \frac{\tilde{e} - E}{\hat{E}} \right\|_{\infty} \leq \Psi_B \right\} \quad (2.10)$$

where $\left\| \frac{\tilde{e} - E}{\hat{E}} \right\|_{\infty} = \max \left\{ \left| \frac{\tilde{e}_1 - E_1}{\hat{E}_1} \right|, \left| \frac{\tilde{e}_2 - E_2}{\hat{E}_2} \right|, \dots, \left| \frac{\tilde{e}_{|J|} - E_{|J|}}{\hat{E}_{|J|}} \right| \right\}$.

In my self-scheduling model, $j = t$ and $|J| = T$, thus:

$$BS = \left\{ \tilde{e}_t \in [E_t - \hat{E}_t, E_t + \hat{E}_t] \forall t : \left| \frac{\tilde{e}_t - E_t}{\hat{E}_t} \right| \leq \Psi_B \forall t \right\} \quad (2.11)$$

The same value of box DR, i.e. the same value of $\Psi_B \in [0, 1]$, is adopted for all uncertain electricity prices to control the size of BS . DR in RO approaches gives the decision-maker the capability of changing the robustness of the RO solution.

To construct the BRO-based robust counterpart of the deterministic self-scheduling

model (2.1)-(2.9), only (2.1) is changed since only (2.1) includes the uncertain variables:

$$\begin{aligned} \max_{\Omega} \min_{\tilde{e}_t \in BS} & \left[\sum_{t=1}^T \sum_{u=1}^U (\tilde{e}_t \cdot p_{ut}) - \sum_{t=1}^T \sum_{u=1}^U u_{ut}^{su} \right. \\ & \left. - \sum_{t=1}^T \sum_{u=1}^U f_u(p_{ut}) \right], \quad \text{s.t. (2.2) - (2.9)} \end{aligned} \quad (2.12)$$

Considering BS given in (2.11), the bi-level optimization problem of (2.12) can be reformulated as the single-level optimization problem of (2.13) [25]:

$$\max \left[DT - \Psi_B \cdot \sum_{t=1}^T \sum_{u=1}^U \left(\hat{E}_t \cdot p_{ut} \right) \right], \quad \text{s.t. (2.2) - (2.9)} \quad (2.13)$$

where DT is as given in (2.1). The BRO-based self-scheduling model of (2.13) has MILP form.

2.2.2.2 ERO-based Self-Scheduling Model

Through ERO, the ellipsoidal uncertainty set of electricity market prices, i.e. ES , is modeled using Euclidean norm (2-norm) as given below:

$$ES = \left\{ \tilde{e}_j \in [E_j - \hat{E}_j, E_j + \hat{E}_j] \quad \forall j \in J : \left\| \frac{\tilde{e} - E}{\hat{E}} \right\|_2 \leq \Psi_E \right\} \quad (2.14)$$

$$\text{where } \left\| \frac{\tilde{e} - E}{\hat{E}} \right\|_2 = \sqrt{\left[\frac{\tilde{e} - E}{\hat{E}} \right] \cdot \left[\frac{\tilde{e} - E}{\hat{E}} \right]} = \sqrt{\sum_{j=1}^{|J|} \left[\frac{\tilde{e}_j - E_j}{\hat{E}_j} \right]^2}.$$

Hence,

$$ES = \left\{ \tilde{e}_t \in [E_t - \hat{E}_t, E_t + \hat{E}_t] \quad \forall t : \sqrt{\sum_{t=1}^T \left[\frac{\tilde{e}_t - E_t}{\hat{E}_t} \right]^2} \leq \Psi_E \right\} \quad (2.15)$$

In the *ERO* approach, the ellipsoidal DR of $\Psi_E \in [0, \sqrt{|J|}]$ (i.e., $[0, \sqrt{T}]$) controls the solution robustness. The robust counterpart of the ERO approach can be obtained

from (2.12) by changing the argument of the 'min' operator from $\tilde{e}_t \in BS$ to $\tilde{e}_t \in ES$. Subsequently, the ERO-based robust counterpart can be constructed as follows [25]:

$$\max \left[DT - \Psi_E \cdot \sqrt{\sum_{t=1}^T \left([\widehat{E}_t]^2 \cdot \left[\sum_{u=1}^U p_{ut} \right]^2 \right)} \right], \text{ s.t. (2.2) - (2.9)} \quad (2.16)$$

where DT is as given in (2.1). The ERO-based non-deterministic self-scheduling model of (2.16), which is a mixed-integer second-order cone programming (MISOCP) model with convex (hull) [36], is solved as a mixed-integer quadratic constrained programming (MIQCP) problem [37].

2.2.2.3 PRO-based Self-Scheduling Model

PRO uses 1-norm to formulate the polyhedral uncertainty set PS of electricity market prices as given in (2.17):

$$PS = \left\{ \tilde{e}_j \in [E_j - \widehat{E}_j, E_j + \widehat{E}_j] \quad \forall j \in J : \left\| \frac{\tilde{e} - E}{\widehat{E}} \right\|_1 \leq \Psi_P \right\} \quad (2.17)$$

where $\left\| \frac{\tilde{e} - E}{\widehat{E}} \right\|_1 = \left| \frac{\tilde{e}_1 - E_1}{\widehat{E}_1} \right| + \left| \frac{\tilde{e}_2 - E_2}{\widehat{E}_2} \right| + \dots + \left| \frac{\tilde{e}_{|J|} - E_{|J|}}{\widehat{E}_{|J|}} \right|$, therefore

$$PS = \left\{ \tilde{e}_t \in [E_t - \widehat{E}_t, E_t + \widehat{E}_t] \quad \forall t : \sum_{t=1}^T \left| \frac{\tilde{e}_t - E_t}{\widehat{E}_t} \right| \leq \Psi_P \right\} \quad (2.18)$$

The polyhedral DR of $\Psi_P \in [0, |J|]$ (i.e. $[0, T]$) is used to control the solution robustness. Considering PS instead of BS in (2.12), the following PRO-based robust counterpart can be obtained [25]:

$$\max [DT - (\Psi_P \cdot v)] \quad (2.19)$$

$$\text{s.t.} \quad v \geq \widehat{E}_t \cdot \sum_{u=1}^U p_{ut} \quad v \geq 0, \quad \forall t, \quad (2.2) - (2.9) \quad (2.20)$$

where DT is as given in (2.1). The PRO-based self-scheduling model of (2.19)-(2.20) has MILP form.

The last term within the brackets of (2.13), (2.16) and (2.19) represents the protection functions (PFs). By changing box DR, ellipsoidal DR, and polyhedral DR (i.e. Ψ_B , Ψ_E , and Ψ_P), the magnitude of the PF and so the solution robustness of the BRO-based, ERO-based, and PRO-based non-deterministic self-scheduling models, respectively, can be adjusted.

2.2.2.4 BERO-based Self-Scheduling Model

BERO employs the intersection of box and ellipsoidal uncertainty sets, denoted by BES , presented in (2.21):

$$BES = BS \cap ES = \left\{ \tilde{e}_t \in [E_t - \hat{E}_t, E_t + \hat{E}_t] \quad \forall t : \right. \\ \left. \left| \frac{\tilde{e}_t - E_t}{\hat{E}_t} \right| \leq \Psi_B \quad \forall t, \quad \sqrt{\sum_{t=1}^T \left[\frac{\tilde{e}_t - E_t}{\hat{E}_t} \right]^2} \leq \Psi_E \right\} \quad (2.21)$$

As shown in [38], the following property for infinite-norm and 2-norm of the n -dimensional vector X holds:

$$|X|_\infty \leq |X|_2 \leq \sqrt{n} \cdot |X|_\infty \quad (2.22)$$

Similarly, for the uncertain electricity market prices during the scheduling period (i.e., \tilde{e}_t for $t = 1, \dots, T$), it can be concluded that:

$$\left\| \frac{\tilde{e} - E}{\hat{E}} \right\|_\infty \leq \left\| \frac{\tilde{e} - E}{\hat{E}} \right\|_2 \leq \sqrt{T} \cdot \left\| \frac{\tilde{e} - E}{\hat{E}} \right\|_\infty \quad (2.23)$$

Also, $\left\| \frac{\tilde{e} - E}{\hat{E}} \right\|_\infty \leq \Psi_B$ and $\left\| \frac{\tilde{e} - E}{\hat{E}} \right\|_2 \leq \Psi_E$, as shown in (2.21). Accordingly, in the proposed BERO model, $\Psi_E \in [\Psi_B, \Psi_B \cdot \sqrt{T}]$ where $\Psi_B \in [0, 1]$.

The robust counterpart of BERO method, presented in (2.24)-(2.25), is obtained by replacing BS with $BS \cap ES$ in (2.12). The last two terms of (2.24) are the combination of the last terms of (2.13) and (2.16); (2.25) presents the relationship among power

and auxiliary variables of the PFs of BERO [27]. The BERO model of (2.24)-(2.25) is an MISOCP problem with convex (hull) [36], which is solved as an MIQCP [37].

$$\max \left[DT - \left(\Psi_B \cdot \sum_{t=1}^T h_t \right) - \left(\Psi_E \cdot \sqrt{\sum_{t=1}^T (q_t)^2} \right) \right] \quad (2.24)$$

$$\text{s.t.} \quad h_t + q_t \geq \widehat{E}_t \cdot \sum_{u=1}^U p_{ut} \quad h_t \geq 0, q_t \geq 0, \forall t, \quad (2.2) - (2.9) \quad (2.25)$$

where DT is as given in (2.1).

2.2.2.5 BPRO-based Self-Scheduling Model

The intersection of box and polyhedral uncertainty sets, denoted as BPS , is used in BPRO approach [26]:

$$\begin{aligned} BPS = BS \cap PS = \left\{ \tilde{e}_t \in \left[E_t - \widehat{E}_t, E_t + \widehat{E}_t \right] \quad \forall t : \right. \\ \left. \left| \frac{\tilde{e}_t - E_t}{\widehat{E}_t} \right| \leq \Psi_B \quad \forall t, \quad \sum_{t=1}^T \left| \frac{\tilde{e}_t - E_t}{\widehat{E}_t} \right| \leq \Psi_P \right\} \end{aligned} \quad (2.26)$$

where similar to the DRs of BERO in Subsection 2.2.2.4, it can be shown that the DRs should satisfy $\Psi_B \in [0, 1]$ and $\Psi_P \in [\Psi_B, \Psi_B \cdot T]$. The robust counterpart of BPRO approach is given in (2.27)-(2.28), which is an MILP problem [26]:

$$\max \left[DT - (\Psi_P \cdot v) - \left(\Psi_B \cdot \sum_{t=1}^T h_t \right) \right] \quad (2.27)$$

$$\text{s.t.} \quad v + h_t \geq \widehat{E}_t \cdot \sum_{u=1}^U p_{ut} \quad v \geq 0, h_t \geq 0 \quad \forall t, \quad (2.2) - (2.9) \quad (2.28)$$

where DT is as given in (2.1).

2.2.2.6 Stochastic Programming-based Self-Scheduling Model

The stochastic programming framework models uncertain variables by considering their various likely realizations known as scenarios. Here, two-stage CVaR-based

stochastic programming (CVaR-SP) approach is used to model non-deterministic self-scheduling problem. Within this approach, which is given in (2.29)-(2.35), the first-stage including commitment decision variables, and the second-stage comprising dispatch decision variables are scenario independent/dependent, respectively:

$$\begin{aligned} \max & \left[(1 + \lambda) \left\{ \sum_{s=1}^{N_s} \Pi_s \left(\sum_{t=1}^T \sum_{u=1}^U (E_{ts} \cdot p_{uts}) \right. \right. \right. \\ & \left. \left. - \sum_{t=1}^T \sum_{u=1}^U f_u(p_{uts}) \right) - \sum_{t=1}^T \sum_{u=1}^U u_{ut}^{su} \right\} \\ & \left. - \lambda \left(\mu + \frac{1}{1 - \alpha} \sum_{s=1}^{N_s} \Pi_s \beta_s \right) \right] \end{aligned} \quad (2.29)$$

s.t. (2.2)-(2.6)

$$P_u^{\min} \cdot z_{ut} \leq p_{uts} \leq P_u^{\max} \cdot z_{ut} \quad \forall u, \forall t, \forall s \quad (2.30)$$

$$p_{uts} \leq p_{u(t-1)s} + RU_u \cdot z_{u(t-1)} + SUR_u \cdot x_{ut} \quad \forall u, \forall t, \forall s \quad (2.31)$$

$$p_{u(t-1)s} \leq p_{uts} + RD_u \cdot z_{ut} + SDR_u \cdot y_{ut} \quad \forall u, \forall t, \forall s \quad (2.32)$$

$$(p_{uts} - p_{uts'}) \geq m_{ut}^{ss'} \cdot (E_{ts} - E_{ts'}) \quad \forall u, \forall t, \forall s, s' \quad (2.33)$$

$$(p_{uts} - p_{uts'}) = r_{ut}^{ss'} \cdot \sum_{n=1}^t B_{un}^{ss'} \quad \forall u, \forall t, \forall s, s' \quad (2.34)$$

$$\begin{aligned} \beta_s \geq & \sum_{s'=1}^{N_s} \pi_{s'} \left[\sum_{t=1}^T \sum_{u=1}^U (E_{ts'} \cdot p_{uts'}) - \sum_{t=1}^T \sum_{u=1}^U f_u(p_{uts'}) \right] \\ & - \left[\sum_{t=1}^T \sum_{u=1}^U (E_{ts} \cdot p_{uts}) - \sum_{t=1}^T \sum_{u=1}^U f_u(p_{uts}) \right] - \mu \quad \beta_s \geq 0 \quad \forall s \end{aligned} \quad (2.35)$$

The compact form of (2.29) is $\max [(1 + \lambda).EP - \lambda.CVaR]$ obtained from $\max [EP + \lambda.CRP]$ where EP is the expected profit, CRP is the conditional robust profit, and λ is a weight factor to model the financial risk of the self-scheduling problem. Higher/lower values of λ lead to more risk-averse/risk-seeker models. In this stochastic approach, the constraints (2.2)-(2.6) of the deterministic model are directly applied, while the

scenario-based version of the constraints (2.7)-(2.9), in the form of (2.30)-(2.32), is considered. Constraints (2.33) and (2.34) present non-decreasing and non-anticipativity constraints, respectively, which are essential to obtain reasonable solution in the SP model. In non-decreasing constraint (2.33), the non-negative auxiliary variable $m_{ut}^{ss'}$ is used to ensure that p_{uts} is more than $p_{uts'}$ if E_{ts} is more than $E_{ts'}$. In non-anticipativity constraint (2.34), the binary parameter $B_{un}^{ss'}$ is 0, if the realization of the uncertain price variables in hour t are the same in two scenarios s and s' , otherwise 1. The free auxiliary variable $r_{ut}^{ss'}$ is used to ensure that p_{uts} and $p_{uts'}$ can take any value if $\sum_{n=1}^t B_{un}^{ss'} = 0$, otherwise $p_{uts} = p_{uts'}$ [22]. The CVaR constraint of the model is shown in (2.35). For the mathematical details of this approach, the interested reader can refer to [22]. The CVaR-SP model of (2.29)-(2.35) has MILP form.

2.2.2.7 IGDT-based Self-Scheduling Model

The IGDT focuses on decision making under severe uncertainty. Under severe lack of information, uncertainty is considered as the gap between what is known (historical data) and what needs to be known (actual data) to make competent decisions [30]. There are different IGDT models such as Energy-bound, Minkowski-norm, Slope-bound, Fourier-bound, Hybrid info-gap, and so forth, which are quadratic or non-linear [30]. Since the envelope-bound model is a proficient linear and convex approach to characterize the forecast uncertainties [30], in line with previous research work in the power system area [23, 24, 39, 40, 41, 42], this uncertainty model is used in this chapter of the dissertation instead of other non-linear and non-convex ones to characterize the forecast uncertainties of electricity prices in the self-scheduling problem of GenCos. The uncertainty set of envelope-bound-based IGDT, denoted by IS , is as follows:

$$IS = \left\{ \tilde{e}_t : \left| \frac{\tilde{e}_t - E_t}{E_t} \right| \leq \theta \quad \forall t \right\} \quad (2.36)$$

The IGDT includes robust and opportunistic approaches to quantify pernicious and propitious variations of uncertain variables by means of robustness and opportuneness immunity functions [30]. The robust approach in the self-scheduling problem of GenCos focuses on pernicious variations of uncertain electricity prices on the profit (i.e. the realized electricity prices are lower than their forecasted values) and finds the greatest variations of the uncertain electricity prices when the minimum profit is not lower than a critical value (with guarantee). The opportunistic approach in the self-scheduling problem of GenCos focuses on propitious variations of uncertain electricity prices on the profit (i.e. the realized electricity prices are higher than their forecasted values) and finds the lowest variations of the uncertain electricity prices when the maximum profit is higher than a target value (but without guarantee). This research focuses on the robust approach of IGDT, which a risk-averse decision-maker desires to use.

The generic form of robust approach is as follows:

$$\max \theta \tag{2.37}$$

s.t. minimum requirements are always satisfied

Thus, the robust IGDT model of the self-scheduling problem becomes as follows:

$$\begin{aligned} & \text{s.t.} \quad \sum_{t=1}^T \sum_{u=1}^U [(1 - \theta) E_t \cdot p_{ut}] - \sum_{t=1}^T \sum_{u=1}^U u_{ut}^{su} \\ & \quad - \sum_{t=1}^T \sum_{u=1}^U f_u(p_{ut}) \geq (1 - \sigma) \cdot DP, \quad (2.2)-(2.9) \end{aligned} \tag{2.38}$$

where DP is the deterministic profit obtained from (2.1)-(2.9). The IGDT model has a mixed-integer non-linear programming (MINLP) form.

2.2.3 Construction of Hourly Offer Curve

The construction of hourly offer curve is designed based on the price forecast confidence intervals, since confidence intervals for price forecasts can capture price volatility better than point price forecasts [43]. Then, the GenCos can efficaciously control the profit volatility. For the sake of fair comparisons, the same historical prices are used to find E_t^{\min} and E_t^{\max} of the confidence intervals for all non-deterministic self-scheduling models presented in the previous section.

2.2.3.1 RO-based Hourly Offer Curve for Models 1-5

1. Set initial values: $i = 0$, $E_t = E_t^{\max} \forall t$, $DR = DR^{\max}$. The highest DR is considered, since price forecast error typically occurs in all hours of a day [19, 44, 45].
2. Set $Diff_t = (E_t^{\max} - E_t^{\min})/N_i \forall t$.
3. Based on the models 1-5, solve the robust optimization approaches for the interval:

$$E_t \in [E_t^{\max} - i \times Diff_t, E_t^{\max}] \forall t$$
 [19, 33].
4. $i = i + 1$, if $i < N_i$, go to Step 3, otherwise the offer curve is obtained.

2.2.3.2 SP-based Hourly Offer Curve for Model 6

1. Set $Diff_t = (E_t^{\max} - E_t^{\min})/N_s \forall t$ and $\Pi_s = 1/N_s$ [46, 47].
2. Set $E_{ts} = E_t^{\max} - s \times Diff_t \forall t, \forall s \in N_s$.
3. Solve the CVaR-SP model of (2.29)-(2.35) by means of $E_{ts} \forall t, \forall s \in N_s$.

2.2.3.3 IGDT-based Hourly Offer Curve for Model 7

1. Set $j = 0$, $E_t = E_t^{\max} \forall t$, also obtain DP^{\max} and DP^{\min} as deterministic profit for E_t^{\max} and E_t^{\min} , respectively.

2. Set $Diff_{DP} = (DP^{\max} - DP^{\min}) / N_j$.
3. $DP = DP^{\max}$ and $\sigma_j = (j \times Diff_{DP}) / DP^{\max}$.
4. Solve the IGDT model of (2.37)-(2.38) for σ_j .
5. $j = j + 1$, if $j < N_j$, go to Step 3, otherwise the offer curve is obtained.

2.2.4 Post-Optimization Procedure

To correctly and practically assess the efficiency of the non-deterministic self-scheduling approaches, their performance should be evaluated in the real market environment, i.e. with the realized market prices. To address this issue, a post-optimization procedure (POP) is proposed in this chapter of the dissertation to determine the actual profit of each approach in different real-market-environment cases. After constructing the hourly offer curve of every method, the real clearing prices are used in the POP to determine the actual profit associated with each offer curve. For every hourly offer curve, the real clearing price of the market determines the accepted power from the GenCo, and thereby its profit for that hour.

For clarity, the schematic of the proposed self-scheduling framework including pre-optimization, optimization, and post-optimization procedures, is illustrated in Figure 2.1.

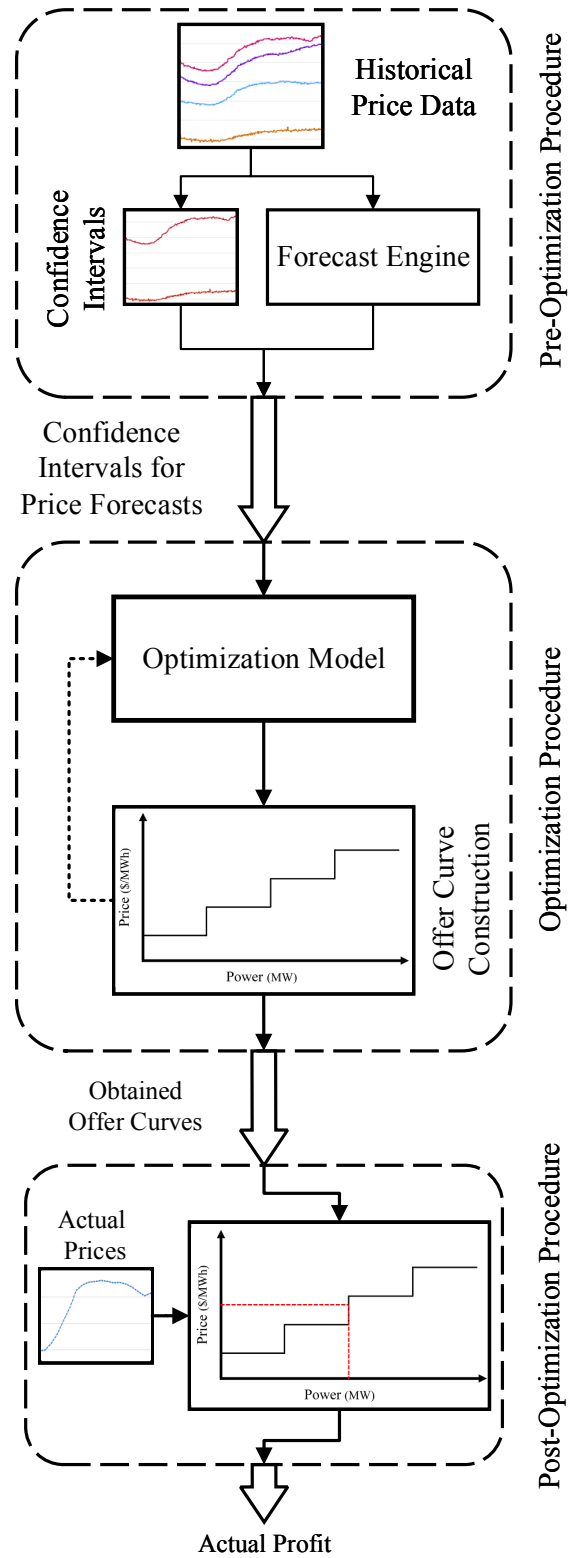


Figure 2.1: Schematic of the proposed self-scheduling framework.

2.3 Case Studies

In this section, all non-deterministic self-scheduling methods discussed in the previous section are implemented on the IEEE 30-bus [48] and IEEE 118-bus test systems [49] (the generator data for two test systems is presented in Appendix B). It is assumed the GenCo has 6, and 54 thermal generating units in the first and second test systems, respectively, and that the data obtained from [48, 49] pertains to these units. Real price data for four months, including January, April, July, and October of the years 2010 to 2013 in the electricity market of New York Independent System Operator (NYISO) [50] is used as the historical data to determine the interval $[E_t^{\min}, E_t^{\max}]$. Additionally, the real price data of these four months of the year 2014 in NYISO electricity market is used as the clearing price for the offer curves. Thus, the test period, i.e. the four months of the year 2014, is different from the setup period. Accordingly, the performance of each non-deterministic self-scheduling method is evaluated by the out-of-sample data. For each hour of the test period, i.e. the four months of the year 2014, the obtained interval $[E_t^{\min}, E_t^{\max}]$ is shifted such that its mean value becomes the price forecast of that hour [16]. Every non-deterministic self-scheduling model uses the shifted price interval to construct its hourly offer curve as described in the previous section. Moreover, $N_i = 100$, $N_s = 100$, $N_j = 100$ are considered for RO approaches, CVaR-SP model and IGDT method, respectively. In line with previous research work in the area, such as [19], N_i is considered equal to 100. And for the sake of fair comparisons, N_j and N_s are also considered equal to 100. In this case, the offer curves of all robust approaches would have 100 blocks. In CVaR-SP model, $\alpha = 0.99$ and $\lambda = 100$ are adopted [21, 22]. All numerical experiments of this chapter of the dissertation have been performed by CPLEX solver (for MILP and MISOCP models) and BARON solver (for MINLP models) in GAMS environment [51] on a 64-bit Windows-based server with 60 GB of RAM and 24 Intel Xeon processors clocking at 3.33 GHz.

It is assumed in the RO models, $DR = DR^{\max}$ in the numerical experiments of this section based on the reason described in the previous section.

Tables 2.1 and 2.2 present the POP results of the deterministic and robust approaches for the four months of the year 2014 in NYISO. In January, July, and October there are 744 (24×31), and in April there are 720 (24×30) hourly offer curves. It is seen that for $DR = DR^{\max}$ the profits of BRO, BERO, and BPRO become the same (the proof is provided in Appendix C). Moreover, for the same DR, ERO is less conservative than PRO and BRO is less conservative than ERO (the proof is provided in Appendix D). In each column of Tables 2.1 and 2.2, the bolded value expresses the maximum profit among all discussed methods and the related technique is indicated in the last row.

Table 2.1: Actual profit of deterministic and robust approaches for four months using the IEEE 30-bus test system (\$)

App.	DR^{\max}	$0.75 \times DR^{\max}$	$0.50 \times DR^{\max}$	$0.25 \times DR^{\max}$
Deterministic	51,089,643	10,685,023	4,046,865	3,287,281
BRO	52,708,930	11,529,019	4,308,318	3,400,501
ERO	51,822,839	10,765,150	4,224,054	3,381,691
PRO	50,705,777	10,430,887	3,957,208	3,271,716
BERO	52,708,930	11,529,019	4,308,318	3,400,501
BPRO	52,708,930	11,529,019	4,308,318	3,400,501
CVaR-SP	60,425,869	10,625,768	4,130,990	3,367,875
IGDT	44,342,860,	9,743,124	3,187,930	2,783,550
Selected	CVaR-SP	BRO/BERO BPRO	BRO/BERO BPRO	BRO/BERO BPRO

Table 2.2: Actual profit of deterministic and robust approaches for four months using the IEEE 118-bus test system (\$)

App.	DR^{Max}	$0.75 \times DR^{\text{Max}}$	$0.50 \times DR^{\text{Max}}$	$0.25 \times DR^{\text{Max}}$
Deterministic	471,258,168	61,072,434	18,601,805	15,178,593
BRO	474,637,872	62,772,835	20,595,063	15,927,308
ERO	472,270,721	62,241,532	19,527,073	15,624,733
PRO	470,798,359	60,612,528	18,337,130	14,680,805
BERO	474,637,872	62,772,835	20,595,063	15,927,308
BPRO	474,637,872	62,772,835	20,595,063	15,927,308
CVaR-SP	564,601,839	61,902,364	19,117,962	15,405,367
IGDT	352,420,273	54,543,388	17,133,489	14,027,273
Selected	CVaR-SP	BRO/BERO BPRO	BRO/BERO BPRO	BRO/BERO BPRO

To more accurately evaluate the POP results, three days of the test period with different price behaviors have been considered. The actual clearing prices realized in the market are mostly higher than, mostly lower than, and close to the mean values of the expected ranges in these three test days, which are January 18, April 14, and July 7, respectively. It is worth to mention that these evaluations can be generalized as all days can be categorized into the above-mentioned three types of days.

Tables 2.3 and 2.4 show the impact of different DR values on the POP results of the RO approaches for the three days in 2014 in NYISO. By decreasing DR from DR^{max} to $0.25 \times DR^{\text{max}}$ (in the steps of $0.25 \times DR^{\text{max}}$), the conservatism level of each RO approach reduces. The following points can be seen from Tables 2.3 and 2.4:

1. On the first test day (i.e. January 18), the actual clearing prices realized in the market are mostly higher than the mean values of the expected ranges. In this case, the less/more conservative methods lead to higher/lower profit. Therefore,

the least conservative approach, i.e. BRO, obtains the highest profit on this test day.

2. On the second test day (i.e. April 14), the actual clearing prices are mostly lower than the mean values of the expected ranges. On this test day, the less/more conservative methods lead to lower/higher profit and the most conservative approach, i.e. PRO, obtains the highest profit.
3. On the third test day (i.e. July 7), the actual clearing prices are close to the mean values of the expected ranges. On this day, ERO, which is less conservative than PRO and more conservative than BRO, leads to the highest profit.
4. BERO/BPRO are less conservative than ERO/PRO and more conservative than BRO.

Table 2.3: Actual profit of RO approaches vs. DR for the IEEE 30-bus test system (\$)

Day	App.	DR^{Max}	$0.75 \times DR^{\text{Max}}$	$0.50 \times DR^{\text{Max}}$	$0.25 \times DR^{\text{Max}}$
January 18 th	BRO	329,503	337,932	345,425	351,324
	ERO	317,545	323,951	332,168	341,873
	PRO	283,910	305,980	314,775	323,031
	BERO	329,503	335,902	339,571	343,320
	BPRO	329,503	334,194	336,042	342,882
April 14 th	BRO	515,700	512,371	510,148	507,274
	ERO	519,315	517,854	514,125	512,969
	PRO	525,437	522,761	519,186	516,316
	BERO	515,700	513,410	511,845	510,109
	BPRO	515,700	514,872	512,768	511,623
July 7 th	BRO	430,610	431,485	432,811	433,328
	ERO	437,693	438,729	440,004	441,983
	PRO	424,853	425,982	428,552	429,250
	BERO	430,610	432,942	434,710	435,532
	BPRO	430,610	432,254	433,558	434,390

Table 2.4: Actual profit of RO approaches vs. DR for the IEEE 118-bus test system (\$)

Day	App.	DR^{Max}	$0.75 \times DR^{\text{Max}}$	$0.50 \times DR^{\text{Max}}$	$0.25 \times DR^{\text{Max}}$
January 18 th	BRO	1,698,159	1,731,237	1,781,518	1,797,305
	ERO	1,619,552	1,662,324	1,699,042	1,746,495
	PRO	1,269,494	1,528,546	1,645,453	1,686,445
	BERO	1,698,159	1,721,165	1,745,129	1,773,516
	BPRO	1,698,159	1,715,569	1,730,930	1,764,231
April 14 th	BRO	3,216,165	3,186,802	3,114,267	3,093,979
	ERO	3,247,017	3,226,484	3,206,519	3,173,068
	PRO	3,347,114	3,309,194	3,246,771	3,220,232
	BERO	3,216,165	3,196,611	3,146,469	3,114,757
	BPRO	3,216,165	3,207,036	3,177,934	3,147,114
July 7 th	BRO	1,946,799	1,949,798	1,952,537	1,953,489
	ERO	2,131,164	2,139,315	2,141,716	2,145,541
	PRO	1,881,772	1,891,269	1,906,837	1,925,260
	BERO	1,946,799	1,955,492	1,961,201	1,965,030
	BPRO	1,946,799	1,951,798	1,955,489	1,959,772

Table 2.5: Actual profit of robust approaches vs. forecast error for the IEEE 30-bus test system (\$)

Forecast error	App.	January 18 th	April 14 th	July 7 th
Original error	Deterministic	307,440	516,092	432,120
	BRO	329,503	515,700	430,610
	ERO	321,545	519,315	437,693
	PRO	286,910	525,437	424,853
	CVaR-SP	318,724	519,186	435,934
	IGDT	280,265	521,883	421,785
	Selected	BRO	PRO	ERO
0.5×Original error	Deterministic	343,585	537,960	462,087
	BRO	341,033	521,564	451,470
	ERO	329,684	543,850	460,532
	PRO	296,350	532,990	443,694
	CVaR-SP	355,480	556,273	487,425
	IGDT	288,540	526,500	438,224
	Selected	CVaR-SP	CVaR-SP	CVaR-SP
2×Original error	Deterministic	249,378	486,124	401,356
	BRO	258,638	490,508	404,950
	ERO	263,152	497,550	407,327
	PRO	269,789	503,685	410,540
	CVaR-SP	260,850	494,442	405,898
	IGDT	275,780	506,967	412,890
	Selected	IGDT	IGDT	IGDT

Table 2.6: Actual profit of robust approaches vs. forecast error for the IEEE 118-bus test system (\$)

Forecast error	App.	January 18 th	April 14 th	July 7 th
Original error	Deterministic	1,407,548	3,225,150	1,972,900
	BRO	1,698,159	3,216,165	1,946,799
	ERO	1,619,552	3,247,017	2,131,164
	PRO	1,269,494	3,347,114	1,881,772
	CVaR-SP	1,475,327	3,238,478	2,057,170
	IGDT	1,196,083	3,249,557	1,475,970
	Selected	BRO	PRO	ERO
0.5×Original error	Deterministic	1,886,543	4,745,230	2,445,980
	BRO	1,795,289	4,561,480	2,141,588
	ERO	1,755,845	4,878,188	2,284,994
	PRO	1,362,530	4,674,811	2,044,199
	CVaR-SP	2,075,485	5,043,600	3,408,220
	IGDT	1,240,546	4,664,170	1,991,751
	Selected	CVaR-SP	CVaR-SP	CVaR-SP
2×Original error	Deterministic	987,860	2,847,950	1,114,752
	BRO	1,008,476	2,908,185	1,136,588
	ERO	1,067,628	2,971,476	1,164,949
	PRO	1,116,361	2,967,949	1,279,036
	CVaR-SP	1,045,623	2,938,120	1,150,422
	IGDT	1,142,334	3,046,693	1,377,099
	Selected	IGDT	IGDT	IGDT

Tables 2.5 and 2.6 demonstrate the actual profit of BRO, ERO, PRO, CVaR-SP, and IGDT obtained from POP considering different price forecast errors. Note that

according to Appendix C, BRO, BERO, and BPRO lead to the same profit for $DR = DR^{\max}$.

In each column of Tables 2.5 and 2.6, the bolded value shows the maximum profit among all non-deterministic approaches and the associated method is indicated in the last row. Based on Tables 2.5 and 2.6, it is concluded that:

1. The actual profit of the deterministic model is not always less/more than that of the non-deterministic models in all cases. The deterministic actual profit in several cases is higher/lower than the non-deterministic actual profits, since those non-deterministic models are more/less conservative than the deterministic model, or price forecast is more/less accurate. While price forecast is less accurate (e.g. forecast error = $2 \times$ original error), the actual profit of the deterministic model is less than that of the non-deterministic models. Therefore, improving the price forecast accuracy increases the deterministic profit.
2. With the original price forecast errors, i.e. the errors obtained from the employed price forecast method [52], BRO, PRO, and ERO attain the highest profit in January 18, April 14, and July 7, respectively.
3. If half of the original price forecast errors are considered, i.e. if 200% more accurate price forecast method could be used, the CVaR-SP obtains the highest profit in the three test days. This can be explained as follows. The performance of CVaR-SP depends heavily on its scenarios. When the price forecast errors become half, much more accurate scenarios can be constructed and so the performance of CVaR-SP greatly improves. Indeed, with half forecast errors, the performance of all non-deterministic approaches of Tables 2.5 and 2.6 improve, but the amount of improvement of CVaR-SP is more than the other methods such that it becomes the most profitable method in this case.
4. If the price forecast errors doubles, i.e. if 200% less accurate price forecast method

is used, the performance of all non-deterministic approaches of Tables 2.5 and 2.6 degrades. In this case, which is just the opposite of the previous case, the performance of CVaR-SP degrades more than the other approaches such that it obtains the lowest profits. On other hand, the IGDT method that gained the lowest improvement in the previous case, suffers from the lowest degradation in this case, since it is the most robust non-deterministic approach in Tables 2.5 and 2.6. The IGDT method builds offer curves for the greatest level of uncertainty which guarantees the profit does not become worse than a definite threshold.

The above points can help a GenCo select the most advantageous self-scheduling approach based on the price information and price forecast method that it has as well as the robustness level that it desires.

The offer curves of unit 39 in hour 10 on January 18th, April 14th, and July 7th are illustrated in Figure 2.2. These offer curves are associated with the results of the original forecast error of the IEEE 118-bus test system presented in Table 2.6. The offer curves in Figure 2.2 demonstrate that BRO, PRO, and ERO compared to other approaches obtain highest profits for unit 39 in hour 10 on January 18th, April 14th, and July 7th, respectively.

Table 2.7 compares the computation time of different robust methodologies for one scheduling day. Table 2.7 shows that a) the MILP approaches of BRO, PRO, BPRO, and CVaR-SP have low computation times in the range of 160s to 334s, b) the MISOCP approaches of ERO and BERO have higher computation times of 3,556s and 7,355s, c) the MINLP approach of IGDT has the highest computation time of 24,729s based on the complexity of their models.

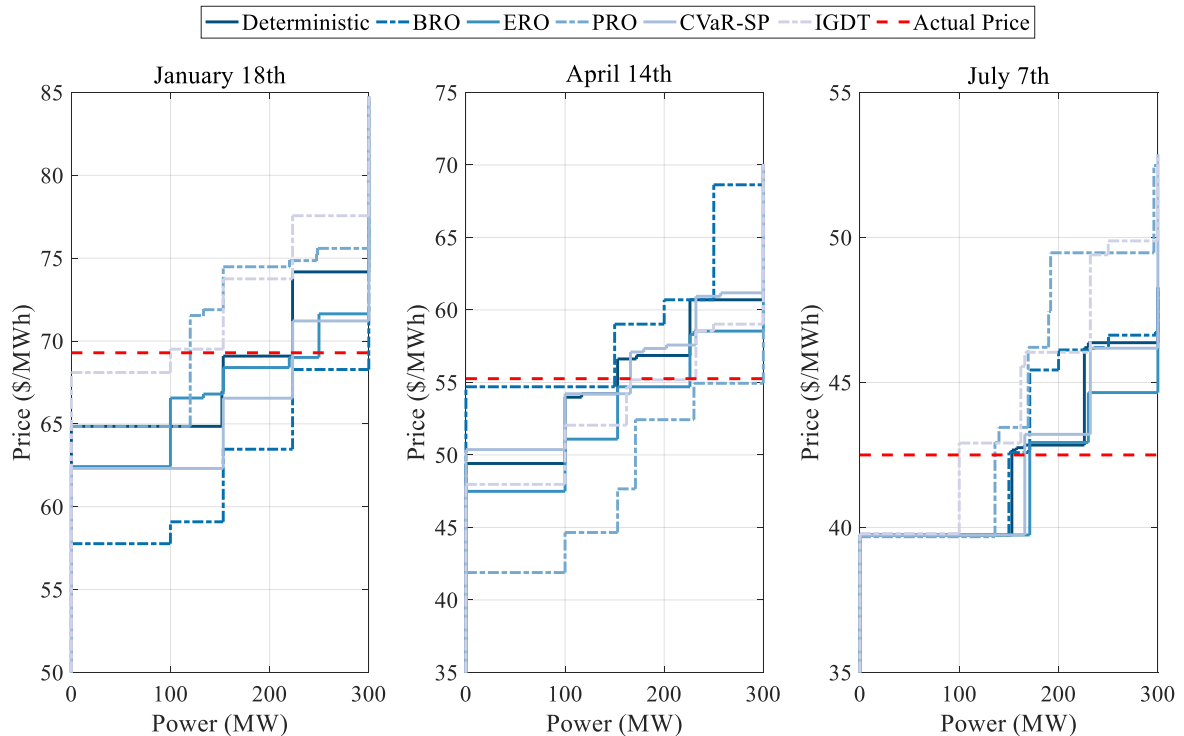


Figure 2.2: Offer curves of unit 39 in hour 10 on January 18th, April 14th, and July 7th.

Table 2.7: Computation time (s) of the robust approaches on the test case

App.	BRO	ERO	PRO	BERO	BPRO	CVaR-SP	IGDT
Time	232	3,556	334	7,355	261	160	24,729

Table 2.8 presents a summary of the self-scheduling strategies for different real-market-environment cases. The self-scheduling strategies can help GenCos in making the most appropriate self-scheduling decision based on the price information and price forecast method that they have adopted as well as the robustness level that they desire in their solution. In Table 2.8, “Actual” term refers to the actual clearing prices realized in the market and “Mean Value” term refers to the mean values of the expected ranges. Note that since price forecast error typically occurs in all hours of a day, it is assumed in the RO models $DR = DR^{\max}$, and according to Appendix C, BRO, BERO, and BPRO lead to the same profit for $DR = DR^{\max}$.

Table 2.8: Summary of the self-scheduling strategies for difference real-market-environment cases

Cases \ Strategies	BRO	ERO	PRO	CVaR-SP	IGDT
More Accurate Forecasted Price				•	
Actual > Mean Value	•				
Actual \approx Mean Value		•			
Actual < Mean Value			•		
Less Accurate Forecasted Price					•

2.4 Conclusion

Various non-deterministic self-scheduling approaches have been presented in recent years. These approaches are mostly based on RO methodologies, SP frameworks and IGDT models. Which of the self-scheduling methods is appropriate for a specific GenCo depends on many factors including the company's objectives, model complexity, available data, and computation time. The main motivation of this study was to evaluate and compare the performance of various robust self-scheduling methodologies. These robust methodologies have different uncertainty modeling approaches, as well as a range of tools for controlling the conservativeness of their solutions.

In addition to recasting the robust methodologies in more applicable forms, offer curve constructing strategy for each method has been presented. Moreover, to practically evaluate the performance of various methodologies, a POP has been proposed to determine the actual profit of each method in different real-market-environment cases. The conclusions drawn from the evaluations can help GenCos select and model the most appropriate non-deterministic self-scheduling approach based on the price information and price forecast method that they have adopted, as well as the robustness level that they desire in their solution.

Analyzing and comparing the performance of the non-deterministic approaches for multi-auctions self-scheduling model as well as considering different sources of uncertainty, such as electricity market price, renewable resources and so on, are set aside to be studied as future work [53].

CHAPTER 3: The ROLE OF DEMAND RESPONSE AS AN ALTERNATIVE TRANSMISSION EXPANSION SOLUTION IN A CAPACITY MARKET

Demand response cannot only be used as a power supply resource to produce a megawatt in high power prices or when the reliability of the grid is threatened, but can also be applied to resolve a transmission expansion planning problem instead of implementing a costly and complex transmission upgrade solution. Essentially, the demand response resources (DRRs) can relieve the capacity requirement for a load area, and thereby relieve the import transmission requirement. This section of the dissertation explores the role of DRRs as an alternative solution to the required transmission upgrades in the context of a proposed capacity market modeled based on Pennsylvania-New Jersey-Maryland (PJM) capacity market model. Numerical results show that the DRRs can indeed replace the needed transmission upgrades.

Nomenclature

A. Indices

b	Index of offering/bidding curve's blocks.
c	Index of curtailment service providers.
l	Index of load deliverability areas.
r	Index of generation resources.

B. Parameters

$CETL_l$	Capacity Emergency Transfer Limit which is the transmission import capability limit for locational deliverability area (LDA) l .
$CETO_l$	Capacity Emergency Transfer Objective which is the transmission import capability requirement for LDA l .

$P_{c,b}^{\text{DR,max}}$	Upper limit of the bidding demand response resource capacity of block b of curtailment service provider c .
$P_{r,b}^{\text{GR,max}}$	Upper limit of the offering generation resource capacity of block b of generation recourse r .
$P_{l,b}^{\text{VRR,max}}$	Upper limit of the bidding variable resource requirement of block b of LDA l .
$RelReq_l$	Reliability requirement in LDA l .
$UCAP_l$	Unforced Capacity which is the capacity availability rating in LDA l .
$\pi_{c,b}^{\text{DR}}$	Bidding price of block b of curtailment service provider c .
$\pi_{r,b}^{\text{GR}}$	Offering price of block b of generation recourse r .
π_l^{TU}	Transmission upgrade price of LDA l .
$\pi_{l,b}^{\text{VRR}}$	Bidding price of variable resource requirement of block b of LDA l .

C. Sets

B	Set of offering/bidding curve's blocks.
C	Set of curtailment service providers.
L	Set of load deliverability areas.
R	Set of generation resources.

D. Variables

$P_{c,b}^{\text{DR}}$	Bidding demand response resource capacity of block b of curtailment service provider c .
$P_{r,b}^{\text{GR}}$	Offering resource capacity of block b of generation recourse r .
P_l^{TU}	Transmission upgrade capacity of LDA l .
$P_{l,b}^{\text{VRR}}$	Bidding variable resource requirement of block b of LDA l .
$P_{l,b}^{\text{VRR-DR}}$	Auxiliary variable to model variable resource requirement decrement due to demand response resource bidding.

3.1 Introduction

3.1.1 Background and Motivation

In some markets such as Pennsylvania-New Jersey-Maryland (PJM), and Independent System Operator New England (ISO-NE), capacity markets are also developed in addition to the most well-known energy markets (day-ahead and real-time markets) and ancillary services market. The capacity market is designed to guarantee that adequate amounts of necessary resources can be available to ensure the reliability of the grid. Generally, to mitigate market power concerns, the energy price or bids in some energy markets are capped which allows generators to cover only their short-term variable costs. To cover long-term fixed costs, a second revenue stream is developed via a capacity market. As an augmented mechanism, capacity markets can increase the revenues received by the cleared generators in the market. This is in addition to the revenue received by the same generators in the energy markets. While the majority of the revenue for each participating generator comes from energy markets, the revenue that can be received from the capacity market can substantially improve the business viability and profitability of the generator.

The important roles that demand response (DR) plays in a major wholesale electricity market have been recognized gradually and more widely. It is widely believed that the DR can bring many benefits to the system. The most important benefit of demand response is improved resource-efficiency of electricity production due to closer alignment between customers' electricity prices and the value they place on electricity [13]. Notably, Federal Energy Regulatory Commission (FERC) Order 745 sets standards for demand response practices and pricing in wholesale markets and brought the practice under the agency's jurisdiction. This federal regulatory authority to regulate demand response programs in wholesale markets was recently upheld by U.S. Supreme Court which reaffirmed that demand response is primarily a wholesale market function [12]. In fact, in all electricity markets in the US, DR can participate

in any relevant energy market in which DR can influence the system reliability and the market price on equal footing with the supply side resources. The same DRs are also allowed to participate in any capacity market. Similar to the situation of DR role in energy markets, DR can also impact the system reliability and market clearing price in capacity markets.

In [54], a demand curve-based approach instead of a fixed demand is proposed for PJM capacity market which makes revenues more predictable for generators, and reduce consumers costs. In [55], the authors evaluate the application of capacity market for hydrothermal systems with a significant portion of hydro generation. A game-theory based simulation is presented to assess the performance of the model under different levels of competitive conditions. A dynamic capacity investment framework is proposed in [56] to evaluate the impact of different capacity market design scenarios, and the results are compared based on affordability, reliability, and sustainability criterion. The authors in [57] present an investigation on the process and trends of demand response procurement and energy efficiency in the New England capacity market, and the design of the integration mechanisms. The integration of DR into PJM capacity market incremental auction is proposed in [58], and its impact on the market clearing solution and prices is discussed. Therefore, to the best of my knowledge, there is no existing research work that uses DR in the capacity market as a transmission expansion planning solution.

3.1.2 Contributions

The main contributions of this chapter of the dissertation can be summarized as follows:

1. Proposing a novel integrated capacity market and demand response model as an alternative solution to the transmission expansion planning problem.
2. Including the use of the demand response resources as power supply resources

to participate in the capacity market.

3.2 PJM Capacity Market

PJM's capacity market, also known as the Reliability Pricing Model (RPM), guarantees long-term grid reliability by obtaining the adequate amount of necessary power supply resources to meet the minimum requirement of energy demand three years in the future. A capacity market can be analogous to an insurance policy which allows for an additional cost (payment to generators which perform well) in return for the availability of generating resources to maintain the reliability of the system. Reliability is extremely important for the power system particularly during extreme events such as ice storms. In this way, consumers have greater protection from power interruptions and price spikes. By matching energy supply with future energy demand, PJM's capacity market produces long-term price signals to attract required energy-related investments and power supply resources required to provide consumer needs for electricity, years into the future.

The RPM is a multi-auction structure including the following market mechanisms [59]:

1. *Base Residual Auction* (BRA) is run during the month of May three years prior to the start of the Delivery Year.
2. *Incremental Auctions* (IAs) are conducted at least three times after the BRA to adjust resource procurement that are known prior to the beginning of the Delivery Year.
3. *Conditional Incremental Auction* (CIA) may be held if a backbone transmission line is delayed, additional capacity procurement in a Locational Deliverability Area (LDA) is needed to remedy the corresponding reliability problem.
4. *Bilateral Market* gives power supply resources an opportunity to cover any

auction commitment shortages. It also provides load serving entities (LSEs) the opportunity to hedge against the locational reliability charge.

Figure 3.1 illustrates the structure of the above mentioned auctions of RPM.

The LSEs that provide electricity to consumers in the PJM market have obligations to procure sufficient generation capacities to meet their projected peak loads now and in the future. This required capacity can be acquired via bilateral contracts or those entities (PJM members) can secure these resources for the future through the PJM capacity market (BRA, IAs, and CIA). The essential elements of the capacity market are [60]:

1. Capacity procurement three years prior to it is needed through a competitive auction.
2. Locational pricing for capacity that changes to reflect limitations on the transmission system and to account for the differing needs for capacity in different areas.
3. A variable resource requirement curve (VRR) or demand curve, which is the energy demand load formula used to set the price paid to market participants for capacity.

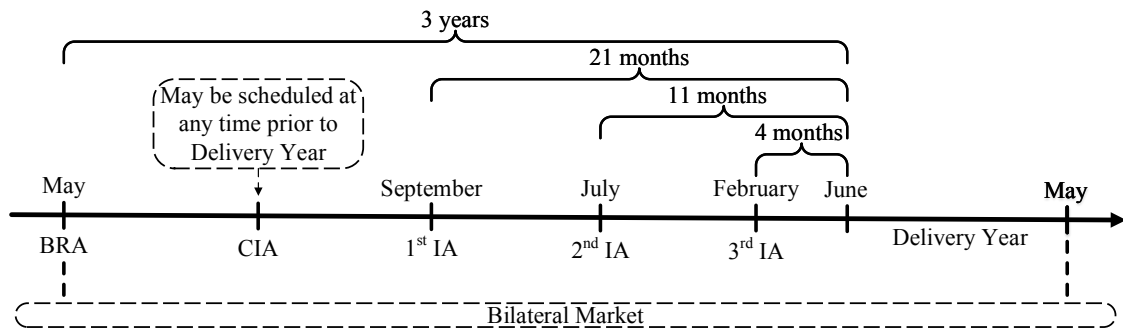


Figure 3.1: PJM capacity market (i.e. RPM) structure.

Capacity market participants offer or bid power supply resources into the market that either increase energy supply or reduce demand, respectively. These resources comprise new generators, upgrades for existing generators, demand response, energy efficiency and transmission upgrades (TUs). When a participant bids these supply resources into the market, the participant is committed to increase their supply or reduce their demand by the amount they offered, three years into the future.

Having adequate amounts of supply resources is necessary but not sufficient for system reliability. The potential power supply from these resources must be able to be transported to the load centers where the power is needed. If there is a transmission limitation to a load area, the load area needs to rely on more expensive resources located in that area, or the transmission limitation needs to be resolved. The market clearing price (MCP) of each LDA's - locational marginal price (LMP) - may be higher than the system MCP if additional capacity is needed in the LDA. In other words, LMP for that import-constrained load area is higher than those for load areas where there is no import limitation. LDAs are defined based on transmission capacity transfer capability into an area. Those load areas or load deliverability areas are shown in Figures 3.2 and 3.3 [61]. Figure 3.2 shows the fundamental level of LDAs, called zonal LDAs, while Figure 3.3 shows the larger LDAs, called global LDAs, which represent a collection of some zonal LDAs.

3.3 Proposed Integrated Capacity Market and Demand Response Model

In this section, first the capacity market model including transmission upgrade solution is described in detail. Then, a comprehensive and integrated model of a capacity market and demand response model is proposed. Note that those models are applied to Base Residual Auction (BRA) without loss of generality, and they can easily be extended to other capacity market auctions such as IAs.

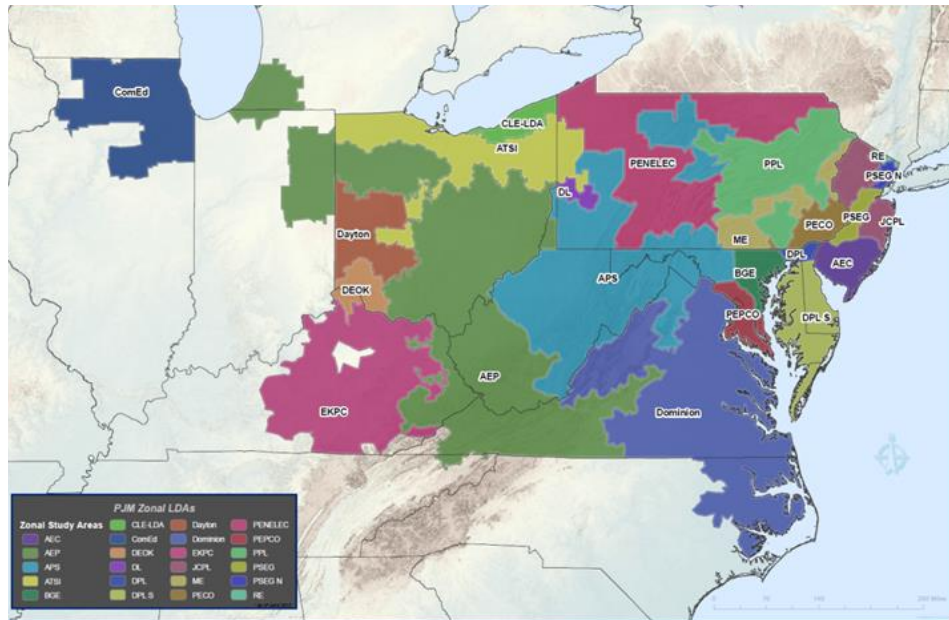


Figure 3.2: Zonal LDAs.

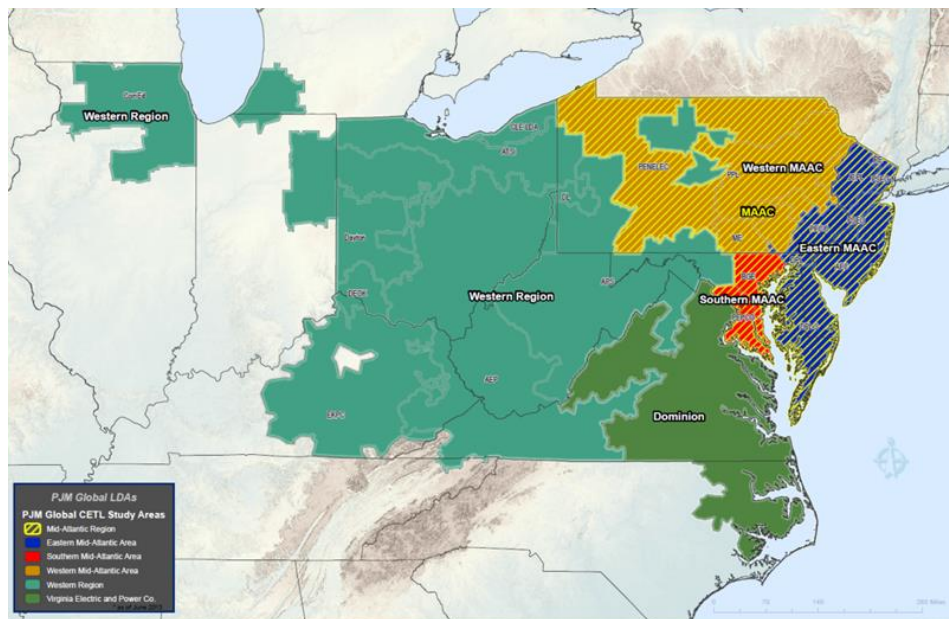


Figure 3.3: Global LDAs.

3.3.1 Capacity Market Model Considering Transmission Upgrade

The objective of a capacity market is to minimize the total cost which is achieved by minimizing the cost of selling capacity from generation resources, and maximizing the obtained revenue of purchased capacity from the demand side. The actual capacity

markets in the real-world is cleared for several years forward. For example, the capacity market in PJM (i.e. RPM) is cleared for the next three years. Similarly, the Forward Capacity Auctions (FCA) for the capacity market in New England market, known as Forward Capacity Market (FCM), are held three years prior to the operating period [62].

In a capacity market, as in any other markets, there are buyers and sellers of the capacity resources. The buyers of the capacity resources are generally LSEs that have obligations to serve load for their respective service territories. The sellers of the capacity market are generally the owners of the generating units. The mathematical formulations of the reliability pricing model of PJM capacity market are proposed in (3.1)-(3.7). The objective function (3.1) shows the minimization of the capacity market cost [63].

$$\text{Minimize } \sum_{r=1}^R \sum_{b=1}^B (\pi_{r,b}^{\text{GR}} \cdot P_{r,b}^{\text{GR}}) \quad (3.1a)$$

$$- \sum_{l=1}^L \sum_{b=1}^B (\pi_{l,b}^{\text{VRR}} \cdot P_{l,b}^{\text{VRR}}) \quad (3.1b)$$

$$+ \sum_{l=1}^L (\pi_l^{\text{TU}} \cdot P_l^{\text{TU}}) \quad (3.1c)$$

There are three components in the proposed objective function (OF) in (3.1). The first term (3.1a) is the cost of accepted generation resource offers; the second term (3.1b) represents the revenue obtained from variable resource requirements (VRRs) as the demand of all regions, and the last term i.e. (3.1c) is the cost that an independent system operator (ISO) or a regional transmission organization (RTO) should pay for new transmission capacity as the transmission upgrades to solve the transmission expansion planning problem (TEP). An example of generation offering and VRR bidding curves is shown in Figure 3.4, in which the intersection of the rising generation offers with decrement VRR bids, determines the clearing values of the price and the

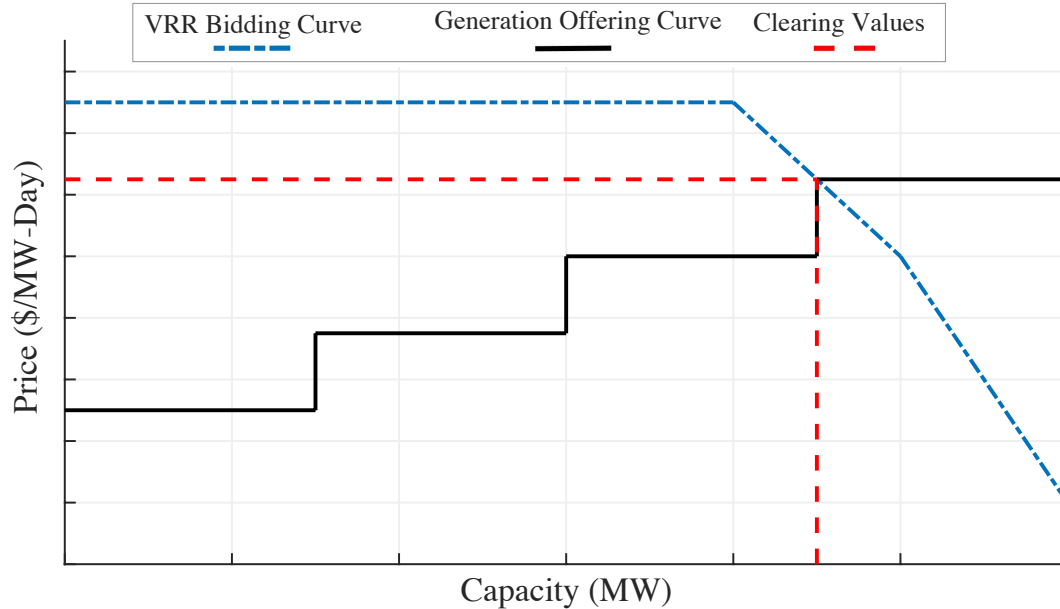


Figure 3.4: Generation offering and VRR bidding curves.

capacity. It is worth mentioning that the regions are referred to as LDAs in the PJM capacity market.

Constraints (3.2) and (3.3) represent the limits of each block of the offered resource capacities and VRR, respectively.

$$P_{r,b}^{\text{GR}} \leq \left(P_{r,b}^{\text{GR,max}} - P_{r,(b-1)}^{\text{GR,max}} \right) \quad \forall r, \forall b \quad (3.2)$$

$$P_{l,b}^{\text{VRR}} \leq \left(P_{l,b}^{\text{VRR,max}} - P_{l,(b-1)}^{\text{VRR,max}} \right) \quad \forall l, \forall b \quad (3.3)$$

In the above inequalities, the amount of the capacity in each block i.e. left-hand-side (LHS) can change between the upper level of the block minus the upper level of the previous block, i.e. right-hand-side (RHS).

The objective function is subject to a number of equality and inequality constraints. Constraint (3.4) guarantees that the amount of the available resource in each LDA meet the reliability requirements which show the target level of reserves required to

meet reliability standards and principles.

$$\sum_{r \subseteq l} \sum_{b=1}^B P_{r,b}^{\text{GR}} \geq \text{RelReq}_l \quad \forall l \quad (3.4)$$

where $\text{RelReq}_l = \text{UCAP}_l - \text{CETO}_l \quad \forall l$, $\text{UCAP}_l = \text{PeakLoadForecast} \times \text{FPR}$, and Forecast Pool Requirement (FPR) includes installed reserve margin, and forced outage rates. CETO_l is transmission import capacity requirement to meet the area reliability criterion of Loss of Load Expectation (LOLE) of one occurrence in 25 years; if the CETO of an LDA is positive, it means there is import capacity in the LDA and the required amount due to reliability issue (i.e. RelReq_l) would decrease; if the CETO of an LDA is negative, there is export capacity from the LDA to other LDAs, and the RelReq_l should increase.

The constraint (3.5) represents the balance of available supply resource, demand load, and CETO in each LDA. For positive CETO of an LDA, the difference between requested load and available resource cannot be more than the import capacity in the LDA; and for negative CETO of an LDA, the difference between available resource and requested load cannot be less than the export capacity in the LDA.

$$\sum_{b=1}^B P_{l,b}^{\text{VRR}} - \sum_{r \subseteq l} \sum_{b=1}^B P_{r,b}^{\text{GR}} \leq \text{CETO}_l \quad \forall l \quad (3.5)$$

For each LDA, if the transmission import capability limits, called Capacity Emergency Transfer Limit (CETL), is less than CETO , transmission upgrade can be used as the solution of the TEP through the constraint (3.6). In other words, if $\text{CETL} \leq \text{CETO}$ for a specific LDA, the transmission facilities in the LDA require an upgrade.

$$\text{CETO}_l \leq \text{CETL}_l + \sum_{b=1}^B P_{l,b}^{\text{TU}} \quad \forall l \quad (3.6)$$

Note that in (3.6), the absolute values of CETO and CETL should be used. In

both import and export (i.e. positive, and negative of $CETO/CETL$, respectively), the capacity limit ($CETL$) should be more than the capacity objective ($CETO$).

Equation (3.7) ensures that the total available supply resources in the capacity market is equal to the total demand loads of all LDAs in the capacity market.

$$\sum_{r=1}^R \sum_{b=1}^B P_{r,b}^{\text{GR}} - \sum_{l=1}^L \sum_{b=1}^B P_{l,b}^{\text{VRR}} = 0 \quad (3.7)$$

The dual variable associated with the balance constraint (3.7) represents the MCP for LDAs which do not have import limitation. There are different capacity prices in different regions if there are import constraints to those regions. If an LDA is import-constrained, the LMP of that location increases. In other words, LMP of each LDA is equal to the MCP plus a dual variable associated with the balance constraint (3.5) in the LDA.

3.3.2 Integrated Capacity Market and Demand Response Model

Transmission upgrade is a very expensive and physically limited solution. However, Demand Response (DR) is a relatively inexpensive and easy alternative solution which avoids the complexity of adding new transmission line structure. DR can be categorized into two types. The first type is Price Responsive Demand (PRD) in which consumers are not paid directly for reductions in their electricity use, but they save money on their bills. The second type is Demand Response Resources (DRRs) in which large customers or end-use customers, through curtailment service providers (CSPs), submit their curtailment and reduction bids to the market, and if the bids are accepted, they can receive payments. In this chapter of the dissertation, the DRR is used as an alternative solution of TEP since DRR, unlike PRD, participates in PJM's reliability pricing model capacity market as a supply resource. Indeed, PRD is not applicable in this case, because PRD represents load that will be offline when LMP reaches a certain threshold. PRD is only treated as a predictable change in the amount

of electricity used, not as additional generation resource [64]. Therefore, a novel integrated capacity market and DR model is proposed in (3.8)-(3.17) in which DRR not only plays a role as a solution to the transmission expansion planning problem, but also participates in the capacity market as a power supply resource. However, according to Capacity Performance (CP) requirement introduced by PJM, capacity resources such as generation resources (GRs), and DRRs are required to be capable of sustained, predictable operation that allows the resource to be available throughout the entire delivery year to provide energy and reserves when PJM determines that a power system emergency condition exists. Only resources that meet the requirements of the capacity performance resource product-type is used in PJM capacity market effective with the 2020/2021 delivery year and beyond [59, 65].

$$\text{Minimize } \sum_{r=1}^R \sum_{b=1}^B (\pi_{r,b}^{\text{GR}} \cdot P_{r,b}^{\text{GR}}) \quad (3.8a)$$

$$- \sum_{l=1}^L \sum_{b=1}^B (\pi_{l,b}^{\text{VRR}} \cdot [P_{l,b}^{\text{VRR}} - P_{l,b}^{\text{VRR-DR}}]) \quad (3.8b)$$

$$+ \sum_{l=1}^L (\pi_l^{\text{TU}} \cdot P_l^{\text{TU}}) \quad (3.8c)$$

$$+ \sum_{c=1}^C \sum_{b=1}^B (\pi_{c,b}^{\text{DR}} \cdot P_{c,b}^{\text{DR}}) \quad (3.8d)$$

The first and three terms of (3.8) (i.e. (3.8a) and (3.8c)) similar to (3.1a) and (3.1c) represent the cost of available generation resources, and the cost of transmission upgrades, respectively. But, there is a difference in the second term (3.8b). By increasing the amount of the accepted DR (i.e. $P_{l,b}^{\text{VRR-DR}}$), the VRR revenue decreases. The last term (3.8d) shows the cost of the accepted demand response bids.

Constraints (3.9) and (3.10) are similar to (3.2) and (3.3), respectively, and con-

straint (3.11) presents the limits of each block of the DR.

$$P_{r,b}^{\text{GR}} \leq \left(P_{r,b}^{\text{GR,max}} - P_{r,(b-1)}^{\text{GR,max}} \right) \quad \forall r, \forall b \quad (3.9)$$

$$P_{l,b}^{\text{VRR}} \leq \left(P_{l,b}^{\text{VRR,max}} - P_{l,(b-1)}^{\text{VRR,max}} \right) \quad \forall l, \forall b \quad (3.10)$$

$$P_{c,b}^{\text{DR}} \leq \left(P_{c,b}^{\text{DR,max}} - P_{c,(b-1)}^{\text{DR,max}} \right) \quad \forall c, \forall b \quad (3.11)$$

It is worth mentioning that limits of constraints (3.9)-(3.11) are obtained according to the offers and bids submitted to the market.

Since the capacity value and price of each block of DR and VRR bidding curves might be different, to model the impact of the DR on the VRR, an auxiliary variable (i.e. $P_{l,b}^{\text{VRR-DR}}$) is introduced. Based on equation (3.12), the total DR of all blocks of CSPs in an LDA is equal to the total blocks of the auxiliary variable in the LDA. Constraint (3.13) limits each block of the auxiliary variable similar to the VRR bidding curve.

$$\sum_{c \subseteq l} \sum_{b=1}^B P_{c,b}^{\text{DR}} = \sum_{b=1}^B P_{l,b}^{\text{VRR-DR}} \quad \forall l \quad (3.12)$$

$$P_{l,b}^{\text{VRR-DR}} \leq \left(P_{l,b}^{\text{VRR,max}} - P_{l,(b-1)}^{\text{VRR,max}} \right) \quad \forall l, \forall b \quad (3.13)$$

Constraints (3.14)-(3.17) are the reformulated form of the constraints (3.4)-(3.7) in which the impact of DR is modeled. In (3.14), DR can help generation resources to meet the reliability requirement in each LDA. Instead of using more expensive resources, DR may be used to satisfy the reliability standards.

$$\sum_{r \subseteq l} \sum_{b=1}^B P_{r,b}^{\text{GR}} + \sum_{c \subseteq l} \sum_{b=1}^B P_{c,b}^{\text{DR}} \geq \text{RelReq}_l \quad \forall l \quad (3.14)$$

Also, based on constraint (3.15), DR can reduce demand, and then, by increasing the

DR usage in each area, fewer LDAs are required to import capacity from other areas.

$$\sum_{b=1}^B P_{l,b}^{\text{VRR}} - \sum_{r \subseteq l} \sum_{b=1}^B P_{r,b}^{\text{GR}} - \sum_{c \subseteq l} \sum_{b=1}^B P_{c,b}^{\text{DR}} \leq CETO_l \quad \forall l \quad (3.15)$$

DRR, in constraints (3.14) and (3.15), plays a role as a power supply resource to participate in the capacity market, but it is not the only application of DRR in my proposed capacity market model. In constraint (3.16), DRR is used as the alternative solution of TEP. When in an LDA, $CETL$ is less than $CETO$, both solutions (i.e. TU, and DRR) can be used, and it depends on the price and capacity limit of each solution. For instance, if DRR's capacity is not enough to meet the required transmission capacity limit, transmission upgrade would also be used.

$$CETO_l \leq CETL_l + \sum_{c \subseteq l} \sum_{b=1}^B P_{c,b}^{\text{DR}} + \sum_{b=1}^B P_{l,b}^{\text{TU}} \quad \forall l \quad (3.16)$$

Constraint (3.17) shows the modified balance equation in which DR can easily help to achieve the balance between generation, and demand sides.

$$\sum_{r=1}^R \sum_{b=1}^B P_{r,b}^{\text{GR}} + \sum_{c=1}^C \sum_{b=1}^B P_{c,b}^{\text{DR}} - \sum_{l=1}^L \sum_{b=1}^B P_{l,b}^{\text{VRR}} = 0 \quad (3.17)$$

3.4 Case Studies

In this section, the proposed integrated methodology is implemented on BRA of 2020/2021 PJM capacity market data [61]. For generation resource and demand response - one-block offering curves, and for VRR - three-block bidding curves [59] are considered. All case studies have been run using CPLEX within GAMS [51] on a Macintosh-based computer with 3.3 GHz Intel Core i7 processor and 16 GB of RAM.

To correctly evaluate the efficiency of the proposed model, its performance should

Table 3.1: The capacity market cost, revenue, and costs vs. different maximum capacity of DR (\$/Day)

	$0 \times P_{c,b}^{\text{DR,max}}$	$0.25 \times P_{c,b}^{\text{DR,max}}$	$0.50 \times P_{c,b}^{\text{DR,max}}$	$0.75 \times P_{c,b}^{\text{DR,max}}$	$1 \times P_{c,b}^{\text{DR,max}}$
Capacity Market Cost	47,168,850	26,377,019	5,588,237	-15,200,554	-31,578,796
Generation Cost	11,778,870	11,675,050	11,577,830	11,480,600	11,383,370
VRR Revenue	42,707,820	42,928,860	43,153,450	43,378,040	43,587,430
Upgrade Cost	78,097,800	57,466,200	36,834,600	16,203,000	0
DR Cost	0	164,629	329,257	493,886	625,264

be assessed with respect to different core parameters. In the following, the impacts of DR, generation capacity, and *CETO* on the proposed model are discussed in detail.

3.4.1 Impact of DR on the Proposed Model

Table 3.1 presents the capacity market cost (3.8), generation cost (3.8a), VRR revenue (3.8b), upgrade cost (3.8c), and DR cost (3.8d) versus different maximum capacity of DR. When capacity of DR is zero, the proposed model becomes the model of subsection 3.3.1 and only TU is used to remedy the TEP problem. By increasing the percentage of maximum capacity of DR from 0% to 100%, the total cost of the proposed model decreases from \$47,168,850 to \$-31,578,796 (note that a negative cost is equivalent to a profit), which is mainly due to increasing the effect of DR instead of TU on the capacity market. The cost of TU, which is too high, decreases, and the cost of DR, as the less expensive solution, increases.

Figure 3.5 illustrates the total profit that consumers can benefit from participation in the proposed integrated capacity market and demand response program. As shown in Figure 3.5, the total profit of consumers includes demand response profit (i.e. DR) obtained from selling capacities of reductions in their electricity use to the capacity

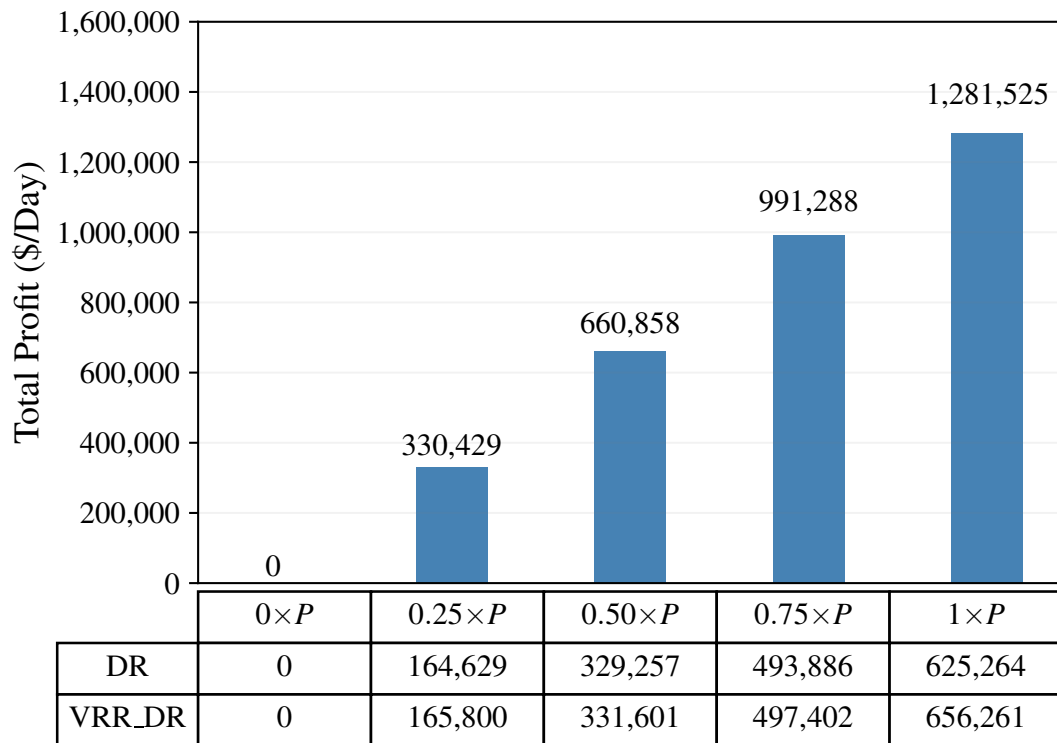


Figure 3.5: Total profit of consumers vs. different maximum capacity of DR (P is $P_{c,b}^{DR,max}$).

market, and saving money on their bills due to decreasing their demands leading to an increase in DR (i.e. VRR_DR). Increasing the capacity of DR in the capacity market allows consumers to be able to obtain more profits.

Figure 3.6 demonstrates the total capacity of generation resource, VRR, upgrade, and DR for different maximum capacity of DR. By increasing the DR's capacity, the total capacity of the generation resource decreases. Since DR is not only used for TEP problem, but also in some LDAs, it participates in the capacity market as a resource, the total capacity of the generation resource decreases.

Although VRR increases when DR increases (top right of Figure 3.6), the final net load (i.e. VRR-DR) decreases from 198,750 to 196,165 (MW-Day). DRs give ISOs/RTOs the opportunity to increase transmission line capacities, by reducing the

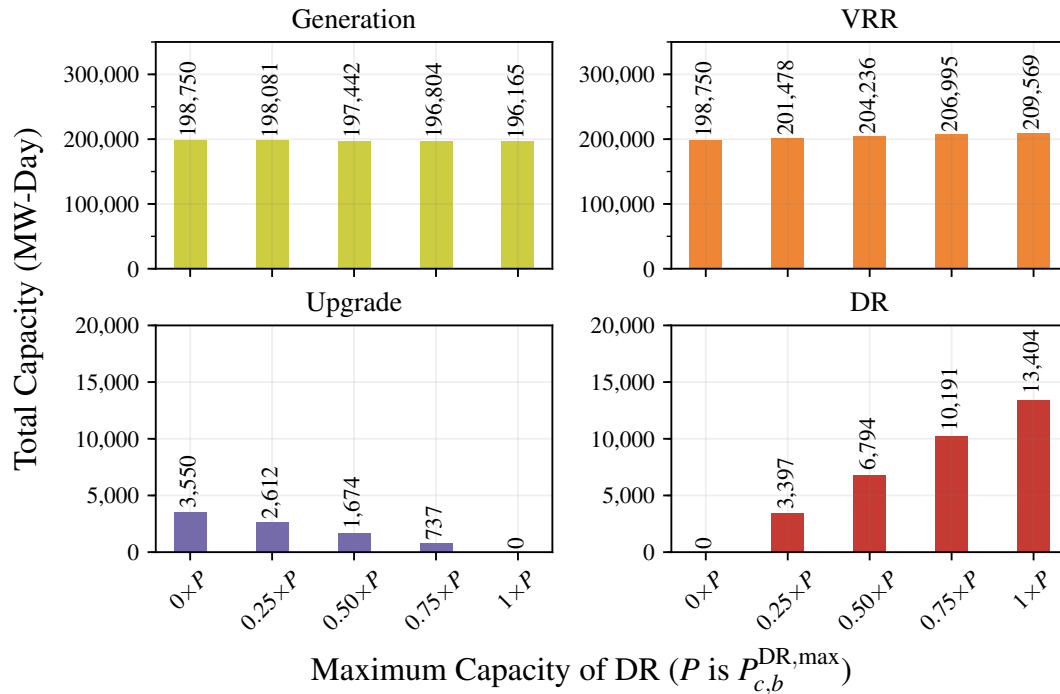


Figure 3.6: Total capacity of generation, VRR, upgrade, and DR vs. different maximum capacity of DR.

load in some areas, whence VRR can increase in other LDAs. In other words, DR increases the flexibility of a market, which is a vital issue for ISOs/RTOs. Consequently, DRs increase the social welfare of a market by reducing the total cost, and increasing the total revenue (Table 3.1).

3.4.2 Impact of Generation Capacities on the Proposed Model

Generation resources are the principal participants of a capacity market, and variation in their capacity impacts the market very noticeably. Figure 3.7 illustrates the total capacity of the generation resource, VRR, and DR for different maximum capacity of the generation resource. It shows that by decreasing the generation resource's capacity, more DR capacity is required to help the reliability requirement to be met (constraint (3.14)). DR tries to compensate the generation decrement, but if the decrement is more than the DR capacity, VRR capacity would decrease. Note that in this experiment for 100% of DR capacity, TU is zero. Therefore, only generation,

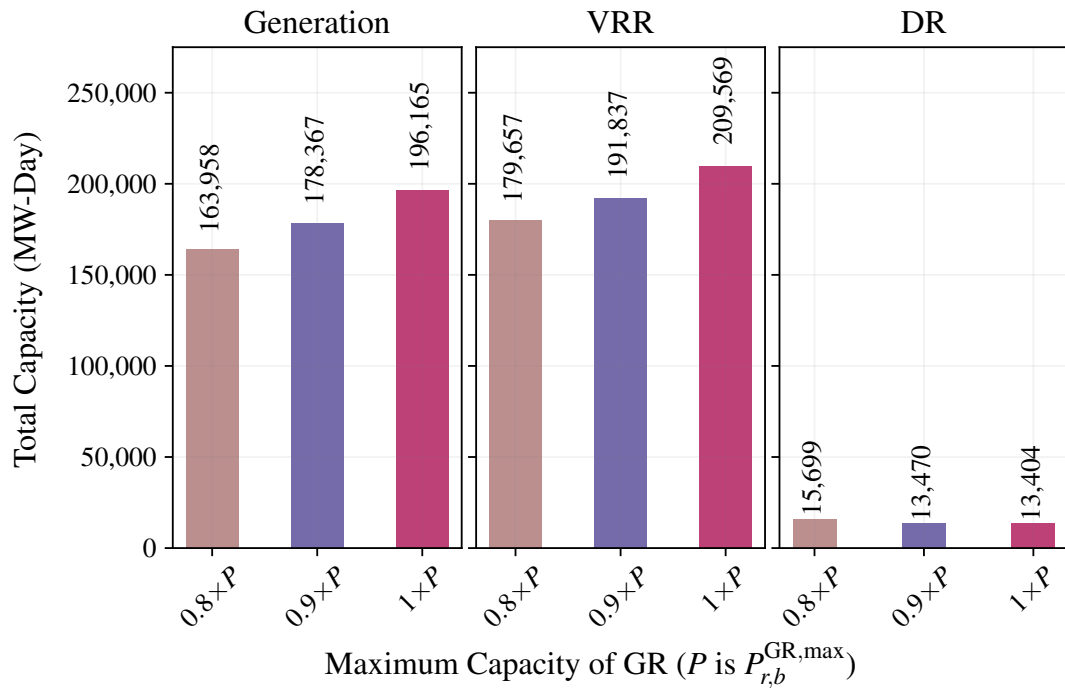


Figure 3.7: Total capacity of generation, VRR, and DR vs. different maximum capacity of generation resource.

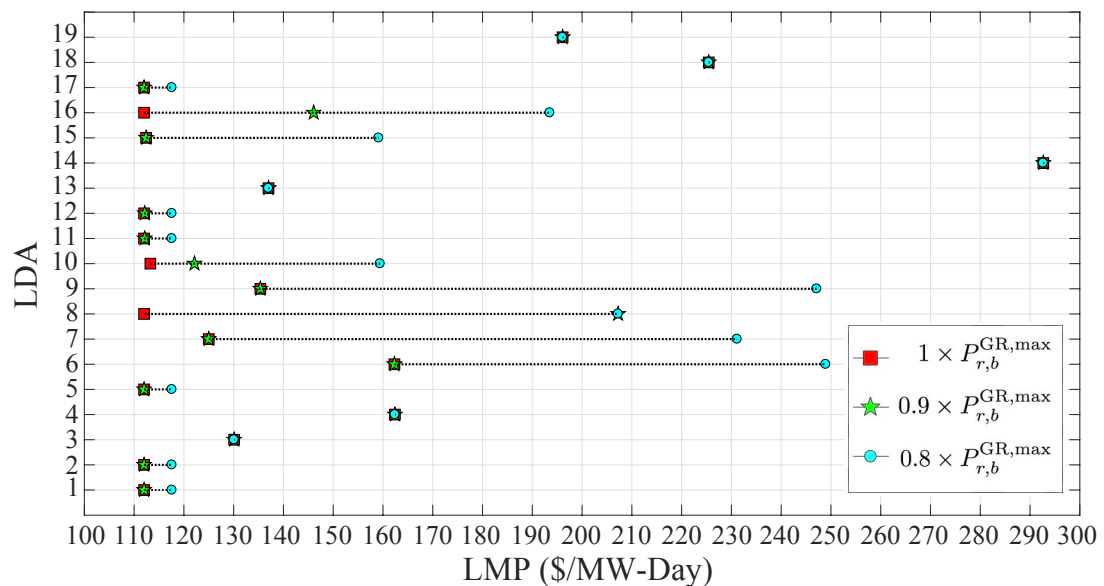


Figure 3.8: Capacity market locational marginal price vs. different maximum capacity of generation resource.

VRR, and DR are presented. As discussed in section 3.2, the locational price is one

of the essential elements of the capacity market. Figure 3.8 shows the impact of the maximum capacity of the generation resource on the capacity market locational marginal price. By decreasing the generation resource maximum capacity, some LDAs have to import capacity from other LDAs; therefore the LMP increases in these constrained LDAs. For example in LDA number 16, price increases from 112 to 193.51 (\$/MW-Day).

3.4.3 Impact of *CETO* on the Proposed Model

CETO is the final parameter that is examined for its effect on the proposed model. *CETO* not only impacts the decision whether an LDA requires new transmission line, but it can also change the LMP price of each LDA by determining the import capacity for each LDA. Figure 3.9 represents the capacity market LMP for different *CETO* values. When *CETO* decreases, based on constraint (3.14) (or (3.4)), reliability requirement increases. Therefore, in some LDAs, the generation increases; then based on constraint (3.15), the VRR capacity can also increase. Figure 3.4 demonstrates that by increasing the VRR capacity, the bidding price decreases, and by increasing generation capacity, the offering price increases. Therefore, increasing or decreasing the LMP price is related directly to the offering/bidding prices. If an LDA is non-import-constrained, the VRR capacity increases leading to an decrease in the LMP of that location. For example, the LMP of LDA number 1 varies from 112 to 97.07 (\$/MW-Day). For an import-constrained LDA which requires the import capacity, the price increases, since the import capacity is limited and more generation capacity is required, then marginal price increases. For instance, the LMP of LDA number 10 changes from 113.27 to 210.7 (\$/MW-Day).

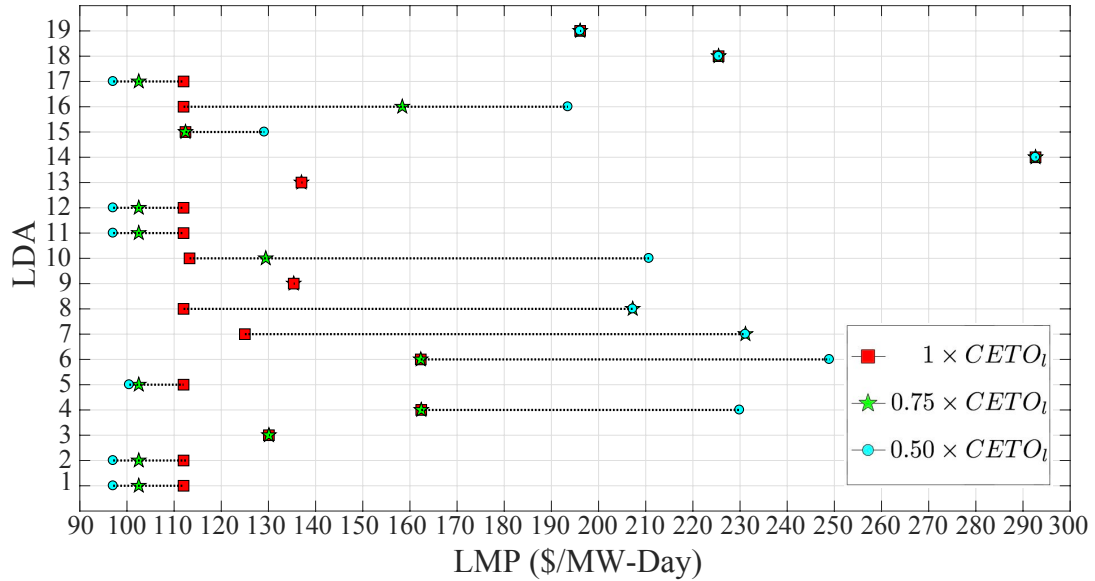


Figure 3.9: Capacity market locational marginal price vs. different $CETO$ values.

3.5 Conclusion

An integrated capacity market and demand response model is developed in which demand response resource can participate in the capacity market to reduce the required transmission capacity as an alternative transmission expansion planning solution instead of the expensive transmission upgrade solution. In addition, demand response resource can be used in the capacity market as a resource to decrease the load to meet the reliability requirement and improve the social welfare of the capacity market. The proposed model is based on the PJM capacity market model (i.e. reliability pricing model). The designed model in this chapter of the dissertation can help ISOs/RTOs to manage the capacity market and transmission expansion planning more efficiently and flexibly. It can also help large consumers or LSEs to manage their loads and earn a profit. To investigate the performance of the proposed framework, it is implemented on the BRA of 2020/2021 PJM capacity market real data, and the influence of several important parameters are investigated in detail [66].

CHAPTER 4: ROBUST TRANSACTIVE ENERGY SYSTEM FRAMEWORK WITH INTEGRATED DEMAND RESPONSE AND DER USING EXTENDED LINEAR DECISION RULES

Increasing the penetration of demand response (DR), energy storage (ES), and plug-in electric vehicles (PEV) exploits the integration of renewable energy (RE) resources and electricity demand, which can lead to addressing resource adequacy, enhancing wholesale electricity market reliability and flexibility, and facilitating customer behavior changes. In this chapter of the dissertation, a design of a novel day-ahead transactive energy system (TES) framework is proposed for the integration of the aggregated DR and PEV as well as other distributed energy resources (DER) including on-site RE resources and behind-the-meter ES systems to improve demand-side energy management. The methodology not only provides the amount of offered DR, but also determines optimal PEV schedules to increase the profit while considering customers' willingness. DR providers and aggregators can take into account the influence of the customers' willingness on their offers by utilizing the proposed comfort index. Finally, to derive a tractable optimization problem, while handling the uncertainty of electricity market clearing prices and renewable power generations, the TES framework is reformulated as an affinely adjustable robust model using extended linear decision rules (ELDR). Simulation results on a large-scale case study demonstrate the applicability and effectiveness of the proposed model.

Nomenclature

A. Indices/Sets

$b \in B$ Index of DR bidding curve blocks.

$l \in L$	Index of affine policy pieces.
$t \in T$	Index of time intervals in a day.
$u \in U$	Index of customers.

B. Parameters

$K_{but}^{LR,I}$	Upper limit of block b of load reduction part of I program for customer u in hour t , $I = \{\text{load curtailment (LC), load shifting (LS)}\}$ (KW).
M	A large enough number.
$N_u^{E,I}$	Number of events of I program for customer u during a scheduling horizon.
$\overline{P}_{ut}^P, \underline{P}_{ut}^P$	Upper and lower boundary of purchased power by customer u in hour t , respectively (KW).
\overline{P}_{ut}^{RE}	Forecasted power of RE of customer u in hour t ; \tilde{P}_{ut}^{RE} and \hat{P}_{lut}^{RE} are the uncertain parameter and the variation range of RE resource, respectively (KW).
$\overline{P}_u^{\Lambda, \text{ch}}, \overline{P}_u^{\Lambda, \text{dch}}$	Upper boundary of charge and discharge of Λ for customer u , respectively, $\Lambda = \{\text{ES, PEV}\}$ (KW).
$\overline{rd}_u^{LR}, \underline{rd}_u^{LR}$	Upper and lower boundary of load reduction duration of customer u , respectively (h).
$\overline{SOC}_u^\Lambda, \underline{SOC}_u^\Lambda$	Upper and lower boundary of Λ state of charge for customer u , respectively, $\Lambda = \{\text{ES, PEV}\}$ (KWh).
ΔT	Duration of a time interval.
$\eta_u^{\Lambda, \text{ch}}, \eta_u^{\Lambda, \text{dch}}$	Charging and discharging efficiency of Λ system for customer u , respectively, $\Lambda = \{\text{ES, PEV}\}$.
$\lambda_1, \lambda_2, \lambda_3, \lambda_4$	Transactive energy control coefficients.
μ_u^Λ	Self-discharge rate of Λ system for customer u , $\Lambda = \{\text{ES, PEV}\}$.
π_{but}^{LR}	Load reduction incentive rate for customer u in block b and hour t ;
π_{ut}^{LR}	is the base value for π_{but}^{LR} (\$/KWh).
π_{ut}^X	Residential rate of X event for customer u in hour t , $X = \{\text{S, P}\}$

(\$/KWh).

$\bar{\pi}_t^{X,LMP}$ Forecasted electricity market locational marginal price of X in hour t ; $\tilde{\pi}_t^{X,LMP}$ and $\hat{\pi}_{lt}^{X,LMP}$ are uncertain parameter and variation range of X, X = {selling (S), purchasing (P)} (\$/KWh).

ρ_{but}^{LR} Load reduction comfort index for customer u in block b and hour t .

ρ_{ut}^{LS} Load shifting comfort index for customer u in hour t .

C. Variables

$P_{but}^{h,LR}, P_{ut}^{h,X}$ Non-adjustable auxiliary variables relating to the ELDR of P_{but}^{LR} and P_{ut}^X , respectively, X = {S, P} (KW).

P_{ut}^I Household compensated power of I program for customer u in hour t , I = {LC, LS} (KW).

P_{but}^{LR} Load reduction power offered through customer u in block b and hour t ; $P_{but}^{LR,I}$ is a component of P_{but}^{LR} related to I program, I = {LC, LS} (KW).

P_{ut}^{RE-G} Total power of RE and grid for customer u in hour t (KW).

$P_{Y,lbut}^{w,LR}, P_{Y,lut}^{w,X}$ Adjustable auxiliary variables relating to the ELDR of P_{but}^{LR} and P_{ut}^X , respectively, Y = {S, P, RE} and X = {S, P} (KW).

P_{ut}^X Power of X event for customer u in hour t , X = {S, P} (KW).

$P_{ut}^{\Lambda,ch}, P_{ut}^{\Lambda,dch}$ Charging and discharging power of Λ system of customer u in hour t , respectively, Λ = {ES, PEV} (KW).

SOC_{ut}^{Λ} State of charge of Λ system for customer u in hour t (KWh), Λ = {ES, PEV}.

$x_{ut}^{LR,I}, y_{ut}^{LR,I}$ Binary variables indicating startup and shutdown status of customer u for I in hour t , respectively, I = {LC, LS}.

$z_{ut}^{\Lambda,ch}, z_{ut}^{\Lambda,dch}$ Binary variables indicating charge/discharge status of Λ system for customer u in hour t .

z_{ut}^{\star} Binary variable indicating status of customer u for \star in hour t (1/0)

for online/offline), $\star = \{LR, LC; LR, LS; P; \text{home}(H)\}$.

$\pi_{lt}^{X,LMP}, P_{ut}^{RE}$ Continuous auxiliary modeling variables, $X = \{S, P\}$.

4.1 Introduction

4.1.1 Background and Motivation

Orders 719 and 745 of the U.S. Federal Energy Regulatory Commission (FERC) are addressing demand response (DR) as a means to help improve the competitiveness of the wholesale electricity markets by facilitating regional transmission organizations (RTO) and independent system operators (ISO) to reduce wholesale electricity prices, increase awareness of energy usage, enhance reliability, and mitigate market power [12, 67].

All customers including those in commercial, industrial, and residential sectors can participate in DR and demand-side energy management (DSEM) at the wholesale market level [13, 66, 68]. However, based on the U.S. Energy Information Administration (EIA), retail customers including those in the residential as well as small commercial and industrial sectors are the largest part in electricity demand. For instance, in 2016, the residential sector at 38%, was the highest percentage of the total electricity consumption [69]. Thus to involve retail customers in DR programs, demand response providers (DRP) and aggregators offer the power from demand response on behalf of retail customers directly into the wholesale electricity markets. Then, DRPs/aggregators provide incentives and benefits to retail customers as compensation for their flexibility in the timing and amount of their electricity consumption.

Extensive integration of distributed energy resources (DER) comprising of DR, renewable energy (RE) resources, energy storage (ES) systems, and electric vehicles (EV) can facilitate resource adequacy, improve system flexibility, reduce load curtailment, and enable customer behavior changes [70]. Significant research work has been concentrated on the incorporation of DR, RE, ES, and EV into demand-side energy management. In [71], an equilibrium problem with equilibrium constraints is proposed

to model interactions between merchant DR aggregators and merchant ES investors in a competitive electricity market. In [72], a residential dynamic energy management model optimizes the scheduling of controllable appliances and plug-in electric vehicles (PEV) of a single household to minimize the consumer electricity-related expenditures. A two-stage stochastic day-ahead power procurement model for energy consumers is introduced in [73] using DR to adjust energy consumption regarding time-varying electricity price, and ES to mitigate RE fluctuation and volatile prices.

DRPs and aggregators aim to obtain the maximum profit from the wholesale electricity market while a certain level of customers comfort and willingness are retained. The comfort level of thermostatically controlled loads of users (thermal comfort) is determined based on temperature thresholds [74]. In the stochastic model of [75], customers are divided into two subgroups based on the capability and willingness to respond to incentives and participate in DR: the responding group, and the non-responding group. In [76], the loss of customer comfort is modeled by waiting cost term in which a parameter controls the trade-off between minimizing the household payment and waiting time for the operation. A quadratic cost of providing DR is presented in [77], in which a customer's willingness to participate in curtailing its load is modeled by a coefficient between zero and one.

Additionally, non-deterministic methodologies such as stochastic programming [78], and robust optimization [79] have been used for characterizing the uncertainty of electricity market price and RE resources in DSEM problems. The stochastic programming approach uses scenarios to characterize uncertainty sources, and the robust optimization approach models uncertainty sources through bounded interval uncertainty sets [53]. Furthermore, to tackle the computational complexity of large-scale DSEM problems, distributed techniques such as decomposition [80], and alternating direction method of multipliers (ADMM) [81] are utilized. Iterative calculations in the decomposition method may necessitate noticeable computation time, and the

ADMM method requires a convex model. Linear decision rules (LDR) [82, 83] have been developed to overcome the aforementioned issues, and have been applied to solve complex decision-making problems [84, 85, 86, 87, 88]. In LDR-based approaches, linear relationships between the optimization variables and the uncertain parameters are assumed. In this chapter of the dissertation though, piecewise affine policies is used as extended LDRs (ELDR) [89, 90] to capture certain responses of the optimization variables to the uncertain parameters in order to obtain more accurate and realistic results.

4.1.2 Contributions

The main contributions of this chapter of dissertation are twofold:

1) A novel and comprehensive transactive energy system (TES) framework is proposed for the integration of the aggregated load reduction DR such as load curtailment (LC) and load shifting (LS), and PEV in which utilizing other DERs including on-site RE resources and behind-the-meter ES systems can increase the obtained profits from day-ahead electricity markets, and enhance DRPs/aggregators interactions with retail customers. In the proposed framework, load reduction offers and optimal PEV schedules are determined while considering customers willingness. To consider the impact of customers willingness, a comfort index (CI) in the proposed framework is designed.

2) A new ELDR to reformulate the TES as an affinely adjustable robust model is introduced to consider the uncertainties of electricity market clearing prices and renewable power generations. The impact of the budget of uncertainty on the ELDR-based robust TES is evaluated. Also, an out-of-sample procedure is presented to analyze the efficacy and performance of the proposed ELDR-based robust TES encountering different realizations of uncertain parameters.

4.2 Problem Description

4.2.1 Deterministic TES Model

The objective function (OF) of the proposed deterministic TES model (4.1) maximizes the profit of the DRP/aggregator.

$$\begin{aligned}
\text{Max}_{\Omega_1} \sum_{t \in T} \sum_{u \in U} & \left[\sum_{b \in B} \left[\overline{\overline{\pi}}_t^{\text{S,LMP}} - \pi_{but}^{\text{LR}} \right] \cdot P_{but}^{\text{LR}} \right] + \\
& \left[\pi_{ut}^{\text{P}} - \overline{\overline{\pi}}_t^{\text{P,LMP}} \right] \cdot P_{ut}^{\text{P}} + \left[\overline{\overline{\pi}}_t^{\text{S,LMP}} - \pi_{ut}^{\text{S}} \right] \cdot P_{ut}^{\text{S}} + \left[\lambda_1 \cdot P_{ut}^{\text{LC}} + \right. \\
& \left. \lambda_2 \cdot \rho_{ut}^{\text{LS}} \cdot P_{ut}^{\text{LS}} + \lambda_3 \cdot \left[\pi_{ut}^{\text{P}} - \overline{\overline{\pi}}_t^{\text{P,LMP}} \right] \cdot P_{ut}^{\text{ES,dch}} - \lambda_4 \cdot P_{ut}^{\text{S}} \right]
\end{aligned} \tag{4.1}$$

where $\Omega_1 = \left\{ P_{but}^{\text{LR}}, P_{ut}^{\text{S}}, P_{ut}^{\text{P}}, P_{ut}^{\text{LC}}, P_{ut}^{\text{LS}}, P_{but}^{\text{LR,LC}}, P_{but}^{\text{LR,LS}}, z_{ut}^{\text{P}}, z_{ut}^{\text{LR,I}}, x_{ut}^{\text{LR,I}}, y_{ut}^{\text{LR,I}}, z_{ut}^{\Lambda,\text{ch}}, z_{ut}^{\Lambda,\text{dch}}, P_{ut}^{\text{RE-G}}, P_{ut}^{\Lambda,\text{ch}}, P_{ut}^{\Lambda,\text{dch}}, SOC_{ut}^{\Lambda} \right\}$. The first row of (4.1) demonstrates the obtained profit through LR. The first and second terms of the second row of (4.1) represent the profit of purchasing from and selling to the grid, respectively. Also, the transactive energy can be restrained by coefficients λ_1 - λ_4 to control the trade-off between the profit and customers comfort level. λ_1 and λ_2 are capable of increasing the amount of the household power as compensation of the load reduction of LC and LS programs, respectively. Based on λ_3 as well as the purchasing residential and market prices, ES can be utilized instead of purchasing from the grid to decrease a customer's bill. The selling power to the grid can be adjusted to consider the customer's comfort level using the λ_4 coefficient.

A comfort index (CI) is introduced for each customer which includes two components: load reduction CI ρ_{but}^{LR} and load shifting CI ρ_{ut}^{LS} . In ρ_{but}^{LR} , each block represents a different value of the willingness of customer u in hour t for a different amount of LR, in which the higher block is associated with less CI and more LR, $0 \leq \rho_{But}^{\text{LR}} \leq \rho_{but}^{\text{LR}} \leq \rho_{1ut}^{\text{LR}} \leq 1$. The CI appears in π_{but}^{LR} which is a pricing function based on an inclining block rate

structure as an incentive price for the load reduction (LR) strategy:

$$\begin{aligned} \pi_{but}^{\text{LR}} &= [1 + [1 - \rho_{but}^{\text{LR}}]] \cdot \pi_{ut}^{\text{LR}} \\ &\text{if } K_{(b-1)ut}^{\text{LR}} < P_{but}^{\text{LR}} \leq K_{but}^{\text{LR}} \quad \forall b, \forall u, \forall t \end{aligned} \quad (4.2)$$

where K_{0ut}^{LR} and K_{But}^{LR} are the lower and upper limits of LR, respectively. The second CI component, ρ_{ut}^{LS} , shows the willingness of customer u for shifting load to hour t , $0 \leq \rho_{ut}^{\text{LS}} \leq 1$. The shifting CI is used in $\lambda_2 \cdot \rho_{ut}^{\text{LS}} \cdot P_{ut}^{\text{LS}}$ term of (4.1) to manage the household power compensation related to the LS program.

4.2.1.1 Demand Response Constraints

Constraint (4.3) defines the purchasing power bounds.

$$\underline{P}_{ut}^{\text{P}} \cdot z_{ut}^{\text{P}} \leq P_{ut}^{\text{P}} \leq \overline{P}_{ut}^{\text{P}} \cdot z_{ut}^{\text{P}} \quad \forall u, \forall t \quad (4.3)$$

Equation (4.4) states that LR includes LC and LS reductions, and their block limits are modeled through (4.5) and (4.6). The minimum operator in constraint (4.6) forces the block limits if the previous block is not equal to zero. Constraints (4.7)-(4.11) model the duration and number of each LR event, and constraint (4.12) enforces that either reduction events or purchasing can occur for customer u in hour t .

$$P_{but}^{\text{LR}} = P_{but}^{\text{LR,LC}} + P_{but}^{\text{LR,LS}} \quad \forall b, \forall u, \forall t \quad (4.4)$$

$$K_{0ut}^{\text{LR,I}} \cdot z_{ut}^{\text{LR,I}} \leq P_{1ut}^{\text{LR,I}} \leq K_{1ut}^{\text{LR,I}} \cdot z_{ut}^{\text{LR,I}} \quad \forall u, \forall t \quad (4.5)$$

$$P_{but}^{\text{LR,I}} \leq \text{Min} \left\{ [K_{but}^{\text{LR,I}} - K_{(b-1)ut}^{\text{LR,I}}], M \cdot P_{(b-1)ut}^{\text{LR,I}} \right\} \\ \forall b = 2 \dots B, \forall u, \forall t \quad (4.6)$$

$$\underline{rd}_u^{\text{LR,I}} \cdot x_{ut}^{\text{LR,I}} \leq \sum_{n=t}^{t+\underline{rd}_u^{\text{LR,I}}-1} z_{un}^{\text{LR,I}} \quad \forall u, \forall t \quad (4.7)$$

$$x_{ut}^{\text{LR,I}} \leq \sum_{n=t}^{t+\overline{rd}_u^{\text{LR,I}}} y_{ut}^{\text{LR,I}} \quad \forall u, \forall t \quad (4.8)$$

$$\sum_{t \in T} x_{ut}^{\text{LR,I}} \leq N_u^{\text{E,I}} \quad \forall u \quad (4.9)$$

$$z_{ut}^{\text{LR,I}} - z_{u(t-1)}^{\text{LR,I}} - x_{ut}^{\text{LR,I}} + y_{ut}^{\text{LR,I}} = 0 \quad \forall u, \forall t \quad (4.10)$$

$$x_{ut}^{\text{LR,I}} + y_{ut}^{\text{LR,I}} \leq 1 \quad \forall u, \forall t \quad (4.11)$$

$$z_{ut}^{\text{LR,LC}} + z_{ut}^{\text{LR,LS}} + 2 \cdot z_{ut}^{\text{P}} \leq 2 \quad \forall u, \forall t \quad (4.12)$$

where $I = \{\text{LC}, \text{LS}\}$.

4.2.1.2 Transactive Energy Control Constraints

The TES conceptual diagram of the proposed TES is illustrated in Figure 4.1, and its related transactive energy control is proposed in constraints (4.13) and (4.14). Household power compensation, and PEVs can be supplied by ESs as well as the grid. And, only the excess RE can be sold to the grid. Constraints (4.16) and (4.17) enforce that the selling can only occur when there is no purchasing and power compensation. According to (4.18) and (4.19), ESs only be used for household power compensation and PEVs. The amount of LC power compensation should be less than the total amount of LC reduction for customer u in hour t (4.20). Equation (4.21) forces the total amount of LS reduction during a day to be equal to the total amount of the compensated power for customer u during the day.

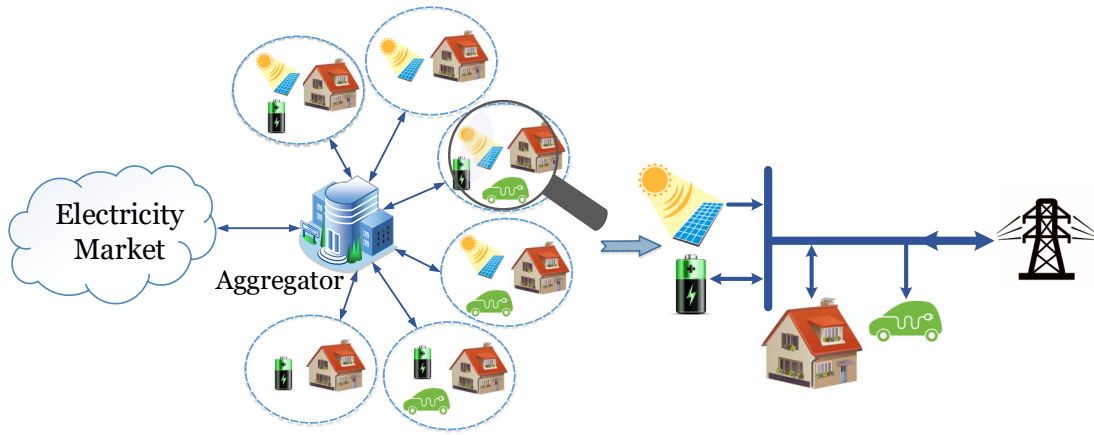


Figure 4.1: TES conceptual diagram.

$$P_{ut}^{\text{LC}} + P_{ut}^{\text{LS}} + P_{ut}^{\text{ES,ch}} + P_{ut}^{\text{PEV,ch}} = P_{ut}^{\text{ES,dch}} + P_{ut}^{\text{RE-G}} \quad \forall u, \forall t \quad (4.13)$$

$$P_{ut}^{\text{RE-G}} = \overline{P}_{ut}^{\text{RE}} + P_{ut}^{\text{P}} - P_{ut}^{\text{S}} \quad \forall u, \forall t \quad (4.14)$$

$$P_{ut}^{\text{G}} = P_{ut}^{\text{P}} - P_{ut}^{\text{S}} \quad \forall u, \forall t \quad (4.15)$$

$$0 \leq P_{ut}^{\text{S}} \leq M. (1 - z_{ut}^{\text{P}}) \quad \forall u, \forall t \quad (4.16)$$

$$0 \leq P_{ut}^{\text{S}} \leq M. (1 - z_{ut}^{\text{H}}) \quad \forall u, \forall t \quad (4.17)$$

$$0 \leq P_{ut}^{\text{LC}} + P_{ut}^{\text{LS}} + P_{ut}^{\text{PEV,ch}} \leq M. z_{ut}^{\text{H}} \quad \forall u, \forall t \quad (4.18)$$

$$P_{ut}^{\text{ES,dch}} \leq \overline{P}_u^{\text{ES,dch}} \cdot z_{ut}^{\text{H}} \quad \forall u, \forall t \quad (4.19)$$

$$\sum_{b \in B} P_{but}^{\text{LR,LC}} \geq P_{ut}^{\text{LC}} \quad \forall u, \forall t \quad (4.20)$$

$$\sum_{t \in T} \sum_{b \in B} P_{but}^{\text{LR,LS}} = \sum_{t \in T} P_{ut}^{\text{LS}} \quad \forall u \quad (4.21)$$

Without loss of generality, it assumed solar photovoltaics (PV) to be representative of RE resources, and behind-the-meter battery storage (BS) to represent ES systems.

4.2.1.3 Battery Storage and Plug-in Electric Vehicle Constraints

The charge and discharge limits of BS and PEV units are represented in constraints (4.22) and (4.23), respectively. The status of charging and discharging of BS and PEV units are indicated in constraint (4.24). The state of charge (SOC) limits of BS and PEV units, as well as the relationship of SOC at hour $t + 1$ to SOC, and the related power at hour t are declared in constraints (4.25) and (4.26), respectively.

$$P_{ut}^{\Lambda,\text{ch}} \leq \overline{P}_u^{\Lambda,\text{ch}} \cdot z_{ut}^{\Lambda,\text{dch}} \quad \forall u, \forall t \quad (4.22)$$

$$P_{ut}^{\Lambda,\text{dch}} \leq \overline{P}_u^{\Lambda,\text{dch}} \cdot z_{ut}^{\Lambda,\text{ch}} \quad \forall u, \forall t \quad (4.23)$$

$$z_{ut}^{\Lambda,\text{ch}} + z_{ut}^{\Lambda,\text{dch}} \leq 1 \quad \forall u, \forall t \quad (4.24)$$

$$\underline{SOC}_u^\Lambda \leq SOC_{ut}^\Lambda \leq \overline{SOC}_u^\Lambda \quad \forall u, \forall t \quad (4.25)$$

$$SOC_{ut}^\Lambda = (1 - \mu_u^\Lambda) \cdot SOC_{u(t-1)}^\Lambda + (\eta_u^{\Lambda,\text{ch}} \cdot P_{ut}^{\Lambda,\text{ch}} - \frac{1}{\eta_u^{\Lambda,\text{dch}}} \cdot P_{ut}^{\Lambda,\text{dch}}) \cdot \Delta T \quad \forall u, \forall t \quad (4.26)$$

where $\Lambda = \{\text{ES}, \text{PEV}\}$.

4.2.2 ELDR-based Robust TES Framework

4.2.2.1 Uncertainty Sets and Decision Policies

The uncertain parameters including electricity prices and the PV power generations are defined in a polyhedral uncertainty set as follows:

$$\text{US} = \left\{ \begin{array}{l} \tilde{\pi}_t^{\text{S,LMP}} = \overline{\overline{\pi}}_t^{\text{S,LMP}} - \sum_{l \in L} \pi_{lt}^{\text{S,LMP}} \quad \forall t \\ \tilde{\pi}_t^{\text{P,LMP}} = \overline{\overline{\pi}}_t^{\text{P,LMP}} + \sum_{l \in L} \pi_{lt}^{\text{P,LMP}} \quad \forall t \\ \tilde{P}_{ut}^{\text{RE}} = \overline{\overline{P}}_{ut}^{\text{RE}} - \sum_{l \in L} P_{ut}^{\text{RE}} \quad \forall u, \forall t \\ 0 \leq \frac{\pi_{lt}^{\text{X,LMP}}}{\overline{\overline{\pi}}_{lt}^{\text{X,LMP}}} \leq 1 \quad : \Pi_{\#,lt}^{\text{X}} \quad \forall l, \forall t \\ 0 \leq \frac{P_{lut}^{\text{RE}}}{\overline{\overline{P}}_{lut}^{\text{RE}}} \leq 1 \quad : \Pi_{\#,lut}^{\text{RE}} \quad \forall l, \forall u, \forall t \\ \sum_{t \in T} \sum_{l \in L} \frac{\pi_{lt}^{\text{X,LMP}}}{\overline{\overline{\pi}}_{lt}^{\text{X,LMP}}} \leq \Theta^{\text{X}} \quad : \Gamma_{\#}^{\text{X}} \\ \sum_{t \in T} \sum_{u \in U} \sum_{l \in L} \frac{P_{lut}^{\text{RE}}}{\overline{\overline{P}}_{lut}^{\text{RE}}} \leq \Theta^{\text{RE}} \quad : \Gamma_{\#}^{\text{RE}} \end{array} \right. \quad (4.27)$$

where $\text{X} = \{\text{S}, \text{P}\}$. $\Pi_{\#,lt}^{\text{X}} \geq 0$, $\Pi_{\#,lut}^{\text{RE}} \geq 0$, $\Gamma_{\#}^{\text{X}} \geq 0$, and $\Gamma_{\#}^{\text{RE}} \geq 0$ are the dual variables, and $\#$ indicates the number associated with each constraint. In the proposed ELDR methodology, to immunize against worst-case uncertainties, the worst-case realization of the uncertain parameters is considered. The uncertain selling LMPs, and uncertain renewable generations take their lower estimates, while the uncertain purchasing LMPs take the upper estimates.

The model variables can be distinguished in terms of being adjustable to the

uncertain data. While, the auxiliary variables (i.e. $P_{but}^{LR,LC}$, $P_{but}^{LR,LS}$, P_{ut}^{LC} , P_{ut}^{LS} , P_{ut}^{RE-G} , $P_{ut}^{\Lambda, ch}$, $P_{ut}^{\Lambda, dch}$, SOC_{ut}^{Λ}) can tune themselves to varying data, the here-and-now decision variables (i.e. $z_{ut}^{LR,I}$, $x_{ut}^{LR,I}$, $y_{ut}^{LR,I}$, z_{ut}^P , $z_{ut}^{\Lambda, ch}$, $z_{ut}^{\Lambda, dch}$) cannot be adjusted to the data. And wait-and-see decision variables (i.e. P_{but}^{LR} , P_{ut}^S , P_{ut}^P) can be provided when parts of the uncertain data become known to adjust themselves to all the data or to a part of it [82]. The ELDR policy between wait-and-see decision variables and uncertain parameters are defined in (4.28)-(4.30), in which P_{but}^{LR} , P_{ut}^S , and P_{ut}^P are parameterized based on a piecewise affine policy and by non-adjustable variables, and adjustable variables related to selling LMPs, purchasing LMPs, and PV power generations.

$$P_{but}^{LR} = P_{but}^{h,LR} + \sum_{l \in L} [P_{S,lbut}^{w,LR} \cdot \pi_{lt}^{S,LMP} + P_{P,lbut}^{w,LR} \cdot \pi_{lt}^{P,LMP} + P_{RE,lbut}^{w,LR} \cdot P_{lut}^{RE}] \quad \forall b, \forall u, \forall t \quad (4.28)$$

$$P_{ut}^S = P_{ut}^{h,S} + \sum_{l \in L} [P_{S,lut}^{w,S} \cdot \pi_{lt}^{S,LMP} + P_{P,lut}^{w,S} \cdot \pi_{lt}^{P,LMP} + P_{RE,lut}^{w,S} \cdot P_{lut}^{RE}] \quad \forall u, \forall t \quad (4.29)$$

$$P_{ut}^P = P_{ut}^{h,P} + \sum_{l \in L} [P_{S,lut}^{w,P} \cdot \pi_{lt}^{S,LMP} + P_{P,lut}^{w,P} \cdot \pi_{lt}^{P,LMP} + P_{RE,lut}^{w,P} \cdot P_{lut}^{RE}] \quad \forall u, \forall t \quad (4.30)$$

In the ELDR-based robust TES formulation, for each uncertainty source, the uncertain parameters and related adjustable variables are divided into several pieces to increase the flexibility and control of the conservativeness and robustness of the optimal solution against any realization of the uncertain parameters. The subinterval limits of adjustable variables are set as follows:

$$P_{Y,lbut}^{w,LR} \leq \text{Min} \left\{ [L_{lbut}^{LR,Y} - L_{(l-1)but}^{LR,Y}], M \cdot P_{Y,(l-1)but}^{w,LR} \right\} \quad \forall l, \forall b, \forall u, \forall t \quad (4.31)$$

$$P_{Y,lut}^{w,P} \leq \text{Min} \left\{ [L_{lut}^{P,Y} - L_{(l-1)ut}^{P,Y}], M.P_{Y,(l-1)ut}^{w,P} \right\} \\ \forall l, \forall u, \forall t \quad (4.32)$$

$$P_{Y,lut}^{w,S} \leq \text{Min} \left\{ [L_{lut}^{S,Y} - L_{(l-1)ut}^{S,Y}], M.P_{Y,(l-1)ut}^{w,S} \right\} \\ \forall l, \forall u, \forall t \quad (4.33)$$

where $Y = \{S, P, RE\}$.

4.2.3 Mathematical Formulation

The robust TES model of (4.1) can be written in the following compact epigraph form:

$$\begin{aligned} & \text{Max}_{\vartheta, \mathbf{z}, \mathbf{y}, \mathbf{p}} \vartheta \\ \text{s.t.} \quad & \mathbf{A}\mathbf{z} + \mathbf{B}\mathbf{y} + \mathbf{C}\mathbf{p} - \mathbf{d}\vartheta \geq \mathbf{R}\boldsymbol{\xi} + \mathbf{r} \quad \forall \boldsymbol{\xi} \in \text{US} \end{aligned} \quad (4.34)$$

The wait-and-see variable \mathbf{p} can take any relationship with uncertain parameter $\boldsymbol{\xi}$ and optimization over all possible relationships makes the model intractable. To make the proposed model tractable, the piecewise affine policy $\mathbf{p} = \mathbf{h} + \mathbf{W}\boldsymbol{\xi}$, i.e. (4.28)-(4.30), is replaced in (4.34), then the worst case reformulation to obtain the robust counterpart is equivalent to the following:

$$\begin{aligned} & \text{Max}_{\vartheta, \mathbf{z}, \mathbf{y}, \mathbf{p}} \vartheta \\ \text{s.t.} \quad & \mathbf{A}\mathbf{z} + \mathbf{B}\mathbf{y} + \mathbf{C}\mathbf{h} - \mathbf{d}\vartheta - \max_{\boldsymbol{\xi} \in \text{US}} (\mathbf{R} - \mathbf{C}\mathbf{W})\boldsymbol{\xi} \geq \mathbf{r} \quad \forall \boldsymbol{\xi} \in \text{US} \end{aligned} \quad (4.35)$$

The constraint (4.35) is still intractable. By using duality theory for the inner maximization over the uncertain parameter $\boldsymbol{\xi}$, the tractable robust counterpart can be obtained. To apply the duality, the inner maximization must be fixed independent of $\boldsymbol{\xi}$. In (4.35), $(\mathbf{R} - \mathbf{C}\mathbf{W})$ is fixed, therefore the reformulated robust counterpart is

equivalent as follows [83, 91]:

$$\begin{aligned}
& \text{Max}_{\vartheta, \mathbf{z}, \mathbf{y}, \mathbf{h}, \mathbf{W}, \mathbf{\Pi}} \vartheta \\
& \text{s.t.} \quad \mathbf{A}\mathbf{z} + \mathbf{B}\mathbf{y} + \mathbf{C}\mathbf{h} - \mathbf{d}\vartheta - \mathbf{\Pi}^T \geq \mathbf{r} \\
& \quad \mathbf{\Pi}^T \mathbf{E} \geq \mathbf{e} (\mathbf{R} - \mathbf{C}\mathbf{W})
\end{aligned} \tag{4.36}$$

where $\mathbf{\Pi} \geq 0$ is equal to $\Pi_{\#,lt}^X$, $\Pi_{\#,lut}^{\text{RE}}$ as well as $0 \leq \frac{\mathbf{E}}{\mathbf{e}} \leq 1$ equals $0 \leq \frac{\pi_{lt}^{\text{X,LMP}}}{\bar{\pi}_{lt}^{\text{X,LMP}}} \leq 1$, and $0 \leq \frac{P_{lut}^{\text{RE}}}{\bar{P}_{lut}^{\text{RE}}} \leq 1$ of the polyhedral uncertainty set US (4.27). Note that according to the constraint $0 \leq \frac{\mathbf{E}}{\mathbf{e}} \leq 1$, the coefficient of the associated dual variable $\mathbf{\Pi}$ in the main constraint equals one [53]. The corresponding ELDR-based formulation of the proposed deterministic TES framework (4.2.1) is provided in Appendix (E). The proposed ELDR-based robust TES model has a mixed-integer linear programming (MILP) form.

4.3 Numerical Results

4.3.1 Data

In this section, numerical analyses are conducted on a 7500-household case study obtained from PecanStreet [92]. The characteristics of the battery storage and the plug-in electric vehicle are taken from [93]. The day-ahead electricity market prices have been derived from the real price data of the electric reliability council of Texas (ERCOT) [94]. And time-of-use rates (TOU) for residential purchasing are available through [95]. To simulate the realistic customer behaviors in the load reduction CI ρ_{but}^{LR} , three time periods including off-peak, mid-peak, and on-peak are considered in which $\text{CI}_{\text{off-peak}}$ and $\text{CI}_{\text{on-peak}}$ have the highest and lowest values, respectively, and for each time period, three blocks are expressed as $\rho_{3ut}^{\text{LR}} \leq \rho_{2ut}^{\text{LR}} \leq \rho_{1ut}^{\text{LR}}$. The maximum deviation of the electricity price and PV power generation forecasts are equal to $0.2 \times \frac{\bar{\pi}_t^{\text{X,LMP}}}{\bar{\pi}_t^{\text{X,LMP}}}$ and $0.5 \times \frac{\bar{P}_{ut}^{\text{RE}}}{\bar{P}_{ut}^{\text{RE}}}$, respectively [34, 88]. The DER penetration considered in this chapter

of the dissertation equals 10%, 20% and 30% for BS, PEV, and PV, respectively. $N_u^{E,I} = 1$, and the minimum and maximum duration of each reduction event are 3 and 6 hours, respectively. Also, it is assumed that $\lambda_1, \lambda_2, \lambda_3$, and λ_4 equal one, as well as $\rho_{ut}^{LS} = 1$. All numerical experiments have been performed using CPLEX within GAMS [51] on a Macintosh-based computer with 3.3 GHz Intel Core i7 processor and 16 GB of RAM.

4.3.2 Evaluation of the Proposed Deterministic TES

Different scenarios are introduced to analyze the impact of DERs on the proposed TES model. The scenarios are as follows: Scen. 1 (DR), Scen. 2 (DR with PV), Scen. 3 (DR with PV, & BS), Scen. 4 (DR with PV, BS, & PEV). Note that the Scen. 4 is equivalent to the proposed deterministic TES framework. Table (4.1) provides the TES profit for different scenarios, and the following observations can be explained:

Scen. 1: The DRP/aggregator profit includes the LR profit, and the benefit obtained from purchased power as shifted loads.

Scen. 2: By adding PV to the basic model (i.e. Scen. 1), although the DRP/aggregator profit reduces, the customers' expense for purchasing power decrease. Due to limited DR events during a day, the remaining PV should be sold. Then, according to the constraint (4.17), the LR profit decreases.

Scen. 3: BS can store excess PV energy generated and the power purchased during the day to use for household compensated power. Therefore, LR and purchasing profits increase, while the selling profit decreases.

Scen. 4: The proposed TES for the integrated DERs including DR, PV, ES, and PEV not only attempts to attain a profitable strategy for DR programs, but also strives to achieve an efficient PEV charging schedule, while considering the customer's willingness. Hence, although LR profit in Scen. 4 is less than in Scen. 3, scheduling the charging PEV increases the purchasing profit, and therefore, the total obtained profit increases.

Table 4.1: The TES profit vs. different scenarios (\$)

Profit	Scen. 1	Scen. 2	Scen. 3	Scen. 4
Total	14,016	12,825	13,474	15,819
Load Reduction	12,011	10,892	11,406	11,107
Purchasing from Grid	2,005	882	1,689	3,744
Selling to Grid	0	1,051	979	968

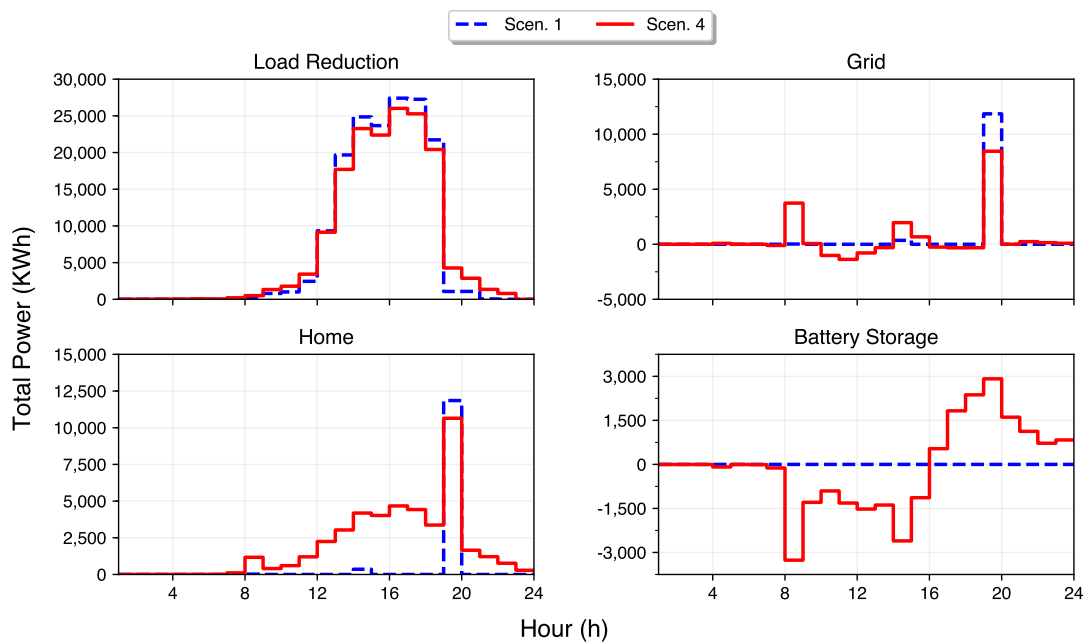


Figure 4.2: Total power of load reduction, grid, home, and battery storage.

The compensation of the total power of Scen. 1, and Scen. 4 is demonstrated in Figure 4.2. Although, the integration of DERs can lead to less LR, the grid power profile is flatter, and the household compensated power is increased which means more comfort for the customers. Note that the positive terms for grid power and BS power are the purchasing power, and BS discharging power, respectively. Also, a negative grid power and BS power refer to sold power, and charging BS power, respectively. Then, according to Table 4.1 and Figure 4.2, utilizing DERs not only is useful for DRPs/aggregators, but also increases the customer's comfort.

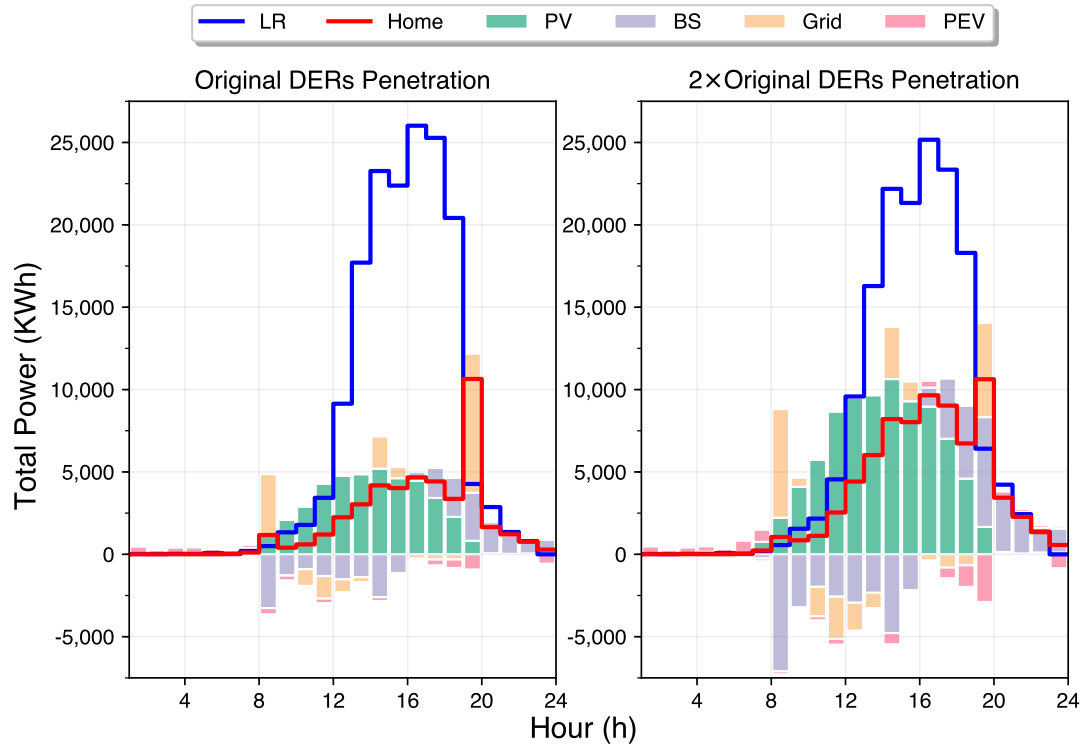


Figure 4.3: Total power of load reduction, grid, home, and battery storage.

The impact of different DER penetration on the proposed TES is illustrated in Figure 4.3. By doubling the original DER penetration (i.e. 20%, 40%, and 60% for ES, PEV, and PV, respectively), more BS can be charged by means of more PV or off-peak grid power. Then PV and BS can be used during peak times to increase the amount of the household compensation and PEV charging power. For instance, in hour 19, an increase in the household compensation and PEV charging power can be supplied by means of the increased PV and BS discharging power, and less power purchase is required. The maximum total power of the load reduction is 26 MWh, which means around 3.5 KWh load reduction for each customer. It is worth mentioning here that the positive PEV power, which is discharging power is determined by customers, and the negative PEV power, which is charging power, is obtained by the proposed TES model.

4.3.3 Evaluation of the Proposed ELDR-based Robust TES

In this section, the performance of the proposed ELDR-based robust TES is compared to the LDR-based robust TES. In the LDR approach, due to 24 hours, the budget uncertainties Θ^S , Θ^P are capable to change between $[0, 24]$. And since only 30% of 7500 customers have PV power, $\Theta^{RE} \in [0, 24 \times 2500]$. While, in the ELDR methodology, since two pieces (i.e. $L = 2$), $\Theta^S \in [0, 2 \times 24]$, $\Theta^P \in [0, 2 \times 24]$, and $\Theta^{RE} \in [0, 2 \times 24 \times 2500]$ are considered. For the sake of fair comparisons, the approaches are compared based on their conservatism levels. For instance, $0.00 \times \Theta^Y$ shows the zero robustness which equals the deterministic TES model, and $1.00 \times \Theta^Y$ represents the maximum robustness.

4.3.3.1 Robust TES vs. Budget of Uncertainty

The impact of the budget of uncertainty on the total profits and the computation time for all scenarios of the proposed TES model are illustrated in Table 4.2. By increasing the robustness level, the total profits of both LDR and ELDR approaches decrease. But, since the ELDR-based robust TES is designed to be less conservative than the LDR model, the total profit of the ELDR model is higher than the LDR model, while, the computational burdens of both the ELDR and the LDR are relatively close. Note that the presented times are the average of the four scenario times. The approaches can rapidly reach to their maximum robustness, even before the maximum budget of uncertainty, since all uncertain parameters have adopted their worst values.

4.3.3.2 Out-of-Sample Procedure

Finally, an out-of-sample procedure is introduced to practically compare the effectiveness and performance of the two methodologies. For the sake of simplicity, the procedure is only applied to Scen. 4 – the most comprehensive scenario of the proposed TES framework. The decision variables of the robust TES model are fixed at the obtained optimal results of the energy transaction schedule for a specific value of

Table 4.2: The total profit (\$) and computation time (s) of the proposed robust TES model vs. budget of uncertainty

Θ^Y	Scen. 1	Scen. 2	Scen. 3	Scen. 4	CPU Time
	LDR-based Robust TES				
$0.00 \times \Theta^Y$	14,016	12,825	13,474	15,819	1,692
$0.25 \times \Theta^Y$	11,369	9,034	9,569	11,713	1,759
$0.50 \times \Theta^Y$	11,369	9,034	9,569	11,713	1,793
$0.75 \times \Theta^Y$	11,369	9,034	9,569	11,713	1,824
$1.00 \times \Theta^Y$	11,369	9,034	9,569	11,713	1,868
LDR-based Robust TES					
$0.00 \times \Theta^Y$	14,016	12,825	13,474	15,819	1,692
$0.25 \times \Theta^Y$	11,577	9,454	10,065	12,280	1,790
$0.50 \times \Theta^Y$	11,577	9,454	10,065	12,280	1,834
$0.75 \times \Theta^Y$	11,577	9,454	10,065	12,280	1,875
$1.00 \times \Theta^Y$	11,577	9,454	10,065	12,280	1,915

the budget of uncertainty. This is the schedule that the DRP/aggregator provides for the customers. Day-ahead LMPs [94], and PV power generations [92] are utilized to obtain the actual profit. Also the deviation of the actual realized PV power generation should be compensated through real-time power purchasing. Therefore, the actual profit includes the customers' schedule with actual LMPs and PV power as well as the real-time purchased power cost. The above-mentioned out-of-sample procedure is run for seven days, and the mean value is presented as the out-of-sample profit in Table 4.3. By changing the budget of uncertainty from zero to $0.04 \times \Theta^Y$ in 0.01 steps, the total profit of the proposed robust TES in both approaches decreases, while in the LDR-based and ELDR-based frameworks, after $0.03 \times \Theta^Y$ and $0.04 \times \Theta^Y$ respectively, the total profits are identical. The out-of-sample results imply that the ELDR-based

Table 4.3: The total profit and out-of-sample results

Θ^Y	Robust TES		Out-of-Sample		Profit Increment	
	(\$)		(\$)		(%)	
	LDR	ELDR	LDR	ELDR	LDR	ELDR
$0.00 \times \Theta^Y$	15,819	15,819	12,594	12,594	0.00	0.00
$0.01 \times \Theta^Y$	13,541	14,306	14,635	14,386	16.21	14.23
$0.02 \times \Theta^Y$	12,528	13,657	15,509	14,863	23.15	18.01
$0.03 \times \Theta^Y$	11,713	12,902	14,497	16,223	15.11	28.82
$0.04 \times \Theta^Y$	11,713	12,280	14,497	15,264	15.11	21.20

robust TES model with the budget of uncertainty $0.03 \times \Theta^Y$ obtains the highest profit \$16,223 with 28.82% increment than the out-of-sample profit of the deterministic model, which indicates the efficacy and flexibility of the proposed framework. Note that increasing the budget of uncertainty to $0.04 \times \Theta^Y$ leads to a reduction in ELDR-based out-of-sample profit, since this robustness is excessively conservative for the uncertainty sources.

4.4 Conclusion

A new TES is proposed for the integrated DERs comprising the aggregated load reduction DR, PEV, on-site RE resources, and behind-the-meter ES systems. Simultaneously, a CI is designed to consider the impact of customer willingness to accept the LR offer and PEV schedule to obtain the optimal profit while enhancing DSEM. A new ELDR is introduced to model the uncertainty sources of electricity market clearing prices and renewable real power generation by reformulating the proposed TES framework as an affinely adjustable robust optimization model. The results on a large-scale case study demonstrate the applicability and effectiveness of the proposed model. The impact of DERs on the TES model has been assessed by considering different scenarios. Also, the performance of the proposed ELDR-based

robust TES has been compared with the LDR-based robust TES with respect to the budget of uncertainty and an out-of-sample procedure. By changing the budget of uncertainty, the ELDR-based robust TES demonstrates less conservative behavior than the LDR-based model. Additionally, the out-of-sample procedure has indicated the effectiveness of the ELDR-based robust TES framework encountering different realizations of uncertain parameters [96].

CHAPTER 5: CONCLUSIONS

In Chapter 2, the performance of various robust self-scheduling methodologies was evaluated and compared. These robust methodologies have different uncertainty modeling approaches, as well as a range of tools for controlling the conservativeness of their solutions. In addition to recasting the robust methodologies in more applicable forms, offer curve constructing strategy for each method has been presented. Moreover, to practically evaluate the performance of various methodologies, a post-optimization procedure has been proposed to determine the actual profit of each method in different real-market-environment cases. The conclusions drawn from the evaluations can help GenCos select and model the most appropriate non-deterministic self-scheduling approach based on the price information and price forecast method that they have adopted, as well as the robustness level that they desire in their solution.

In Chapter 3, an integrated capacity market and DR model was developed in which DRR can participate in the capacity market to reduce the required transmission capacity as an alternative transmission expansion planning solution instead of the expensive transmission upgrade solution. In addition, DRR can be used in the capacity market as a resource to decrease the load to meet the reliability requirement and improve the social welfare of the capacity market. The proposed model was based on the PJM capacity market model. The designed model in this chapter of the dissertation can help ISOs/RTOs to manage the capacity market and transmission expansion planning more efficiently and flexibly. It can also help large consumers or LSEs to manage their loads and earn a profit. To investigate the performance of the proposed framework, it was implemented on the BRA of 2020/2021 PJM capacity market real data, and the influence of several important parameters are investigated

in detail to control the capacity market cost and LMP.

In Chapter 4, a novel TES for the integrated DERs comprising the aggregated load reduction DR, PEV, on-site RE resources, and behind-the-meter ES systems was proposed. Simultaneously, a CI was designed to model the impact of customer willingness to accept the LR offer and PEV schedule to obtain the optimal profit while enhancing DSEM. A new ELDR was introduced to model the uncertainty sources of electricity market clearing prices and renewable real power generation by reformulating the proposed TES framework as an affinity adjustable robust optimization model. The results on a large-scale test system illustrate the applicability and effectiveness of the proposed model. The impact of DERs on the TES model has been evaluated by considering different scenarios. Also, the performance of the proposed ELDR-based robust TES has been compared with the LDR-based robust TES with respect to the budget of uncertainty and an out-of-sample procedure. By changing the budget of uncertainty, the ELDR-based robust TES demonstrates less conservative behavior than the LDR-based model. Additionally, the out-of-sample procedure has indicated the effectiveness of the ELDR-based robust TES framework encountering different realizations of uncertain parameters.

5.1 Contributions

A summary of the main contributions of the dissertation are as follows:

1. The mathematical formulations of different robust approaches including Box RO (BRO), Ellipsoidal RO (ERO), Polyhedral RO (PRO), Box and Ellipsoidal RO (BERO), Box and Polyhedral RO (BPRO), CVaR-SP, and IGDT models are proposed. Also, the characteristics of the uncertainty sets corresponding to BRO, ERO, PRO, BERO, and BPRO are presented by means of relevant theorems and proofs. Previous research work in this area have either only used these approaches [17, 18, 19, 20, 21, 22, 23, 24] or compared these methods without any mathematical proof [31]. Accordingly, to the best of my knowledge,

there is no existing research work that mathematically characterizes the robust approaches [53].

2. Various self-scheduling strategies based on the robust approaches are proposed for GenCos to participate in an electricity market considering the price data and desired robustness level [53].
3. To correctly analyze and compare the performance of these robust methodologies in the uncertain environment of self-scheduling, a post-optimization procedure is proposed. This procedure evaluates the long-run performance of the robust methodologies encountering different realizations of uncertain electricity prices [53].
4. Proposing a novel integrated capacity market and demand response model as an alternative solution to the transmission expansion planning problem [66].
5. Including the use of the demand response resources as power supply resources to participate in the capacity market [66].
6. A novel and comprehensive transactive energy system (TES) framework is proposed for the integration of the aggregated load reduction DR such as load curtailment (LC) and load shifting (LS), and PEV in which utilizing other DERs including on-site RE resources and behind-the-meter ES systems can increase the obtained profits from day-ahead electricity markets, and enhance DRPs/aggregators interactions with retail customers. In the proposed framework, load reduction offers and optimal PEV schedules are determined while considering customers willingness. To consider the impact of customers willingness, a comfort index (CI) in the proposed framework is designed [96].
7. A new ELDR to reformulate the TES as an affinely adjustable robust model is introduced to consider the uncertainties of electricity market clearing prices

and renewable power generations. The impact of the budget of uncertainty on the ELDR-based robust TES is evaluated. Also, an out-of-sample procedure is presented to analyze the efficacy and performance of the proposed ELDR-based robust TES encountering different realizations of uncertain parameters [96].

5.2 Future Work

Analyzing and comparing the performance of the non-deterministic approaches for multi-auctions self-scheduling model as well as considering different sources of uncertainty, such as electricity market price, renewable resources and so on, are set aside to be studied as future work.

The application of the demand response as an alternative solution for different problems such as frequency control in different electricity markets, e.g. real-time or ancillary service markets can be studied in future.

The transactive energy system for commercial or industrial customers considering different types of demand response programs such as critical peak pricing, time-of-use, as well as different DERs can be proposed.

REFERENCES

- [1] Energy Management Systems (EMS) Introduction. 2018. [Online]. Available: https://web.stanford.edu/class/archive/ee/ee392n/ee392n.1116/Lectures/EE392n_Lecture5GE.pdf.
- [2] Advanced Energy Management. 2018. [Online]. Available: https://www.gegridsolutions.com/Software_Solutions/energymanagement.htm.
- [3] Energy Management System. 2018. [Online]. Available: <https://etap.com/packages/energy-management-system>.
- [4] Electric Utility Demand Side Management. 2018. [Online]. Available: <https://www.eia.gov/electricity/data/eia861/dsm/>.
- [5] Demand Side Management. 2018. [Online]. Available: https://www.ema.gov.sg/Demand_Side_Management.aspx.
- [6] D. Lee, H. Shin, and R. Baldick, "Bivariate probabilistic wind power and real-time price forecasting and their applications to wind power bidding strategy development," *IEEE Trans. Power Syst.*, 2018. doi: 10.1109/TPWRS.2018.2830785.
- [7] B. Vatani, S. Mohajeryami, S. Dehghan, and N. Amjady, "Self-scheduling of generation companies via stochastic optimization considering uncertainty of units," *IEEE Power Energy Soc. Gen. Meeting*, pp. 1–5, Jul. 2016.
- [8] N. Amjady, B. Vatani, and H. Sharifzadeh, "Optimum stochastic self-scheduling for genco considering pool auction and bilateral contracts," *Journal of Modeling in Engineering*, vol. 9, no. 24, pp. 21–28, 2011.
- [9] M. R. Ansari, N. Amjady, and B. Vatani, "Stochastic security-constrained hydrothermal unit commitment considering uncertainty of load forecast, inflows to reservoirs and unavailability of units by a new hybrid decomposition strategy," *IET Gener. Transm. Distrib.*, vol. 8, pp. 1900–1915, Dec. 2014.
- [10] J. Lin and B. Vatani, "Impact of capacity market design on power system decarbonization," *14th International Conference on the European Energy Market*, pp. 1–6, Jun. 2017.
- [11] North American Electric Reliability Corporation. 2018. [Online]. Available: <https://www.nerc.com/>.
- [12] Federal Energy Regulatory Commission, "Demand response compensation in organized wholesale energy markets," 2011.
- [13] U.S. Department of Energy, "Benefits of demand response in electricity markets and recommendations for achieving them: A report to the united states congress pursuant to section 1252 of the energy policy act of 2005," 2006.

- [14] N. G. Paterakis, M. Gibescu, A. G. Bakirtzis, and J. P. S. Catalão, “A multi-objective optimization approach to risk-constrained energy and reserve procurement using demand response,” *IEEE Trans. Power Syst.*, vol. 33, pp. 3940–3954, Jul. 2018.
- [15] G. Benysek, J. Bojarski, R. Smolenski, M. Jarnut, and S. Werminski, “Application of stochastic decentralized active demand response (dadr) system for load frequency control,” *IEEE Trans. Smart Grid*, vol. 9, pp. 1055–1062, Mar. 2018.
- [16] M. Shahidehpour, H. Yamin, and Z. Li, *Market operations in electric power systems: forecasting, scheduling, and risk management*. John Wiley & Sons: New York, Apr. 2002.
- [17] R. A. Jabr, “Self-scheduling under ellipsoidal price uncertainty: conic-optimisation approach,” *IET Gener. Transm. Distrib.*, vol. 1, pp. 23–29, Jan. 2007.
- [18] R. A. Jabr, “Worst-case robust profit in generation self-scheduling,” *IEEE Trans. Power Syst.*, vol. 24, pp. 492–493, Feb. 2009.
- [19] L. Baringo and A. J. Conejo, “Offering strategy via robust optimization,” *IEEE Trans. Power Syst.*, vol. 26, pp. 1418–1425, Aug. 2011.
- [20] A. A. Thatte, L. Xie, D. E. Viassolo, and S. Singho, “Risk measure based robust bidding strategy for arbitrage using a wind farm and energy storage,” *IEEE Trans. Smart Grid*, vol. 4, pp. 2191–2199, Dec. 2013.
- [21] L. P. Garces and A. J. Conejo, “Weekly self-scheduling, forward contracting, and offering strategy for a producer,” *IEEE Trans. Power Syst.*, vol. 25, pp. 657–666, May 2010.
- [22] B. Vatani, N. Amjady, and H. Zareipour, “Stochastic self-scheduling of generation companies in day-ahead multi-auction electricity markets considering uncertainty of units and electricity market prices,” *IET Gener. Transm. Distrib.*, vol. 7, pp. 735–744, Jul. 2013.
- [23] B. Mohammadi-Ivatloo, H. Zareipour, N. Amjady, and M. Ehsan, “Application of information-gap decision theory to risk-constrained self-scheduling of gencos,” *IEEE Trans. Power Syst.*, vol. 28, pp. 1093–1102, May 2013.
- [24] M. Kazemi, B. Mohammadi-Ivatloo, and M. Ehsan, “Risk-constrained strategic bidding of gencos considering demand response,” *IEEE Trans. Power Syst.*, vol. 30, pp. 376–384, Jan. 2015.
- [25] A. Ben-Tal, L. El Ghaoui, and A. Nemirovski, *Robust optimization*. Princeton University Press, 2009.
- [26] D. Bertsimas and M. Sim, “The price of robustness,” *Oper. Res.*, vol. 52, pp. 35–53, Jan./Feb. 2004.

- [27] A. Ben-Tal and A. Nemirovski, “Robust solutions of linear programming problems contaminated with uncertain data,” *Math. Program.*, vol. 88, pp. 411–424, Sep. 2000.
- [28] J. R. Birge and F. Louveaux, *Introduction to stochastic programming*. Springer Verlag, 1997.
- [29] R. T. Rockafellar and S. Uryasev, “Optimization of conditional value-at-risk,” *J. Risk*, vol. 2, pp. 21–42, 2000.
- [30] Y. Ben-Haim, *Info-gap decision theory: decisions under severe uncertainty*. 2nd ed., San Diego, CA: Academic Press, 2006.
- [31] Q. P. Zheng, J. Wang, and A. L. Liu, “Stochastic optimization for unit commitment—a review,” *IEEE Trans. Power Syst.*, vol. 30, pp. 1913–1924, Jul. 2015.
- [32] J. Ostrowski, M. F. Anjos, and A. Vannelli, “Tight mixed integer linear programming formulations for the unit commitment problem,” *IEEE Trans. Power Syst.*, vol. 27, pp. 39–46, Feb. 2012.
- [33] L. Fan, J. Wang, R. Jiang, and Y. Guan, “Min-max regret bidding strategy for thermal generator considering price uncertainty,” *IEEE Trans. Power Syst.*, vol. 29, pp. 2169–2179, Sep. 2014.
- [34] S. Dehghan, N. Amjady, B. Vatani, and H. Zareipour, “A new hybrid stochastic-robust optimization approach for self-scheduling of generation companies,” *Int. Trans. Elec. Energy Syst.*, vol. 26, pp. 1244–1259, Jun. 2016.
- [35] M. Carrion and J. M. Arroyo, “A computationally efficient mixed-integer linear formulation for the thermal unit commitment problem,” *IEEE Trans. Power Syst.*, vol. 21, pp. 1371–1378, Aug. 2006.
- [36] S. Boyd and L. Vandenberghe, *Convex optimization*. Cambridge University Press, 2004.
- [37] IBM. 2018. [Online]. Available: <http://www.ibm.com/support/knowledgecenter>.
- [38] G. H. Golub, and C. F. V. Loan, *Matrix Computations*. 3rd ed., Johns Hopkins University Press, 1996.
- [39] M. Ahmadigorji, N. Amjady, and S. Dehghan, “A robust model for multiyear distribution network reinforcement planning based on information-gap decision theory,” *IEEE Trans. Power Syst.*, vol. 33, pp. 1339–1351, Mar. 2018.
- [40] S. Dehghan, A. Kazemi, and N. Amjady, “Multi-objective robust transmission expansion planning using information-gap decision theory and augmented ϵ -constraint method,” *IET Gener. Transm. Distrib.*, vol. 8, pp. 828–840, May 2014.

- [41] A. Soroudi and M. Ehsan, "IGDT based robust decision making tool for dns in load procurement under severe uncertainty," *IEEE Trans. Smart Grid*, vol. 4, pp. 886–895, Jun. 2013.
- [42] K. Chen, W. Wu, B. Zhang, and H. Sun, "Robust restoration decision-making model for distribution networks based on information gap decision theory," *IEEE Trans. Smart Grid*, vol. 6, pp. 587–597, Mar. 2015.
- [43] A. J. Conejo, J. Contreras, R. Espinola, and M. A. Plazas, "Forecasting electricity prices for a day-ahead pool-based electric energy market," *Int. J. Forecast.*, vol. 21, pp. 435–462, Jul.-Sep. 2005.
- [44] R. Dominguez, L. Baringo, and A. J. Conejo, "Optimal offering strategy for a concentrating solar power plant," *Applied Energy*, vol. 98, pp. 316–325, Oct. 2012.
- [45] H. M. I. Pousinho, J. Contreras, P. Pinson, and V. M. F. Mendes, "Robust optimisation for self-scheduling and bidding strategies of hybrid csp-fossil power plants," *Int. J. Elect. Power Energy Syst.*, vol. 67, pp. 639–650, May 2015.
- [46] L. Baringo and A. J. Conejo, "Offering strategy of wind-power producer: a multi-stage risk-constrained approach," *IEEE Trans. Power Syst.*, vol. 31, pp. 1420–1429, Mar. 2016.
- [47] M. Kohansal and H. Mohsenian-Rad, "Price-maker economic bidding in two-settlement pool-based markets: the case of time-shiftable loads," *IEEE Trans. Power Syst.*, vol. 31, pp. 695–705, Jan. 2016.
- [48] O. Alsac and B. Stott, "Optimal load flow with steady-state security," *IEEE Trans. Power Appar. Syst.*, vol. 93, pp. 745–751, May 1974.
- [49] IEEE 118-bus test system. 2018. [Online]. Available: <http://motor.ece.iit.edu/data/PBUData.pdf>.
- [50] New York Independent System Operator, NYISO. 2018. [Online]. Available: <http://www.nyiso.com>.
- [51] N. Rosenthal, "Gams: a user's guide," *GAMS development corporation: Washington, DC*, 2017.
- [52] N. Amjady, *Electric power systems: advanced forecasting techniques and optimal generation scheduling*. Chapter 4, CRC Press, Taylor & Francis, 2012.
- [53] B. Vatani, B. Chowdhury, S. Dehghan, and N. Amjady, "A critical review of robust self-scheduling for generation companies under electricity price uncertainty," *Int. J. Elect. Power Energy Syst.*, vol. 97, pp. 428–439, Apr. 2018.
- [54] B. F. Hobbs, M. Hu, J. G. Inon, S. E. Stoft, and M. P. Bhavaraju, "A dynamic analysis of a demand curve-based capacity market proposal: the PJM reliability pricing model," *IEEE Trans. Power Syst.*, vol. 22, pp. 3–14, Feb. 2007.

- [55] A. N. Zucarato, and E. L. da Silva, "Simulation model to assess the performance of a forward capacity market for hydro-based systems," *IET Gener. Transm. Distrib.*, vol. 6, pp. 1086–1095, Nov. 2012.
- [56] D. Hach, C. K. Chyong, and S. Spinler, "Capacity market design options: a dynamic capacity investment model and a GB case study," *Euro. J. Opr. Res.*, vol. 249, pp. 691–705, Mar. 2016.
- [57] Y. Liu, "Demand response and energy efficiency in the capacity resource procurement: case studies of forward capacity markets in ISO New England, PJM and Great Britain," *Energy Policy*, vol. 100, pp. 271–282, Jan. 2017.
- [58] Y. Xiao, Y. Lee, F. S. Bresler, J. Bastian, and A. Engle, "Integration of demand resource into PJM capacity market incremental auction," *IEEE Power Energy Soc. Gen. Meeting*, 2013.
- [59] PJM Manual 18: PJM Capacity Market. 2018. [Online]. Available: <http://www.pjm.com/~media/documents/manuals/m18.ashx>.
- [60] Capacity Market (RPM), PJM. 2018. [Online]. Available: <https://learn.pjm.com/three-priorities/buying-and-selling-energy/capacity-markets.aspx>.
- [61] PJM. 2018. [Online]. Available: <http://pjm.com>.
- [62] Forward Capacity Market, ISO-New England. 2018. [Online]. Available: <https://www.iso-ne.com/markets-operations/markets/forward-capacity-market>.
- [63] B. Vatani, B. Chowdhury, and J. Lin, "The role of demand response as an alternative transmission expansion solution in a capacity market," *2017 IEEE IAS Annu. Meeting*.
- [64] Price Responsive Demand, PJM. 2018. [Online]. Available: <https://www.pjm.com/~media/about-pjm/newsroom/fact-sheets/price-responsive-demand.ashx>.
- [65] Demand Response Subcommittee, PJM. 2018. [Online]. Available: <http://www.pjm.com/committees-and-groups/subcommittees/drs.aspx>.
- [66] B. Vatani, B. Chowdhury, and J. Lin, "The role of demand response as an alternative transmission expansion solution in a capacity market," *IEEE Trans. Ind. Appl.*, vol. 54, pp. 1039–1046, Mar. 2018.
- [67] Federal Energy Regulatory Commission, "Wholesale competition in regions with organized electric markets." 2008. [Online]. Available: <http://www.ferc.gov>.
- [68] C. L. Su and D. Kirschen, "Quantifying the effect of demand response on electricity markets," *IEEE Trans. Power Syst.*, vol. 24, pp. 1199–1207, Aug. 2009.

- [69] U.S. Energy Information Administration, “Use of electricity.” 2017. [Online]. Available: <https://www.eia.gov>.
- [70] Electric Power Research Institute, “The integrated grid: realizing the full value of central and distributed energy resources.” 2014. [Online]. Available: <https://www.energy.gov/sites/prod/files/2015/03/f20/EPRI%20Integrated%20Grid021014.pdf>.
- [71] Y. Dvorkin, “Can merchant demand response affect investments in merchant energy storage?,” *IEEE Trans. Power Syst.*, vol. 33, pp. 2671–2683, May 2018.
- [72] M. Muratori and G. Rizzoni, “Residential demand response: Dynamic energy management and time-varying electricity pricing,” *IEEE Trans. Power Syst.*, vol. 31, pp. 1108–1117, Mar. 2016.
- [73] J. Leithon, S. Sun, and T. J. Lim, “Demand response and renewable energy management using continuous-time optimization,” *IEEE Trans. Sustain. Energy*, vol. 9, pp. 991–1000, Apr. 2018.
- [74] A. Abiri-Jahromi and F. Bouffard, “Contingency-Type Reserve Leveraged Through Aggregated Thermostatically-Controlled Loads—Part I: Characterization and Control,” *IEEE Trans. Power Syst.*, vol. 31, pp. 1972–1980, May 2016.
- [75] M. Song and M. Amelin, “Purchase bidding strategy for a retailer with flexible demands in day-ahead electricity market,” *IEEE Trans. Power Syst.*, vol. 32, pp. 1839–1850, May 2017.
- [76] A. H. Mohsenian-Rad and A. Leon-Garcia, “Optimal residential load control with price prediction in real-time electricity pricing environments,” *IEEE Trans. Smart Grid*, vol. 1, pp. 120–133, Sep. 2010.
- [77] D. T. Nguyen, M. Negnevitsky, and M. de Groot, “Pool-based demand response exchange—concept and modeling,” *IEEE Trans. Power Syst.*, vol. 26, pp. 1677–1685, Aug. 2011.
- [78] M. Asensio and J. Contreras, “Risk-constrained optimal bidding strategy for pairing of wind and demand response resources,” *IEEE Trans. Smart Grid*, vol. 8, pp. 200–208, Jan. 2017.
- [79] E. M. Moghaddam, M. Nayeripour, J. Aghaei, A. Khodaei, and E. Waffenschmidt, “Interactive robust model for energy service providers integrating demand response programs in wholesale markets,” *IEEE Trans. Smart Grid*. doi: 10.1109/TSG.2016.2615639.
- [80] R. Deng, Z. Yang, F. Hou, M. Y. Chow, and J. Chen, “Distributed real-time demand response in multiseller–multibuyer smart distribution grid,” *IEEE Trans. Power Syst.*, vol. 30, pp. 2364–2374, Sep. 2015.

- [81] Y. Zhang and G. B. Giannakis, “Distributed stochastic market clearing with high-penetration wind power,” *IEEE Trans. Power Syst.*, vol. 31, pp. 895–906, Mar. 2016.
- [82] A. Ben-Tal, A. Goryashko, E. Guslitzer, and A. Nemirovski, “Adjustable robust solutions of uncertain linear programs,” *Math. Program.*, vol. 99, pp. 351–376, Mar. 2004.
- [83] D. Bertsimas and F. J. C. T. de Ruiter, “Duality in two-stage adaptive linear optimization: Faster computation and stronger bounds,” *INFORMS J. Comp.*, vol. 28, pp. 500–511, May 2016.
- [84] J. Warrington, C. Hohl, P. J. Goulart, and M. Morari, “Rolling unit commitment and dispatch with multi-stage recourse policies for heterogeneous devices,” *IEEE Trans. Power Syst.*, vol. 31, pp. 187–197, Jan. 2016.
- [85] R. Domínguez, A. J. Conejo, and M. Carrión, “Investing in generation capacity: A multi-stage linear-decision-rule approach,” *IEEE Trans. Power Syst.*, vol. 31, pp. 4784–4794, Nov. 2016.
- [86] S. Dehghan, N. Amjady, and A. J. Conejo, “Adaptive robust transmission expansion planning using linear decision rules,” *IEEE Trans. Power Syst.*, vol. 32, pp. 4024–4034, Sep. 2017.
- [87] H. Ding, P. Pinson, Z. Hu, J. Wang, and Y. Song, “Optimal offering and operating strategy for a large wind-storage system as a price maker,” *IEEE Trans. Power Syst.*, vol. 32, pp. 4904–4913, Nov. 2017.
- [88] R. A. Jabr, “Linear decision rules for control of reactive power by distributed photovoltaic generators,” *IEEE Trans. Power Syst.*, vol. 33, pp. 2165–2174, Mar. 2018.
- [89] X. Chen and Y. Zhang, “Uncertain linear programs: Extended affinely adjustable robust counterparts,” *Opr. Resr.*, vol. 57, pp. 1469–1482, Mar. 2009.
- [90] A. Ben-Tal, O. E. Housni, and V. Goyal, “A tractable approach for designing piecewise affine policies in dynamic robust optimization.” 2018. [Online]. Available: http://optimization-online.org/DB_FILE/2016/07/5557.pdf.
- [91] B. L. Gorissen, I. Yanikoglu, and D. den Hertog, “A practical guide to robust optimization,” *Omega*, vol. 53, pp. 124 – 137, 2015.
- [92] Pecan Street. 2018. [Online]. Available: <https://www.pecanstreet.org>.
- [93] Tesla. 2018. [Online]. Available: <https://www.tesla.com>.
- [94] Electric Reliability Council of Texas. 2018. [Online]. Available: <http://www.ercot.com>.

- [95] Austin Energy. 2018. [Online]. Available: <https://austinenergy.com>.
- [96] B. Vatani and B. Chowdhury, "Robust transactive energy system framework with integrated demand response and der using extended linear decision rules," *IEEE Trans. Power Syst.* Under Review.
- [97] J. M. Steele, *The Cauchy-Schwarz Master Class: An Introduction to the Art of Mathematical Inequalities*. Cambridge University Press, 2004.

APPENDIX A: The LINEARIZATION OF THE GENERATION COST
FUNCTIONS

The quadratic generation cost function $f_u(\cdot)$ is as follows:

$$f_u(p_{ut}) = a_u + b_u \cdot p_{ut} + c_u \cdot p_{ut}^2 \quad \forall u, \forall t \quad (\text{A.1})$$

By applying the piecewise linear approximation [35] to (A.1), the linearized generation cost function is obtained in (A.2)-(A.6).

$$f_u(p_{ut}) = A_u \cdot z_{ut} + \sum_{l=1}^{N_u^l} (S_{lu} \cdot pb_{lut}) \quad \forall u, \forall t \quad (\text{A.2})$$

$$p_{ut} = P_u^{\min} \cdot z_{ut} + \sum_{l=1}^{N_u^l} pb_{lut} \quad \forall u, \forall t \quad (\text{A.3})$$

$$pb_{(l=1)ut} \leq P_u^{l=1} - P_u^{\min} \quad \forall u, \forall t \quad (\text{A.4})$$

$$pb_{lut} \leq P_u^l - P_u^{l-1} \quad \forall u, \forall t, \forall l = 1, \dots, N_u^l \quad (\text{A.5})$$

$$pb_{N_u^l ut} \leq P_u^{\max} - P_u^{N_u^l - 1} \quad \forall u, \forall t \quad (\text{A.6})$$

where $A_u = a_u + b_u \cdot P_u^{\min} + c_u \cdot (P_u^{\min})^2 \quad \forall u$.

APPENDIX B: THE GENERATOR DATA OF IEEE 30 AND 118-BUS TEST
SYSTEMS

Table B.1: IEEE 30-bus generator data

Bus No.	P_u^{\min} (MW)	P_u^{\max} (MW)	Cost Coefficients		
			a_u (\$/h)	b_u (\$/MWh)	c_u (\$/MW ² h)
1	50	200	0	2.00	0.00375
2	20	80	0	1.75	0.01750
5	15	50	0	1.00	0.06250
8	10	35	0	3.25	0.00834
11	10	30	0	3.00	0.02500
13	12	40	0	3.00	0.02500

Table B.2: IEEE 118-bus generator data

Unit	Bus No.	P_u^{\min} (MW)	P_u^{\max} (MW)	MD_u (h)	MU_u (h)	RD_u (MW/h)	RU_u (MW/h)	$SU_{u\tau}$ (\\$)	Cost Coefficients		
									a_u (\$/h)	b_u (\$/MWh)	c_u (\$/MW ² h)
1001	4	5	30	1	1	15	15	40	31.67	26.2438	0.06966
1002	6	5	30	1	1	15	15	40	31.67	26.2438	0.06966
1003	8	5	30	1	1	15	15	40	31.67	26.2438	0.06966
1004	10	150	300	8	8	150	150	440	6.78	12.8875	0.01088
1005	12	100	300	8	8	150	150	110	6.78	12.8875	0.01088
1006	15	10	30	1	1	15	15	40	31.67	26.2438	0.06966
1007	18	25	100	5	5	50	50	50	10.15	17.8200	0.01280
1008	19	5	30	1	1	15	15	40	31.67	26.2438	0.06966
1009	24	5	30	1	1	15	15	40	31.67	26.2438	0.06966
1010	25	100	300	8	8	150	150	100	6.78	12.8875	0.01088

Unit	Bus No.	P_u^{\min} (MW)	P_u^{\max} (MW)	MD_u (h)	MU_u (h)	RD_u (MW/h)	RU_u (MW/h)	$SU_{u\tau}$ (\\$)	Cost Coefficients		
									a_u (\$/h)	b_u (\$/MWh)	c_u (\$/MW ² h)
1011	26	100	350	8	8	175	175	100	32.96	10.7600	0.00300
1012	27	8	30	1	1	15	15	40	31.67	26.2438	0.06966
1013	31	8	30	1	1	15	15	40	31.67	26.2438	0.06966
1014	32	25	100	5	5	50	50	50	10.15	17.8200	0.01280
1015	34	8	30	1	1	15	15	40	31.67	26.2438	0.06966
1016	36	25	100	5	5	50	50	50	10.15	17.8200	0.01280
1017	40	8	30	1	1	15	15	40	31.67	26.2438	0.06966
1018	42	8	30	1	1	15	15	40	31.67	26.2438	0.06966
1019	46	25	100	5	5	50	50	59	10.15	17.8200	0.01280
1020	49	50	250	8	8	125	125	100	28.00	12.3299	0.00240
1021	54	50	250	8	8	125	125	100	28.00	12.3299	0.00240
1022	55	25	100	5	5	50	50	50	10.15	17.8200	0.01280
1023	56	25	100	5	5	50	50	50	10.15	17.8200	0.01280
1024	59	50	200	8	8	100	100	100	39.00	13.2900	0.00440
1025	61	50	200	8	8	100	100	100	39.00	13.2900	0.00440
1026	62	25	100	5	5	50	50	50	10.15	17.8200	0.01280
1027	65	100	420	10	10	210	210	250	64.16	8.3391	0.01059
1028	66	100	420	10	10	210	210	250	64.16	8.3391	0.01059
1029	69	80	300	8	8	150	150	100	6.78	12.8875	0.01088
1030	70	30	80	4	4	40	40	45	74.33	15.4708	0.04592
1031	72	10	30	1	1	15	15	40	31.67	26.2438	0.06966
1032	73	5	30	1	1	15	15	40	31.67	26.2438	0.06966
1033	74	5	20	1	1	10	10	30	17.95	37.6968	0.02830

Unit	Bus No.	P_u^{\min} (MW)	P_u^{\max} (MW)	MD_u (h)	MU_u (h)	RD_u (MW/h)	RU_u (MW/h)	$SU_{u\tau}$ (\\$)	Cost Coefficients		
									a_u (\$/h)	b_u (\$/MWh)	c_u (\$/MW ² h)
1034	76	25	100	5	5	50	50	50	10.15	17.8200	0.01280
1035	77	25	100	5	5	50	50	50	10.15	17.8200	0.01280
1036	80	150	300	8	8	150	150	440	6.78	12.8875	0.01088
1037	82	25	100	5	5	50	50	50	10.15	17.8200	0.01280
1038	85	10	30	1	1	15	15	40	31.67	26.2438	0.06966
1039	87	100	300	8	8	150	150	440	32.96	10.7600	0.00300
1040	89	50	200	8	8	100	100	400	6.78	12.8875	0.01088
1041	90	8	20	1	1	10	10	30	17.95	37.6968	0.02830
1042	91	20	50	1	1	25	25	45	58.81	22.9423	0.00977
1043	92	100	300	8	8	150	150	100	6.78	12.8875	0.01088
1044	99	100	300	8	8	150	150	100	6.78	12.8875	0.01088
1045	100	100	300	8	8	150	150	110	6.78	12.8875	0.01088
1046	103	8	20	1	1	10	10	30	17.95	37.6968	0.02830
1047	104	25	100	5	5	50	50	50	10.15	17.8200	0.01280
1048	105	25	100	5	5	50	50	50	10.15	17.8200	0.01280
1049	107	8	20	1	1	10	10	30	17.95	37.6968	0.02830
1050	110	25	50	2	2	25	25	45	58.81	22.9423	0.00977
1051	111	25	100	5	5	50	50	50	10.15	17.8200	0.01280
1052	112	25	100	5	5	50	50	50	10.15	17.8200	0.01280
1053	113	25	100	5	5	50	50	50	10.15	17.8200	0.01280
1054	116	25	50	2	2	25	25	45	58.81	22.9423	0.00977

where generation cost function is equal to $f_u(p_{ut}) = a_u + b_u \cdot p_{ut} + c_u \cdot p_{ut}^2$

APPENDIX C:

Theorem: The BRO, BERO, and BPRO models lead to the same result for $DR = DR^{\max}$.

Proof: As (2.24) should be maximized and its last two terms are negative (since $h_t \geq 0 \ \forall t$ and $q_t \geq 0 \ \forall t$ based on (2.25)), in the optimal solution of BERO, the inequality of (2.25) becomes an equality:

$$h_t + q_t = \widehat{E}_t \cdot \sum_{u=1}^U p_{ut} \Rightarrow \sum_{t=1}^T (h_t + q_t) = \sum_{t=1}^T \sum_{u=1}^U \widehat{E}_t \cdot p_{ut} \quad (\text{C.1})$$

Similarly, for (2.28), the following relation in the optimal solution is found:

$$\sum_{t=1}^T (v + h_t) = \sum_{t=1}^T \sum_{u=1}^U \widehat{E}_t \cdot p_{ut} \quad (\text{C.2})$$

The above relations (C.1) and (C.2) can be written as:

$$\sum_{t=1}^T h_t + \sum_{t=1}^T q_t = \sum_{t=1}^T \sum_{u=1}^U \widehat{E}_t \cdot p_{ut} \quad (\text{C.3})$$

$$T \cdot v + \sum_{t=1}^T h_t = \sum_{t=1}^T \sum_{u=1}^U \widehat{E}_t \cdot p_{ut} \quad (\text{C.4})$$

Based on $DR = DR^{\max}$, there are $\Psi_B = 1$, $\Psi_E = \sqrt{|J|} = \sqrt{T}$ and $\Psi_P = |J| = T$ in BERO, and BPRO. Thus, the PF of (2.24), and (2.27) become:

$$\left[\Psi_B \cdot \sum_{t=1}^T h_t \right] + \left[\Psi_E \cdot \sqrt{\sum_{t=1}^T q_t^2} \right] = \sum_{t=1}^T h_t + \sqrt{T} \cdot \sqrt{\sum_{t=1}^T q_t^2} \quad (\text{C.5})$$

$$[\Psi_P \cdot v] + \left[\Psi_B \cdot \sum_{t=1}^T h_t \right] = T \cdot v + \sum_{t=1}^T h_t \quad (\text{C.6})$$

From Cauchy-Schwarz inequality, it is well-known that [97]:

$$\langle \mathbf{a}, \mathbf{b} \rangle \leq \langle \mathbf{a}, \mathbf{a} \rangle^{\frac{1}{2}} \langle \mathbf{b}, \mathbf{b} \rangle^{\frac{1}{2}} \quad (\text{C.7})$$

where $\langle \cdot, \cdot \rangle$ is the inner product. Consider $\mathbf{a} = \{1, 1\}$, $\mathbf{b} = \{q_1, q_2\}$, and based on constraint (2.25).

$$q_1 + q_2 \leq \sqrt{2} \cdot \sqrt{q_1^2 + q_2^2} \quad (\text{C.8})$$

This result can easily be extended to T terms as:

$$\sqrt{T} \cdot \sqrt{\sum_{t=1}^T q_t^2} \geq \sum_{t=1}^T q_t \quad (\text{C.9})$$

Therefore, for $\text{DR} = \text{DR}^{\max}$ to obtain the maximum value of (2.24), the ERO term $(\sqrt{T} \cdot \sqrt{\sum_{t=1}^T q_t^2})$ equals $\sum_{t=1}^T q_t$. Using this result, combining (C.3) with (C.5), and (C.4) with (C.6) yield:

$$\left[\Psi_B \cdot \sum_{t=1}^T h_t \right] + \left[\Psi_E \cdot \sqrt{\sum_{t=1}^T q_t^2} \right] = \sum_{t=1}^T \sum_{u=1}^U \widehat{E}_t \cdot p_{ut} \quad (\text{C.10})$$

$$[\Psi_P \cdot v] + \left[\Psi_B \cdot \sum_{t=1}^T h_t \right] = \sum_{t=1}^T \sum_{u=1}^U \widehat{E}_t \cdot p_{ut} \quad (\text{C.11})$$

The right-hand-side of (C.10) and (C.11) is the last term of (2.13) for $\Psi_B = 1$. Thus, for $\text{DR} = \text{DR}^{\max}$, the BRO, BERO, and BPRO models have the same PF, and thus lead to the same optimal result. Figure C.1 illustrates the uncertainty set of BRO, BERO, and BPRO for $\text{DR} = \text{DR}^{\max}$.

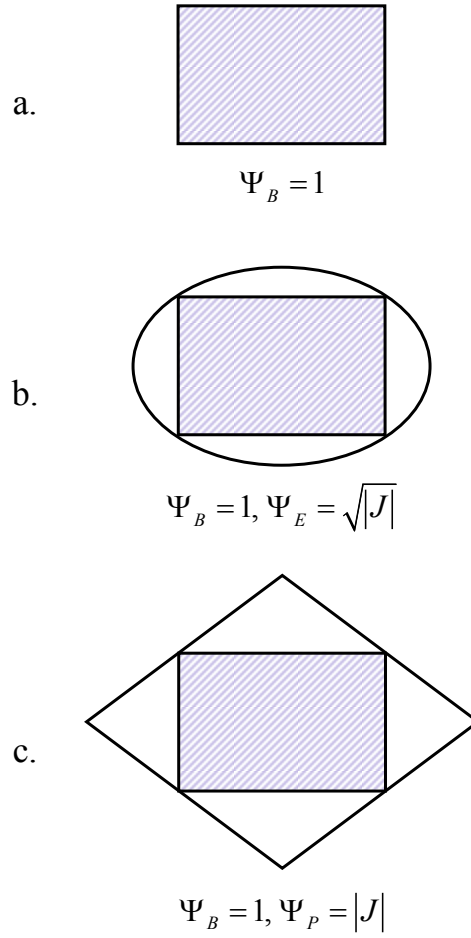


Figure C.1: BRO (a.), BERO (b.), and BPRO (c.) uncertainty set for $DR = DR^{\max}$.

APPENDIX D:

Theorem: In terms of conservativeness, BRO, ERO and PRO are sorted as: $\text{BRO} \leq \text{ERO} \leq \text{PRO}$.

Proof: For $\text{DR} = \text{DR}^{\max}$ the PF of the ERO in (2.16) becomes:

$$\Psi_E \cdot \sqrt{\sum_{t=1}^T \left[\hat{E}_t^2 \cdot \left[\sum_{u=1}^U p_{ut} \right]^2 \right]} = \sqrt{T} \cdot \sqrt{\sum_{t=1}^T \left[\hat{E}_t \cdot \sum_{u=1}^U p_{ut} \right]^2} \quad (\text{D.1})$$

Using (C.8), for this PF it can be written that:

$$\sqrt{T} \times \sqrt{\sum_{t=1}^T \left[\hat{E}_t \cdot \sum_{u=1}^U p_{ut} \right]^2} \geq \sum_{t=1}^T \left[\hat{E}_t \cdot \sum_{u=1}^U p_{ut} \right] \quad (\text{D.2})$$

The right-hand-side of (D.2) is the PF of BRO in (2.13) for $\text{DR} = \text{DR}^{\max}$, i.e. $\Psi_B = 1$. Thus, ERO has a higher PF than BRO and so is more conservative than BRO for $\text{DR} = \text{DR}^{\max}$.

Considering the inequality $v \geq \hat{E}_t \cdot \sum_{u=1}^U p_{ut}$ in (2.20), the PF of the ERO can be written as:

$$\sqrt{T} \cdot \sqrt{\sum_{t=1}^T \left[\hat{E}_t \cdot \sum_{u=1}^U p_{ut} \right]^2} \leq \sqrt{T} \cdot \sqrt{\sum_{t=1}^T v^2} = T \cdot v \quad (\text{D.3})$$

For $\text{DR} = \text{DR}^{\max}$, the PF of the PRO in (2.19) becomes:

$$\Psi_p \cdot v = T \cdot v \quad (\text{D.4})$$

(D.3) and (D.4) yield that PRO has a higher PF than ERO, and so is more conservative than ERO for $\text{DR} = \text{DR}^{\max}$. This result and the previous one proves the theorem for $\text{DR} = \text{DR}^{\max}$. Similarly, this theorem can be proved for the other values of DR.

APPENDIX E:

Constraints (4.5)-(4.13), and (4.18)-(4.26) are not changed in the ELDR-based methodology since they include only the here-and-now, and auxiliary variables. The reformulated constraints (4.1), (4.3), (4.4), and (4.14)-(4.17) are provided in this section. The piecewise affine policies (4.28)-(4.30) are replaced in the associated constraints. Then, to end up with the tractable robust counterpart of the TES model, the duality theory can be applied to reformulate each constraint.

As mentioned in subsection (4.2.3), to apply the duality the inner maximization must be fixed independent of ξ . While, in (4.1) the products of selling LMP and LR power, purchasing LMP and power, and selling LMP and power are dependent to ξ . To remedy this issue a new auxiliary variable $\xi' = \xi \cdot \xi$ is defined. Also, the non-adjustable variable \mathbf{h} is divided into two components \mathbf{h}_1 and \mathbf{h}_2 , and the piecewise affine policy can be rewritten as:

$$\mathbf{p} = \mathbf{h}_1 + \mathbf{h}_2 + \mathbf{W}\xi \quad (\text{E.1})$$

The piecewise affine policy of the product $\mathbf{p}\xi$ can be defined as follows:

$$\mathbf{p}\xi = \mathbf{h}_1 + \mathbf{h}_2\xi + \mathbf{W}\xi' \quad (\text{E.2})$$

Accordingly, the duality theory can be applied to (4.1) using piecewise affine policies (E.1) and (E.2):

$$\text{Max } \vartheta \quad (\text{E.3})$$

s.t.

$$\begin{aligned}
& \sum_{t \in T} \left[\sum_{u \in U} \left[\sum_{b \in B} \left[\overline{\overline{\pi}}_t^{\text{S,LMP}} - \pi_{but}^{\text{LR}} \right] \cdot (P_{but}^{\text{h1,LR}} + P_{but}^{\text{h2,LR}}) \right] + [\pi_{ut}^{\text{P}} - \overline{\overline{\pi}}_t^{\text{P,LMP}}] \cdot (P_{ut}^{\text{h1,P}} + P_{ut}^{\text{h2,P}}) + \overline{\overline{\pi}}_t^{\text{S,LMP}} \right. \\
& \left. - \pi_{ut}^{\text{S}} \cdot (P_{ut}^{\text{h1,S}} + P_{ut}^{\text{h2,S}}) + \lambda_1 \cdot P_{ut}^{\text{LC}} + \lambda_2 \cdot \rho_{ut}^{\text{LS}} \cdot P_{ut}^{\text{LS}} + \lambda_3 \cdot [\pi_{ut}^{\text{P}} - \overline{\overline{\pi}}_t^{\text{P,LMP}}] \cdot P_{ut}^{\text{ES,dch}} - \lambda_4 \cdot (P_{ut}^{\text{h1,S}} + P_{ut}^{\text{h2,S}}) \right] - \sum_{l \in L} (\Pi_{1,lut}^{\text{RE}} \\
& + \Pi_{lut}^{\text{A,4}} + \Pi_{lut}^{\text{A,5}}) \left. \right] - \sum_{l \in L} (\Pi_{1,lt}^{\text{S}} + \Pi_{1,lt}^{\text{P}} + \Pi_{lt}^{\text{A,1}} + \Pi_{lt}^{\text{A,2}} + \Pi_{lt}^{\text{A,3}}) \left. \right] - \Theta^{\text{S}} \cdot \Gamma_1^{\text{S}} - \Theta^{\text{P}} \cdot \Gamma_1^{\text{P}} - \Theta^{\text{RE}} \cdot \Gamma_1^{\text{RE}} - \vartheta \geq 0
\end{aligned} \tag{E.4}$$

$$\begin{aligned}
& \sum_{l \in L} \Pi_{1,lt}^{\text{S}} + \Gamma_1^{\text{S}} \geq \sum_{l \in L} \left[\widehat{\pi}_{lt}^{\text{S}} \cdot \sum_{u \in U} \left[\sum_{b \in B} [(\pi_{but}^{\text{LR}} - \overline{\overline{\pi}}_t^{\text{S,LMP}}) \cdot P_{S,lbut}^{\text{w,LR}} + P_{but}^{\text{h2,LR}}] + (\overline{\overline{\pi}}_t^{\text{P,LMP}} - \pi_{ut}^{\text{P}}) \cdot P_{S,lut}^{\text{w,P}} + [\pi_{ut}^{\text{S}} - \overline{\overline{\pi}}_t^{\text{S,LMP}}] \cdot P_{S,lut}^{\text{w,S}} + P_{ut}^{\text{h2,S}} + \lambda_4 \cdot P_{S,lut}^{\text{w,S}}] \right] \quad \forall t
\end{aligned} \tag{E.5}$$

$$\begin{aligned}
& \sum_{l \in L} \Pi_{1,lt}^{\text{P}} + \Gamma_1^{\text{P}} \geq \sum_{l \in L} \left[\widehat{\pi}_{lt}^{\text{P}} \cdot \sum_{u \in U} \left[\sum_{b \in B} [(\pi_{but}^{\text{LR}} - \overline{\overline{\pi}}_t^{\text{S,LMP}}) \cdot P_{P,lbut}^{\text{w,LR}}] + (\overline{\overline{\pi}}_t^{\text{P,LMP}} - \pi_{ut}^{\text{P}}) \cdot P_{P,lut}^{\text{w,P}} + P_{ut}^{\text{h2,P}} + [\pi_{ut}^{\text{S}} - \overline{\overline{\pi}}_t^{\text{S,LMP}}] \cdot P_{P,lut}^{\text{w,S}} + \lambda_3 \cdot P_{ut}^{\text{ES,dch}} + \lambda_4 \cdot P_{P,lut}^{\text{w,S}}] \right] \quad \forall t
\end{aligned} \tag{E.6}$$

$$\begin{aligned}
& \sum_{l \in L} \Pi_{1,lut}^{\text{RE}} + \Gamma_1^{\text{RE}} \geq \sum_{l \in L} \left[\widehat{P}_{lut}^{\text{RE}} \cdot \sum_{b \in B} [(\pi_{but}^{\text{LR}} - \overline{\overline{\pi}}_t^{\text{S,LMP}}) \cdot P_{RE,lbut}^{\text{w,LR}} + (\overline{\overline{\pi}}_t^{\text{P,LMP}} - \pi_{ut}^{\text{P}}) \cdot P_{RE,lut}^{\text{w,P}} + [\pi_{ut}^{\text{S}} - \overline{\overline{\pi}}_t^{\text{S,LMP}}] \cdot P_{RE,lut}^{\text{w,S}} + \lambda_4 \cdot P_{RE,lut}^{\text{w,S}}] \right] \quad \forall u, \forall t
\end{aligned} \tag{E.7}$$

$$\begin{aligned}
& \sum_{l \in L} \Pi_{lt}^{\text{A,1}} \geq \sum_{l \in L} \widehat{\pi}_{lt}^{\text{S}} \cdot \widehat{\pi}_{lt}^{\text{S}} \cdot \sum_{u \in U} \left[\sum_{b \in B} P_{S,lbut}^{\text{w,LR}} + P_{S,lut}^{\text{w,S}} \right] \quad \forall t
\end{aligned} \tag{E.8}$$

$$\begin{aligned}
& \sum_{l \in L} \Pi_{lt}^{\text{A,2}} \geq \sum_{l \in L} \widehat{\pi}_{lt}^{\text{S}} \cdot \widehat{\pi}_{lt}^{\text{P}} \cdot \sum_{u \in U} \left[\sum_{b \in B} P_{P,lbut}^{\text{w,LR}} + P_{S,lut}^{\text{w,P}} + P_{P,lut}^{\text{w,S}} \right] \quad \forall t
\end{aligned} \tag{E.9}$$

$$\sum_{l \in L} \Pi_{lt}^{A,3} \geq \sum_{l \in L} \hat{\pi}_{lt}^P \cdot \hat{\pi}_{lt}^P \cdot \sum_{u \in U} P_{P,lt}^{w,P} \quad \forall t \quad (\text{E.10})$$

$$\begin{aligned} \sum_{l \in L} \Pi_{lut}^{A,4} &\geq \sum_{l \in L} \hat{\pi}_{lt}^S \cdot \hat{P}_{lut}^{\text{RE}} \cdot \left[\sum_{b \in B} P_{\text{RE},lb}^{w,LR} \right. \\ &\left. + P_{\text{RE},lut}^{w,S} \right] \quad \forall u, \forall t \end{aligned} \quad (\text{E.11})$$

$$\sum_{l \in L} \Pi_{lut}^{A,5} \geq \sum_{l \in L} \hat{\pi}_{lt}^P \cdot \hat{P}_{lut}^{\text{RE}} \cdot P_{\text{RE},lut}^{w,P} \quad \forall u, \forall t \quad (\text{E.12})$$

where $\Pi_{lt}^{A,1} \geq 0$, $\Pi_{lt}^{A,2} \geq 0$, $\Pi_{lt}^{A,3} \geq 0$, $\Pi_{lut}^{A,4} \geq 0$, and $\Pi_{lut}^{A,5} \geq 0$ are the dual variables associated with $\pi_{lt}^{\text{S,LMP}} \cdot \pi_{lt}^{\text{S,LMP}}$, $\pi_{lt}^{\text{S,LMP}} \cdot \pi_{lt}^{\text{P,LMP}}$, $\pi_{lt}^{\text{P,LMP}} \cdot \pi_{lt}^{\text{P,LMP}}$, $\pi_{lt}^{\text{S,LMP}} \cdot P_{lut}^{\text{RE}}$, and $\pi_{lt}^{\text{P,LMP}} \cdot P_{lut}^{\text{RE}}$, respectively.

The constraints (E.13)-(E.20), (E.21)-(E.24), and (E.25)-(4.28) are the reformulated form of the constraints (4.3), (4.4), and (4.14), respectively. Without loss of generality, the equality constraints of (4.4), (4.14), and (4.15) are replaced with the inequality constraints of (E.21), (E.25), and (E.31), respectively [86].

$$\begin{aligned} (P_{ut}^{\text{h1,P}} + P_{ut}^{\text{h2,P}}) - \bar{P}_{ut}^P \cdot z_{ut}^P - \sum_{l \in L} [\Pi_{3.1,lt}^{\text{S}} + \Pi_{3.1,lt}^{\text{P}} \\ + \Pi_{3.1,lut}^{\text{RE}}] - \Theta^{\text{S}} \cdot \Gamma_{3.1}^{\text{S}} - \Theta^{\text{P}} \cdot \Gamma_{3.1}^{\text{P}} - \Theta^{\text{RE}} \cdot \Gamma_{3.1}^{\text{RE}} \geq 0 \quad \forall u, \forall t \end{aligned} \quad (\text{E.13})$$

$$\sum_{l \in L} \Pi_{3.1,lt}^{\text{S}} + \Gamma_{3.1}^{\text{S}} \geq - \sum_{l \in L} \hat{\pi}_{lt}^{\text{S}} \cdot P_{S,lt}^{w,P} \quad \forall u, \forall t \quad (\text{E.14})$$

$$\sum_{l \in L} \Pi_{3.1,lt}^{\text{P}} + \Gamma_{3.1}^{\text{P}} \geq - \sum_{l \in L} \hat{\pi}_{lt}^{\text{P}} \cdot P_{P,lt}^{w,P} \quad \forall u, \forall t \quad (\text{E.15})$$

$$\sum_{l \in L} \Pi_{3.1,lut}^{\text{RE}} + \Gamma_{3.1}^{\text{RE}} \geq - \sum_{l \in L} \hat{P}_{lut}^{\text{RE}} \cdot P_{\text{RE},lut}^{w,P} \quad \forall u, \forall t \quad (\text{E.16})$$

$$\begin{aligned} \bar{P}_{ut}^P \cdot z_{ut}^P - (P_{ut}^{\text{h1,P}} + P_{ut}^{\text{h2,P}}) - \sum_{l \in L} [\Pi_{3.2,lt}^{\text{S}} + \Pi_{3.2,lt}^{\text{P}} \\ + \Pi_{3.2,lut}^{\text{RE}}] - \Theta^{\text{S}} \cdot \Gamma_{3.2}^{\text{S}} - \Theta^{\text{P}} \cdot \Gamma_{3.2}^{\text{P}} - \Theta^{\text{RE}} \cdot \Gamma_{3.2}^{\text{RE}} \geq 0 \quad \forall u, \forall t \end{aligned} \quad (\text{E.17})$$

$$\sum_{l \in L} \Pi_{3.2,lt}^{\text{S}} + \Gamma_{3.2}^{\text{S}} \geq \sum_{l \in L} \hat{\pi}_{lt}^{\text{S}} \cdot P_{S,lt}^{w,P} \quad \forall u, \forall t \quad (\text{E.18})$$

$$\sum_{l \in L} \Pi_{3.2,lt}^{\text{P}} + \Gamma_{3.2}^{\text{P}} \geq \sum_{l \in L} \hat{\pi}_{lt}^{\text{P}} \cdot P_{P,lt}^{w,P} \quad \forall u, \forall t \quad (\text{E.19})$$

$$\sum_{l \in L} \Pi_{3.2,lut}^{\text{RE}} + \Gamma_{3.2}^{\text{RE}} \geq \sum_{l \in L} \widehat{P}_{lut}^{\text{RE}} \cdot P_{\text{RE},lut}^{\text{w,P}} \quad \forall u, \forall t \quad (\text{E.20})$$

$$\begin{aligned} & P_{but}^{\text{LR,LC}} + P_{but}^{\text{LR,LS}} - (P_{but}^{\text{h1,LR}} + P_{but}^{\text{h2,LR}}) - \sum_{l \in L} [\Pi_{4,lt}^{\text{S}} \\ & + \Pi_{4,lt}^{\text{P}} + \Pi_{4,lut}^{\text{RE}}] - \Theta^{\text{S}} \cdot \Gamma_4^{\text{S}} - \Theta^{\text{P}} \cdot \Gamma_4^{\text{P}} - \Theta^{\text{RE}} \cdot \Gamma_4^{\text{RE}} \\ & \geq 0 \quad \forall b, \forall u, \forall t \end{aligned} \quad (\text{E.21})$$

$$\sum_{l \in L} \Pi_{4,lt}^{\text{S}} + \Gamma_4^{\text{S}} \geq \sum_{l \in L} \widehat{\pi}_{lt}^{\text{S}} \cdot P_{\text{S},lbut}^{\text{w,LR}} \quad \forall b, \forall u, \forall t \quad (\text{E.22})$$

$$\sum_{l \in L} \Pi_{4,lt}^{\text{P}} + \Gamma_4^{\text{P}} \geq \sum_{l \in L} \widehat{\pi}_{lt}^{\text{P}} \cdot P_{\text{P},lbut}^{\text{w,LR}} \quad \forall b, \forall u, \forall t \quad (\text{E.23})$$

$$\sum_{l \in L} \Pi_{4,lut}^{\text{RE}} + \Gamma_4^{\text{RE}} \geq \sum_{l \in L} \widehat{P}_{lut}^{\text{RE}} \cdot P_{\text{RE},lbut}^{\text{w,LR}} \quad \forall b, \forall u, \forall t \quad (\text{E.24})$$

$$\begin{aligned} & P_{ut}^{\text{RE-G}} - \overline{\overline{P}}_{ut}^{\text{RE}} - (P_{ut}^{\text{h1,P}} + P_{ut}^{\text{h2,P}}) + (P_{ut}^{\text{h1,S}} + P_{ut}^{\text{h2,S}}) - \\ & \sum_{l \in L} [\Pi_{14,lt}^{\text{S}} + \Pi_{14,lt}^{\text{P}} + \Pi_{14,lut}^{\text{RE}}] - \Theta^{\text{S}} \cdot \Gamma_{14}^{\text{S}} - \Theta^{\text{P}} \cdot \Gamma_{14}^{\text{P}} \\ & - \Theta^{\text{RE}} \cdot \Gamma_{14}^{\text{RE}} \geq 0 \quad \forall u, \forall t \end{aligned} \quad (\text{E.25})$$

$$\sum_{l \in L} \Pi_{14,lt}^{\text{S}} + \Gamma_{14}^{\text{S}} \geq \sum_{l \in L} \widehat{\pi}_{lt}^{\text{S}} \cdot [P_{\text{S},lut}^{\text{w,P}} - P_{\text{S},lut}^{\text{w,S}}] \quad \forall u, \forall t \quad (\text{E.26})$$

$$\sum_{l \in L} \Pi_{14,lt}^{\text{P}} + \Gamma_{14}^{\text{P}} \geq \sum_{l \in L} \widehat{\pi}_{lt}^{\text{P}} \cdot [P_{\text{P},lut}^{\text{w,P}} - P_{\text{P},lut}^{\text{w,S}}] \quad \forall u, \forall t \quad (\text{E.27})$$

$$\begin{aligned} \sum_{l \in L} \Pi_{14,lut}^{\text{RE}} + \Gamma_{14}^{\text{RE}} & \geq \sum_{l \in L} \widehat{P}_{lut}^{\text{RE}} \cdot [P_{\text{RE},lut}^{\text{w,P}} - P_{\text{RE},lut}^{\text{w,S}} \\ & - 1] \quad \forall u, \forall t \end{aligned} \quad (\text{E.28})$$

By replacing equality constraint of (4.14) with the inequality constraint of (4.25), $P_{ut}^{\text{RE-G}}$ variable is unbounded. To resolve this problem, the auxiliary constraints (E.29) and (E.30) are introduced.

$$\begin{aligned} \overline{\overline{P}}_{ut}^{\text{RE}} + \overline{P}_{ut}^{\text{P}} \cdot z_{ut}^{\text{P}} - P_{ut}^{\text{RE-G}} - \sum_{l \in L} \Pi_{\text{A},lut}^{\text{RE}} - \Theta^{\text{RE}} \cdot \Gamma_{\text{A}}^{\text{RE}} \\ \geq 0 \quad \forall u, \forall t \end{aligned} \quad (\text{E.29})$$

$$\sum_{l \in L} \Pi_{\text{A},lut}^{\text{RE}} + \Gamma_{\text{A}}^{\text{RE}} \geq \sum_{l \in L} \widehat{P}_{lut}^{\text{RE}} \quad \forall u, \forall t \quad (\text{E.30})$$

$$(P_{ut}^{h1,P} + P_{ut}^{h2,P}) - (P_{ut}^{h1,S} + P_{ut}^{h2,S}) - P_{ut}^G - \sum_{l \in L} [\Pi_{16,lt}^S + \Pi_{15,lt}^P + \Pi_{15,lt}^{RE}] - \Theta^S \cdot \Gamma_{15}^S - \Theta^P \cdot \Gamma_{15}^P - \Theta^{RE} \cdot \Gamma_{15}^{RG} \geq 0 \quad \forall u, \forall t \quad (\text{E.31})$$

$$\sum_{l \in L} \Pi_{15,lt}^S + \Gamma_{15}^S \geq \sum_{l \in L} \hat{\pi}_{lt}^S \cdot (P_{S,lt}^{w,S} - P_{S,lt}^{w,P}) \quad \forall u, \forall t \quad (\text{E.32})$$

$$\sum_{l \in L} \Pi_{15,lt}^P + \Gamma_{15}^P \geq \sum_{l \in L} \hat{\pi}_{lt}^P \cdot (P_{P,lt}^{w,S} - P_{P,lt}^{w,P}) \quad \forall u, \forall t \quad (\text{E.33})$$

$$\sum_{l \in L} \Pi_{15,lt}^{RE} + \Gamma_{15}^{RE} \geq \sum_{l \in L} \hat{P}_{lut}^{RE} \cdot (P_{RE,lt}^{w,S} - P_{RE,lt}^{w,P}) \quad \forall u, \forall t \quad (\text{E.34})$$

The robust counterpart of the constraints (4.16) and (4.17) are represented in the constraints (E.35)-(E.38) and (E.39)-(E.42).

$$M \cdot (1 - z_{ut}^P) - (P_{ut}^{h1,S} + P_{ut}^{h2,S}) - \sum_{l \in L} [\Pi_{16,lt}^S + \Pi_{16,lt}^P + \Pi_{16,ut}^{RE}] - \Theta^S \cdot \Gamma_{16}^S - \Theta^P \cdot \Gamma_{16}^P - \Theta^{RE} \cdot \Gamma_{16}^{RE} \geq 0 \forall u, \forall t \quad (\text{E.35})$$

$$\sum_{l \in L} \Pi_{16,lt}^S + \Gamma_{16}^S \geq \sum_{l \in L} \hat{\pi}_{lt}^S \cdot P_{S,lt}^{w,S} \quad \forall u, \forall t \quad (\text{E.36})$$

$$\sum_{l \in L} \Pi_{16,lt}^P + \Gamma_{16}^P \geq \sum_{l \in L} \hat{\pi}_{lt}^P \cdot P_{P,lt}^{w,S} \quad \forall u, \forall t \quad (\text{E.37})$$

$$\sum_{l \in L} \Pi_{16,lt}^{RE} + \Gamma_{16}^{RE} \geq \sum_{l \in L} \hat{P}_{lut}^{RE} \cdot P_{RE,lt}^{w,S} \quad \forall u, \forall t \quad (\text{E.38})$$

$$M \cdot (1 - z_{ut}^H) - (P_{ut}^{h1,S} + P_{ut}^{h2,S}) - \sum_{l \in L} [\Pi_{17,lt}^S + \Pi_{17,lt}^P + \Pi_{17,ut}^{RE}] - \Theta^S \cdot \Gamma_{17}^S - \Theta^P \cdot \Gamma_{17}^P - \Theta^{RE} \cdot \Gamma_{17}^{RE} \geq 0 \forall u, \forall t \quad (\text{E.39})$$

$$\sum_{l \in L} \Pi_{17,lt}^S + \Gamma_{17}^S \geq \sum_{l \in L} \hat{\pi}_{lt}^S \cdot P_{S,lt}^{w,S} \quad \forall u, \forall t \quad (\text{E.40})$$

$$\sum_{l \in L} \Pi_{17,lt}^P + \Gamma_{17}^P \geq \sum_{l \in L} \hat{\pi}_{lt}^P \cdot P_{P,lt}^{w,S} \quad \forall u, \forall t \quad (\text{E.41})$$

$$\sum_{l \in L} \Pi_{17,lt}^{RE} + \Gamma_{17}^{RE} \geq \sum_{l \in L} \hat{P}_{lut}^{RE} \cdot P_{RE,lt}^{w,S} \quad \forall u, \forall t \quad (\text{E.42})$$

The final formulation of the ELDR-based robust TES framework is as follows:

$$(\text{E.3})$$

s.t. (4.5)-(4.13), (4.18)-(4.26), (4.31)-(4.33), and (E.4)-(E.42)